FINAL REPORT

INVESTIGATION INTO THE MECHANISM OF DEGRADATION OF SOLAR CELLS WITH SILVER-TITANIUM CONTACTS

Prepared By:

Charles J. Bishop - Technical Leader

Henry Oman - Program Leader

THE BOEING COMPANY
AEROSPACE GROUP
KENT FACILITY
P.O. BOX 3999
SEATTLE, WASHINGTON 98124

Prepared For:

NATIONAL AERONAUTICS AND SPACE ADMINISTRATION

July 1, 1970

Contract NASW-1859

National Aeronautics and Space Administration
Washington, D.C.

Ernst M. Cohn, Project Manager
Office of Advanced Research and Technology

TABLE OF CONTENTS

1.0 SUMMARY, CONCLUSIONS AND RECOMMENDATIONS

The objective of the work described in this report was to determine the fundamental mechanism which causes solar cells with silver-titanium contacts to degrade when stored in humid atmospheres. We used electrochemical tests and physical measurements to characterize the degradation process. Physical measurements included optical and electron micrographs, X-ray diffraction, electron microprobe, mass spectroscopy, and internal reflection spectroscopy.

Micrographs of a Heliotek solar cell showed that the mottled surface is not from true grains of silver. What appeared to be grains were in reality plateaus and ridges in the silicon substrate resulting from the etching process used in preparing the silicon wafers. The mottled surface is simply the contour of the silicon substrate transmitted through the silver layer. No evidence for porosity was seen from the micrographs. The pores were smaller than could be detected by electron microscopy.

Mass spectroscopy identified many contaminants in solar cells, even in supposedly ultraclean silicon wafers which were ready for contact evaporation. The most important contaminants were chloride and fluoride ions. The fluoride ions are residue from the hydrofluoric acid etching processes. Chloride ions come from handling of the product, and as impurities in titanium.

X-ray diffraction analysis did not give meaningful results and we concluded that this method is not sensitive enough to identify the nature of titanium films in solar cells. Electron microprobe data proved that the contact loses adhesion at the silver-titanium interface.

Internal reflection spectroscopy was the most productive physical measurement. It showed that silver is porous, with pores 15 to 65 Å in radius. Water from capillary condensation collects rapidly in the pores when humidity exceeds a critical value. The small diameter of the pores compared to the thickness of the silver films (30,000Å) suggests an interconnected or "spongelike" structure in the silver. The critical humidity at which condensation occurred, and thus the pore size distribution in the silver layer, varied from manufacturer to manufacturer and between samples from one manufacturer. We also found that under certain conditions silicon can contribute to contact degradation probably by the reaction: $Si + 2H_2O \rightarrow 2H_2 + SiO_2$. A one-micron gold film was non-porous to humid air and thus might be a good substitute for silver to protect the chemically active titanium.

In electrochemical tests, polarization measurements and constant potential tests verified the environment in which solar cells degrade in a predictable manner in the laboratory. Polarization measurements showed that degradation could be reproduced and accelerated under controlled laboratory conditions. The measurements indicated that the silver layer on solar cells is porous and that titanium interacts with the chemical solutions.

Rest potential measurements were not useful for predicting solar cell degradation behavior as first thought, and did not yield much information about the degradation process. However, rest potentials of solar cells, when compared with those of silver and silicon in the same solution, again suggested that titanium interacts with the solution.

Exposure of solar cells to chemical environments ranging from strong acids to strong bases produced eventual degradation except in one instance. Calculations showed that surface oxidation of even 50 Å of titanium generates enough hydrogen and pressure to create blisters in solar cells. The hydrogen is generated fast enough to form blisters before it can diffuse away from the blister site. An internal pressure high enough to blow the water out of the pores is unlikely.

As contact degradation progressed we observed that: (1) new blisters appeared with the passage of time, (2) old blisters grew to random sizes and then stopped growing, with no relation to final blister size or to time, and (3) silver peeled away in areas where no blisters appeared.

The presence of fluoride and chloride ions, even in small concentrations, accelerated degradation. However, contacts free of halogen contaminants also degraded in humid atmospheres.

We observed that blisters are not necessarily accompanied by changes in the solar cell current-voltage (I-V) curve, hence an I-V curve is not a good indicator of degradation. Blisters tend to first form at cell edges, and with further degradation appear in the contact interior. This was attributed to exposed titanium at cell edges. Blisters are less likely to form on the sun-facing side of the cell, and this side usually exhibits silver separation first. The narrow grids allow hydrogen to escape easier, and expose more titanium to the atmosphere because of edge effects.

Studies of titanium corrosion in fluoride solutions showed that normally passive titanium will actively corrode in one-normal solutions of pH of 5 or less. The data indicate that active corrosion occurs in even more neutral fluoride solutions at elevated temperatures. Polarization data at room temperature showed no active corrosion at $\mathrm{pH} > 6$ while other data indicated that fluoride solutions with $\mathrm{pH} > 6$ enhanced degradation of solar cells. Calculations showed that the expected corrosion currents are too low to be measured by our polarization equipment, possibly explaining this disagreement. A second possibility is that the thin film of titanium in solar cells behaves differently than the thick films used in the polarization studies. Titanium dissolves in the fluoride solutions by the probable reaction: $\mathrm{Ti} + 6\mathrm{F}^- \rightarrow \mathrm{TiF}_6^{=} + 4e^-$. There was also evidence of Ti^{+3} in the solutions.

Similar polarization studies with chloride ion solutions at room temperature produced no visible corrosion. Again, either the corrosion currents are below the sensitivity of our instrument, or the thin film of titanium in a solar cell is highly reactive towards these solutions. Coupling of titanium with platinum, a noble metal, reduced the corrosion rate of the titanium in the presence of fluoride ion but did not halt it.

Present day (1970) solar cells consistently degraded when exposed to high humidity. Degradation behavior varied; some cells had no blisters, yet silver separated; some contacts blistered, others did not; in some silver separated only along edges, in others all over. Some cells showed signs of resistance to electrical degradation as seen on I-V curves, yet had silver separation, indicating that the useful life of the cell was reduced. Most cells degraded on the critical sun-facing side of the cell.

The major conclusions about humidity degradation of solar cells with silver-titanium contacts are:

- In a humid atmosphere moisture will rapidly condense by capillary condensation in the silver layer of the solar-cell contact whenever a critical humidity is exceeded. The degree and nature of the silver porosity depends on many factors in contact manufacturing such as substrate temperature, deposition rates, and vacuum.
- Titanium and titanium hydride very likely react electrochemically with the condensed water producing titanium oxide and hydrogen as observed by others (Ref. 1, 16). The oxides formed are probably non-protective and allow further degradation to occur.
- Elevated temperatures accelerate the degradation process.
- Solar cells and the condensing moisture contain varying amounts of halide ions (F^- and Cl^-) which accelerate solar-cell contact degradation.
- CO_2-containing atmospheres are acidic, enhancing the corrosion of titanium.
- Contact of solar cells with an aqueous solution has the potential of promoting contact degradation.
- Exposure of all present-day (1970) solar cells with silver-titanium contacts to $\sim$ 100% relative humidity caused contact degradation.
- I-V curves by themselves are not good indicators of solar cell degradation.

Based on the results obtained in this research we make the following recommendations:

Immediate

- Continue solder dipping the solar cells. The layer of solder, about 25 microns thick, or eight times the thickness of the typical three micron silver contact, is an adequate barrier against moisture penetration.
- Continue storing of solderless cells in a dry atmosphere. Note, however, that the condensation process is relatively fast ($<$ 24 hours) once the critical humidity is exceeded. Also, there is always the possibility of moisture entering the contact during handling, cleaning of the cell surface, attachment of cover glasses, and other processes taking place during assembly of arrays from the individual cells.

Near Future

- Solar cell manufacturing processes should be reviewed with the objective of reducing contamination by halogens which accelerate the degradation. Humidity should be controlled in manufacturing and storage areas. The purity of water and other chemicals used in cell manufacturing should be controlled.

- In applications where the 5 to 20% extra weight of solder-dipped cells cannot be tolerated, the silver-palladium-titanium contact devised by AEG-Telefunken (Ref. 11) can be used. Initial tests of these cells have been encouraging with respect to stability in humid atmospheres. It has been shown however, that alloying with noble metals reduces the corrosion rate of titanium but does not halt it. A "dirty" titanium-palladium-alloyed solar-cell contact which was contaminated with fluoride could conceivably corrode in an acidic atmosphere. There remains unanswered the question of whether there is sufficient reduction in corrosion rate of the silver-palladium-titanium contact to provide contact integrity for the desired lifetime of the cell. The use of palladium as a separate diffusion barrier layer to prevent water from reaching the titanium film would be more effective than the titanium-palladium alloy. Optimization and testing of such a contact would be needed.

- Replace the porous silver with a non-porous layer, such as gold. Gold is commonly used to achieve ohmic contacts to semiconductors. It also has the advantage that it does not oxidize as readily as silver.

Long-Term

- The humidity problem with silver-titanium contacts comes from the presence of the very reactive titanium layer. Replacing this layer with a non-reactive substance would eliminate the problem. In the semiconductor industry silver-titanium contacts have not been used for many years. Present day technology relies on newer contacts such as gold-platinum or aluminum. Gold-platinum forms a strong, ohmic contact of the type needed in solar cells (Ref. 32, 33). The platinum is sputtered onto the silicon and transformed to platinum silicide by heating. Because platinum is quite expensive, the sputtering technique uses directional bombardment to reduce waste. We recommend that eventually the solar cell contact be of a type such as gold-platinum.

2.0 INTRODUCTION

Silver-titanium ohmic contacts have been applied to recent American solar cells by a process described in a patent awarded to Lepselter in 1963 (Ref. 1). Silver alone will not make a good mechanical contact with silicon into which dopants have been diffused to form a junction. Use of an active metal such as titanium between the silver and silicon results in a good mechanical and ohmic contact. A typical contact consists of about 1000 angstroms (Å) of titanium and three microns of silver evaporated onto the silicon, and subsequently sintered for several minutes at 600°C. Oxidation of some of the titanium during sintering reduces the naturally occurring silicon oxide, enabling the titanium to bond solidly to the silicon. The resulting structure (Figure 1) provides a low electrical resistance connection and an adherent mechanical bond.

The first silver-titanium contacts were coated with solder to simplify interconnecting individual cells into an array. The solder coating increased the weight of the solar cells, so cells with solderless silver-titanium contacts soon became popular.

In 1967 at the 6th IEEE Photovoltaic Specialists Conference several papers described degradation of solar cells with these solderless silver-titanium contacts following storage in humid atmospheres at room temperature. Elevated temperatures were said to accelerate the degradation. This degradation appears in the form of hydrogen containing (Ref. 2) blisters on the contact area as shown in Figure 2. Further degradation reduces output power as seen in the current-voltage (I-V) curve of an illuminated cell (Figure 3). Peeling of the back contact and grid lines can occur in the final stages of degradation (Figure 4).

Humidity testing produced confusing results. Cell behavior varied from vendor to vendor and even from batch to batch from a single vendor (Ref. 3, 4). The Boeing Company was therefore contracted by NASA Headquarters (Contract NASW-1859) to determine the fundamental mechanism that degrades solar cells with silver-titanium contacts. The results of that study are presented in this report (Ref. 5, 6).

It is appropriate to note other work on the subject of contact degradation. 3M (Ref. 7, 8, 9), Texas Instruments (Ref. 2, 10), and AEG-Telefunken (Ref. 11) conducted similar research. Their results, along with unpublished data from other groups, are discussed in this report whenever pertinent to the theory of solar cell contact humidity degradation.

Important contributions to this study have been made by Dr. T. R. Beck of the Boeing Scientific Research Laboratories who acted as consultant, and W. F. Springgate who directed early phases of the work.

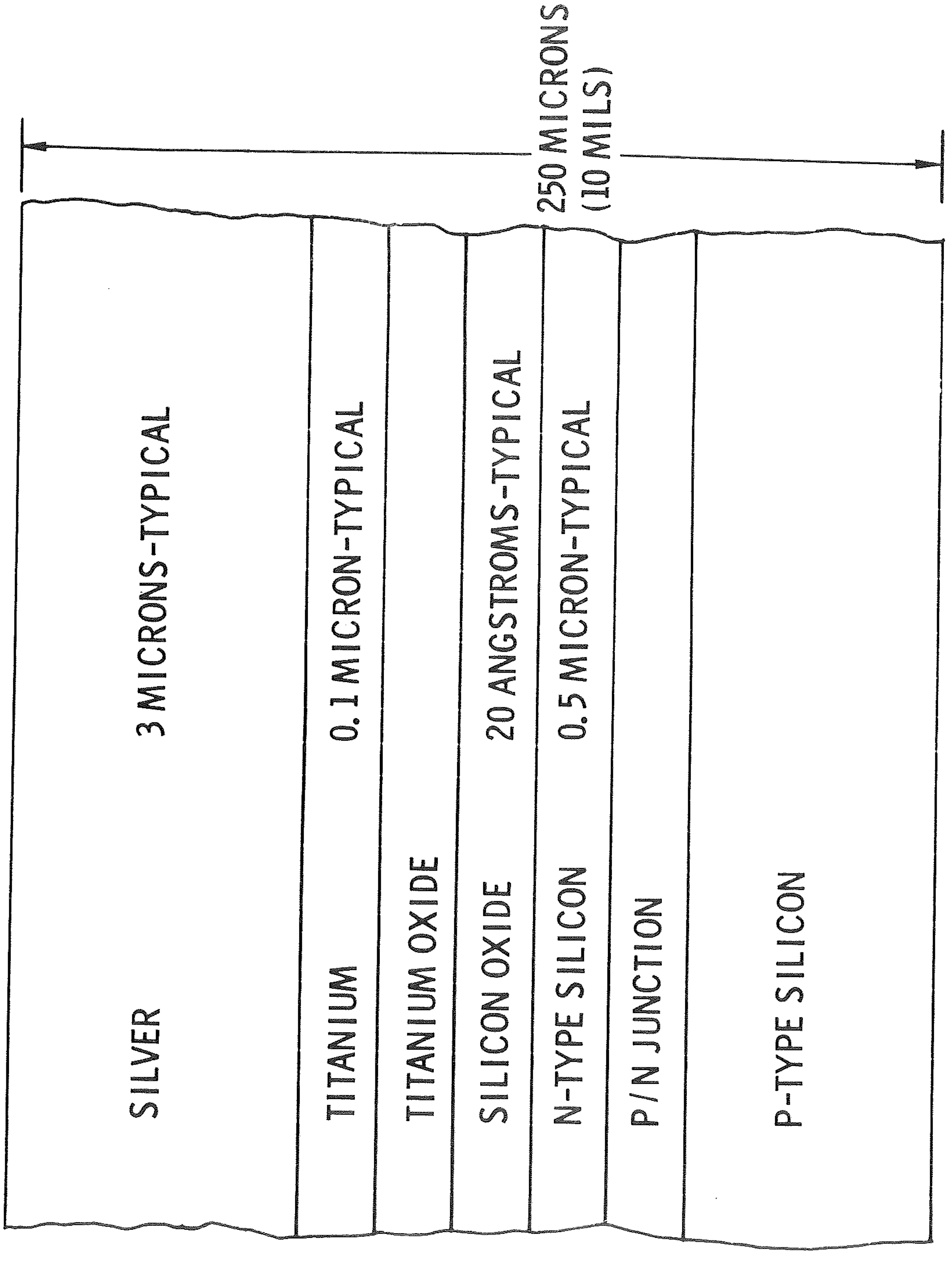

NOT TO SCALE

Figure 1: SOLAR CELL COMPOSITION

Figure 2: BLISTERED BACK OF SOLAR CELL

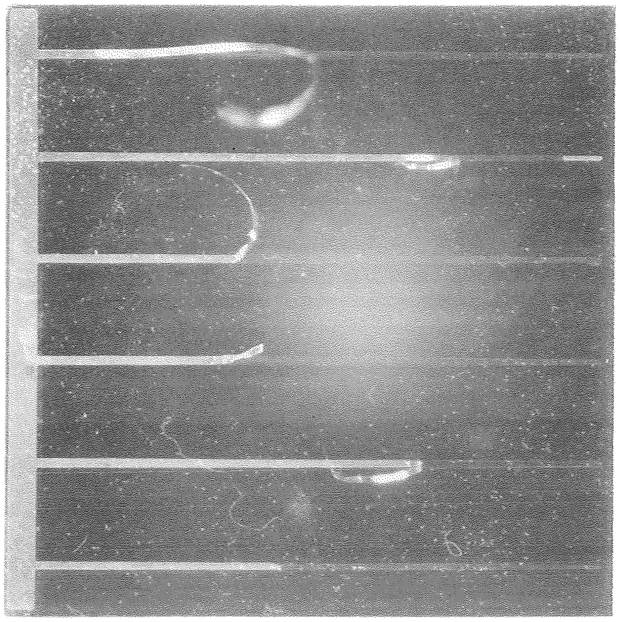

Figure 4: PEELING GRIDS ON A SOLAR CELL

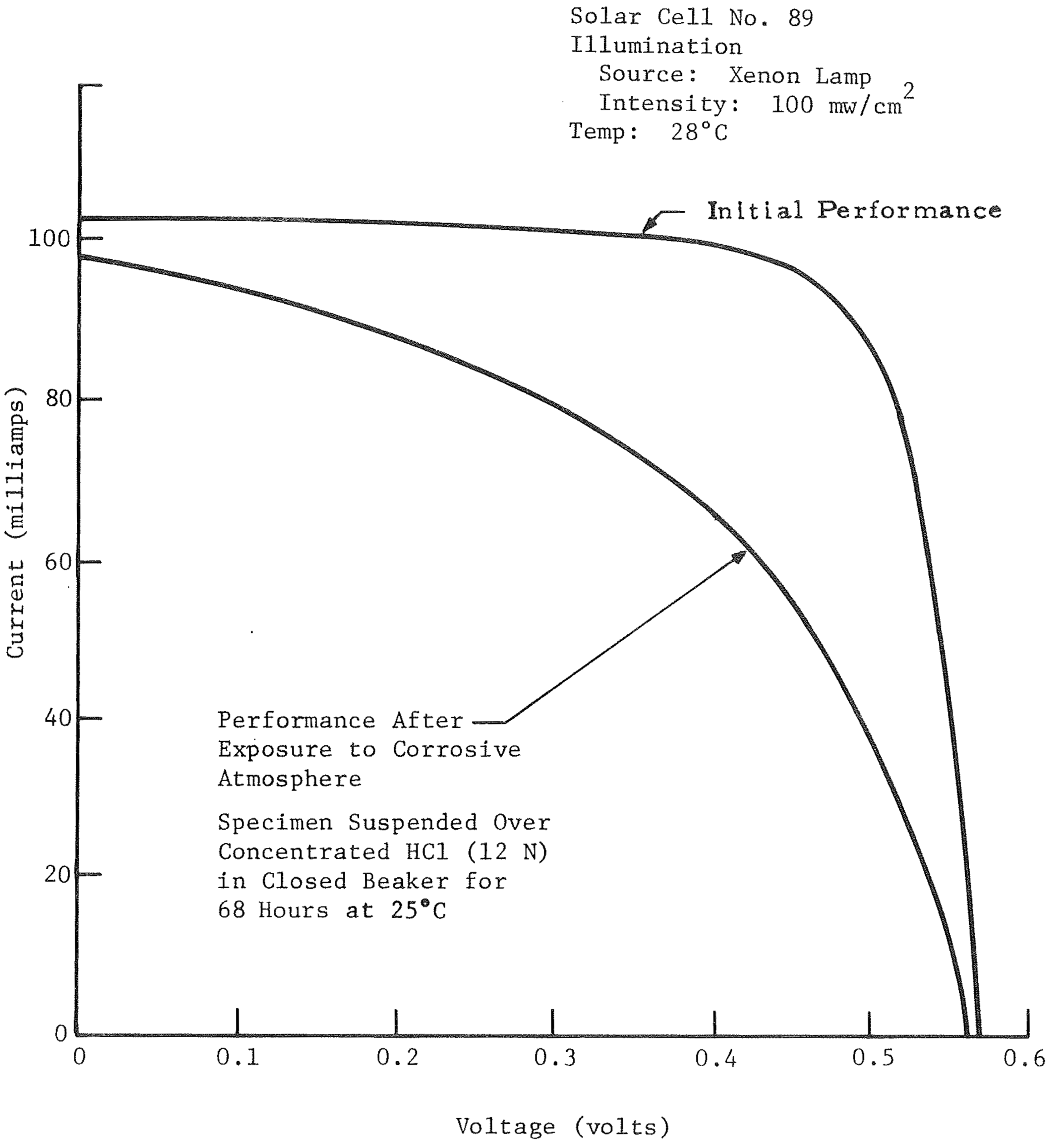

Figure 3 : PERFORMANCE DEGRADATION OF A SOLAR CELL

3.0 TECHNICAL ACHIEVEMENTS

Two theoretical models have been postulated to explain the degradation mechanism (Ref. 5). Model I involves the diffusion of atomic hydrogen through the silver layer to the titanium-silver interface where combination into molecular hydrogen occurs, giving rise to blisters. The second model postulates capillary condensation of water in the silver layer with subsequent electrochemical corrosion of the titanium via the reaction:

$$Ti + 2H_2O \rightarrow TiO_2 + 2H_2\uparrow$$

A coordinated program of chemical and physical measurements was used to characterize the degradation mechanism in the cells. In this section are described the individual experiments performed and the results obtained.

Present day solar cells degrade erratically (Ref. 3, 4) and manufacturing processes change from time to time. For these reasons we chose to study solar cells already at Boeing which showed a previous history of rather consistent contact degradation. These solar cells, which were used in most of the tests, were standard N-on-P cells, 2 by 2-cm, 8 mils thick, and had a resistivity of 1 to 3 ohm-cm. They had been manufactured before 1967 by Heliotek and will be referred to as "LASA" cells. Solar cells and silicon blanks manufactured with today's methods were later obtained from Centralab and Heliotek. We thank Mr. K. S. Ling of Centralab and Mr. E. L. Ralph of Heliotek for providing these new cells and blanks.

We did most of our experimental work on the solar cell back contact which, because of its size, was easier to study. The grids on the sun-facing surface of the cell are produced in the same way as the back contact, hence our conclusions can in general be extended to the grids as well.

3.1 Physical Measurements

Characterization of the solar cell surface, its constituents, and its behavior during the degradation process is a key to understanding the degradation mechanism. Degraded and undegraded solar cells and silicon wafers were examined with optical and electron microscopy, X-ray diffraction, mass spectroscopy, and internal reflection spectroscopy.

3.1.1 Optical and Electron Micrographs

Optical micrographs of the sun-facing and back surfaces, taken with a 5 MM metallograph having a 400-watt Xenon light source, are shown in Figures 5, 6, and 7 for LASA, present Centralab, present Heliotek solar cells. Sun-facing areas of all three cell types appear similar except for small differences in grid length and bar contact width. Views of the back contact (Figures 5 and 7) show a mottled surface with "grain-like" characteristics in Heliotek's LASA and present day 1970 cells. The notch in Figure 7 was for identification.

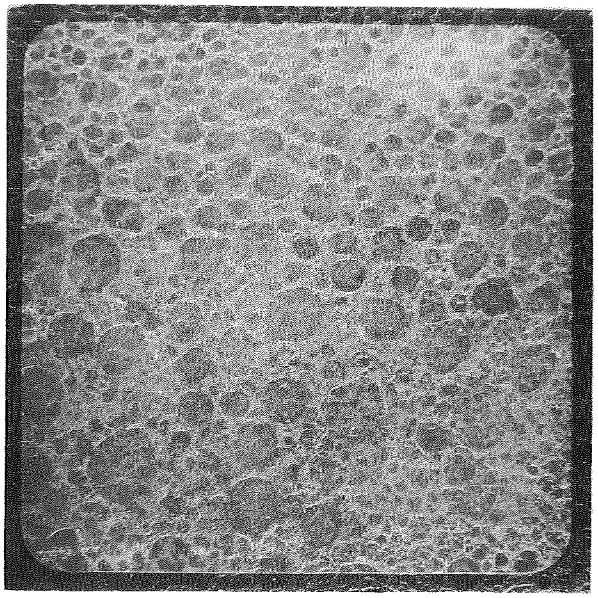

Back Contact

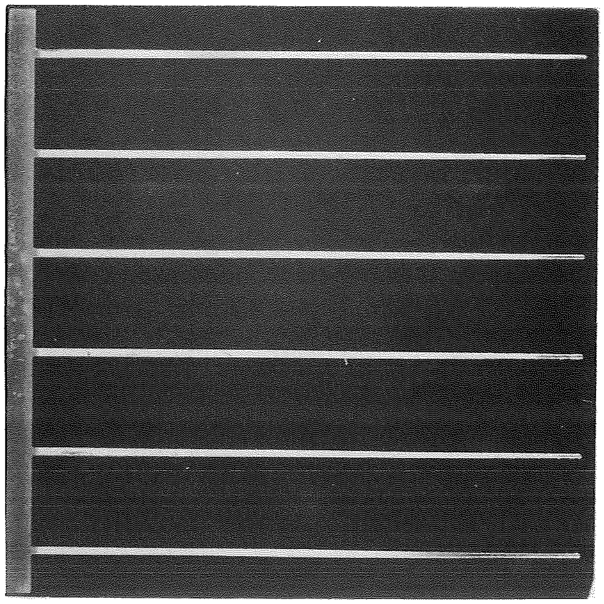

Front Contact

Figure 5 : HELIOTEK SOLAR CELL (LASA)

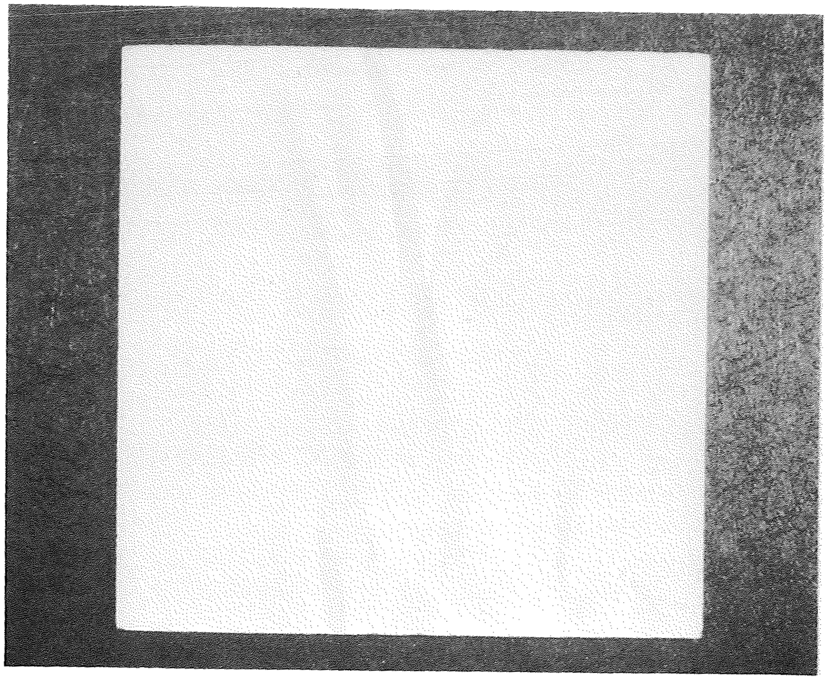

Back Contact

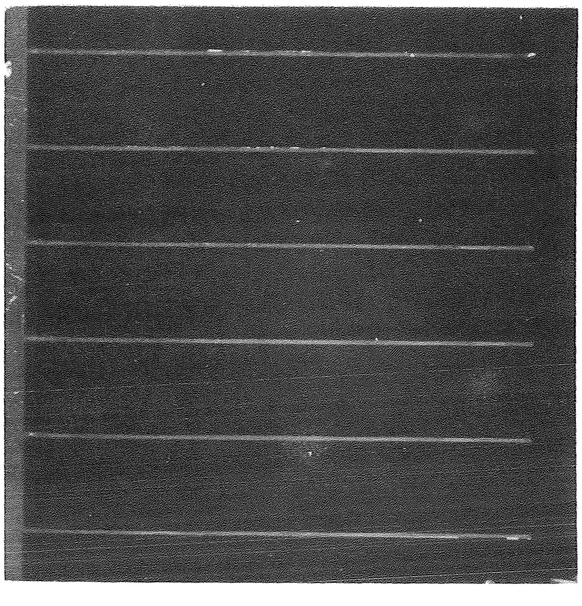

Front Contact

Figure 6: CENTRALAB SOLAR CELL

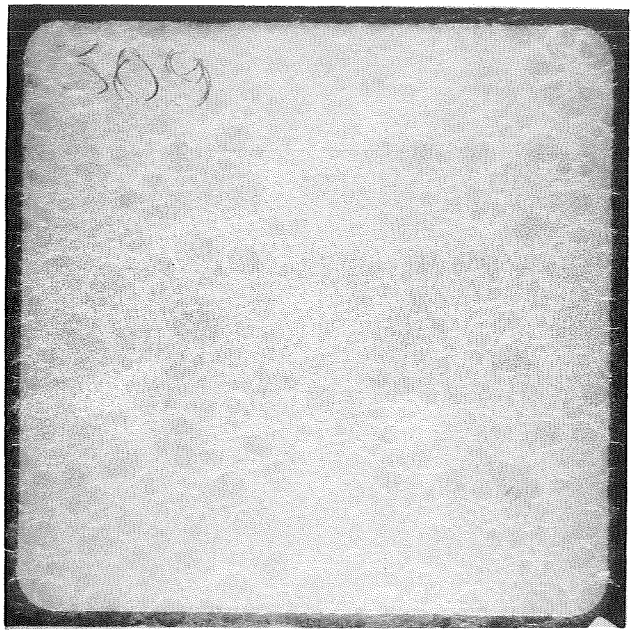

Back Contact

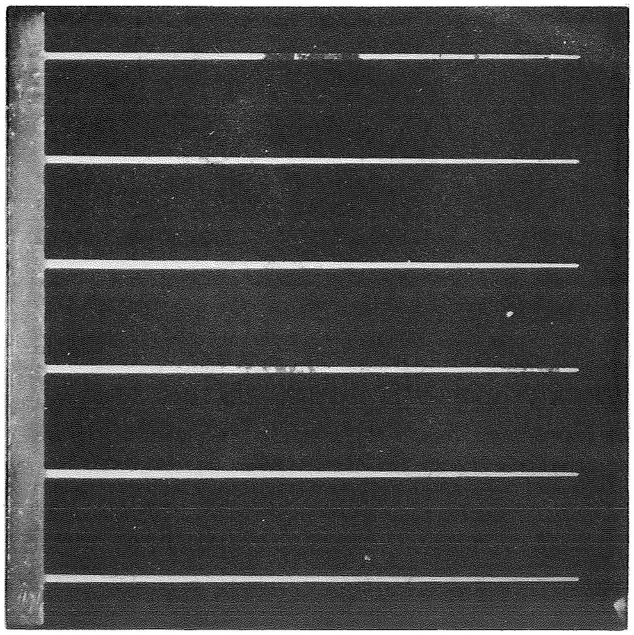

Front Contact

Figure 7: HELIOTEK SOLAR CELL

Examination of the mottled surface at a higher magnification shows a series of plateaus with no grain boundary (Figures 8 and 9). In particular, Figure 9 shows a continuous surface pattern through a ridge that has a grain boundary appearance at low magnification. The blisters were observed to be located at these plateau boundaries. A metallographic cross section of a solar cell shows rather sharp steps in the silicon substrate, supporting the contention that the apparent grains are substrate plateaus (Figure 10).

The fine grain structure observed optically is well delineated by electron microscopy, using a JEM 7 (JEOLCO) microscope at 80KV. The replicas were prepared by a two stage technique using acetate tape for replicating, and germanium and carbon for shadowing. The boundaries appear to contain a precipitate, and small pores are prevalent within the grain (Figures 11, 12, 13). We believe that the pores are thermal etch pits generated during sintering.

To resolve the question of whether the mottled surface is a characteristic of the silicon, samples of silicon wafers taken from the processing line prior to deposition of the silver-titanium contact were obtained from Heliotek. Micrographs (Figures 14 and 15) show that the mottled surface appears also on the blank. This type of mottling is generated in the chemical etching process which is used by Heliotek. It is commonly called "orange peel" and is characteristic of hydrofluoric (HF) etchants. Its appearance depends on buffering and temperature of the etchant solution. Lapping of the wafer with a mild abrasive at an angle of 5° (Figures 16 and 17) shows the uneven structure created by the etching process. The mottled surface seen on the backs of completed solar cells is obviously due to the silver simply transmitting the contours of the silicon substrate.

The micrographs show differences in manufacturing methods used by the two solar cell suppliers. Figure 18 shows the back contact of a Centralab solar cell. The silver has an entirely different appearance. Lapping of Centralab silicon blanks (Figure 19) shows a different type of structure which results from Centralab's different processing. Other silver-layer variations result from differences in the vacuum used, deposition rate of silver, substrate temperature, and other factors. The micrographs show no evidence of large pores that can transmit water. Micrographs indicate the "etch pits" which appear in some micrographs (Figure 13) are approximately 300 Å in diameter, whereas the thickness of the silver layer is typically 30,000 Å, making it unlikely that the etch pits go all the way through the contact.

The important conclusions from the micrograph work are:

- The mottled surface of Heliotek cells is not from true grains of silver, but rather results from the silver layer transmitting the contour of the silicon substrate.
- No evidence for a porous silver layer was seen. Any porosity, if it exists, is therefore of smaller size than could be detected by electron microscopy.

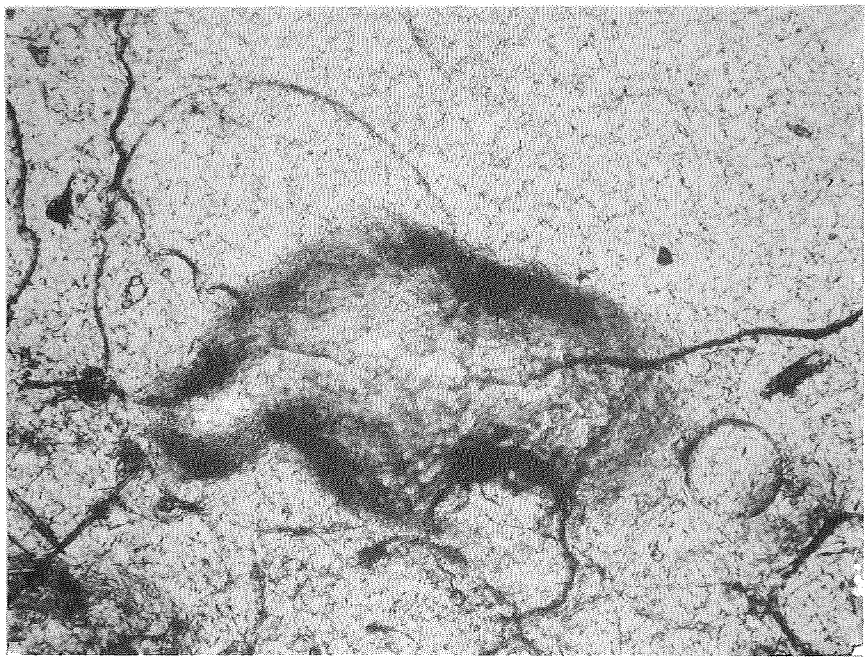

Figure 8: BLISTERED AREA(200X)

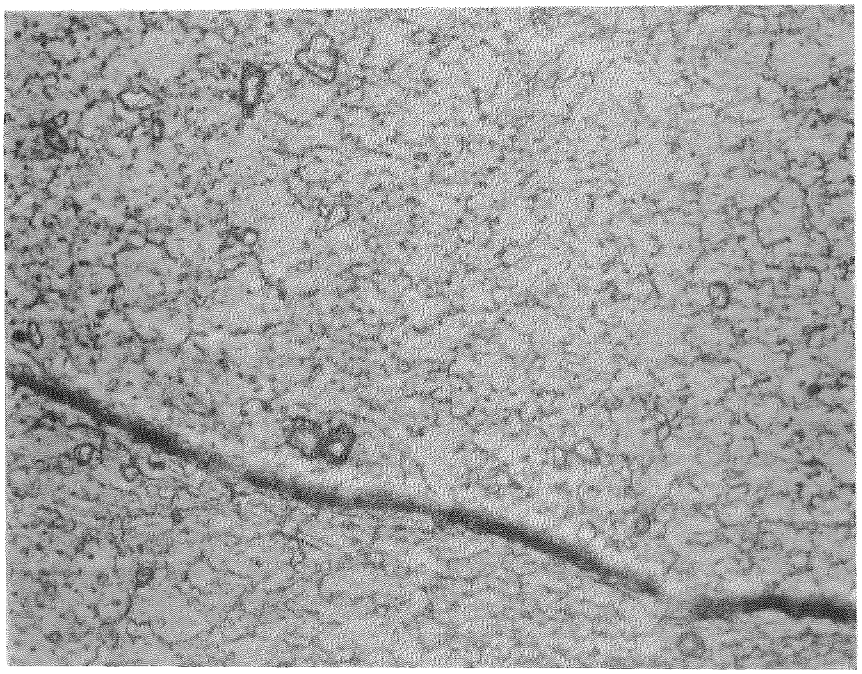

Figure 9 : CONTACT SURFACE (500X)

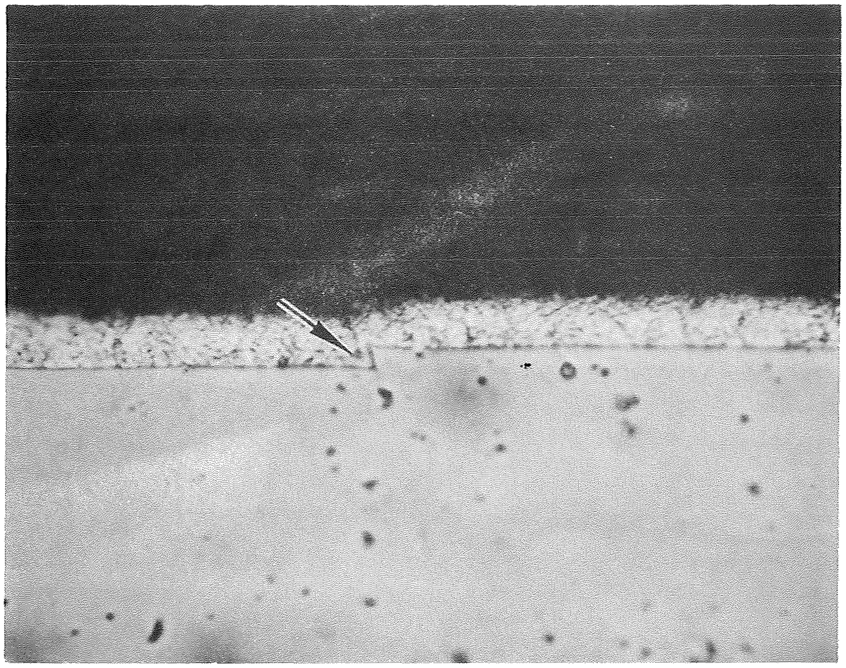

Figure 10: METALLOGRAPHIC PROFILE OF CELL CROSS SECTION (1400X)

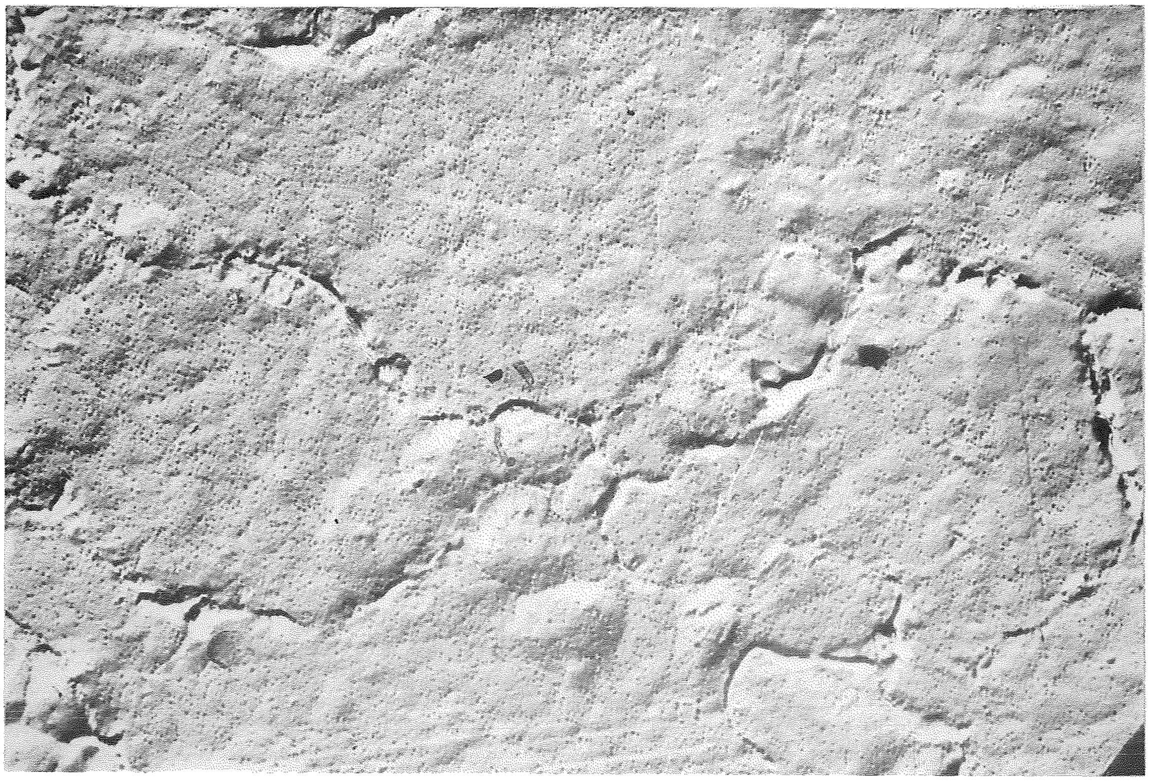

Figure 11: ELECTRON MICROGRAPH (8000X) OF CONTACT SURFACE

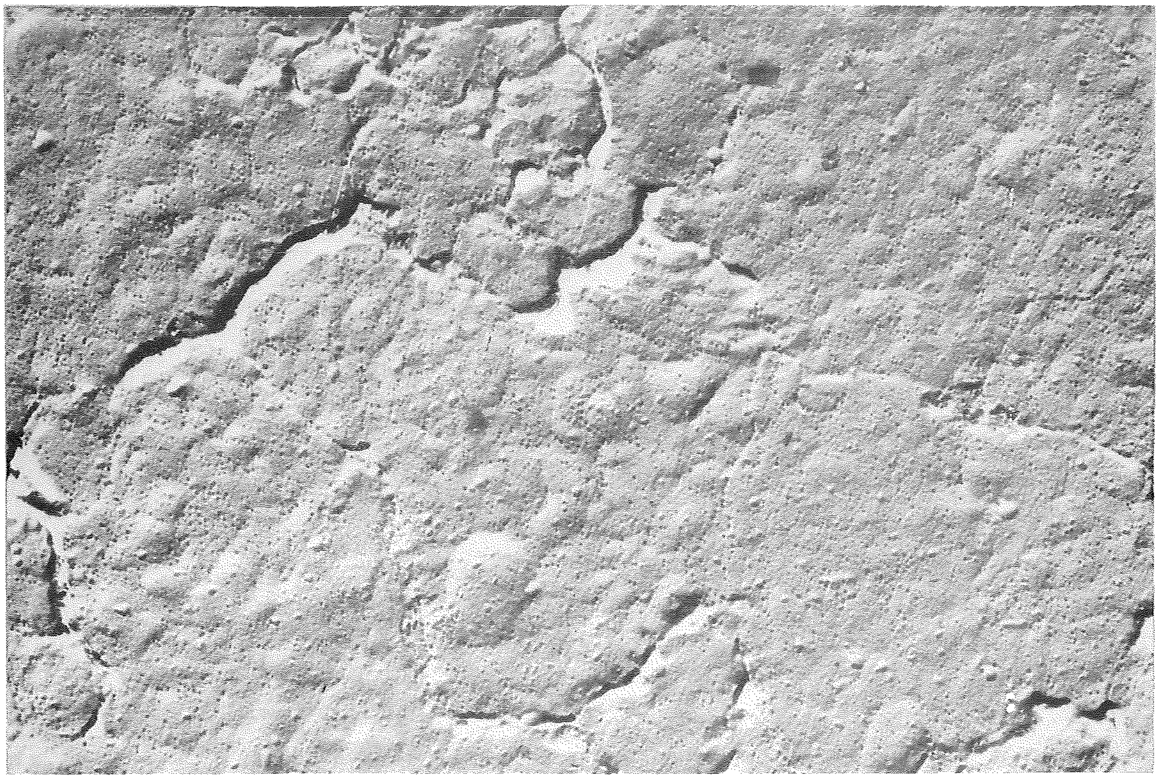

Figure 12: ELECTRON MICROGRAPH (8000X) OF CELL CONTACT

Figure 13: ELECTRON MICROGRAPH (31000X) OF CELL CONTACT

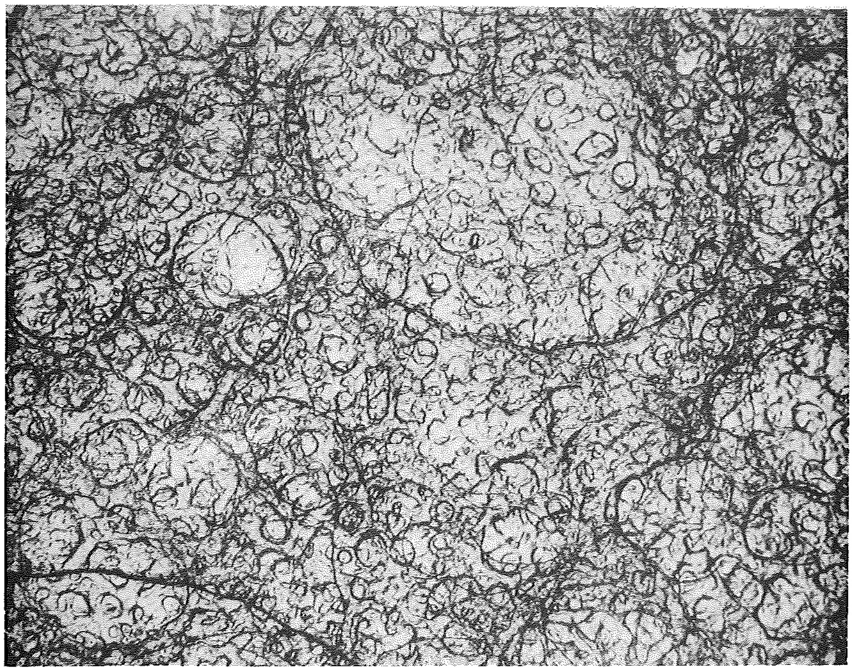

Figure 14: SILICON WAFER PRIOR TO DEPOSITION OF CONTACTS (45X)

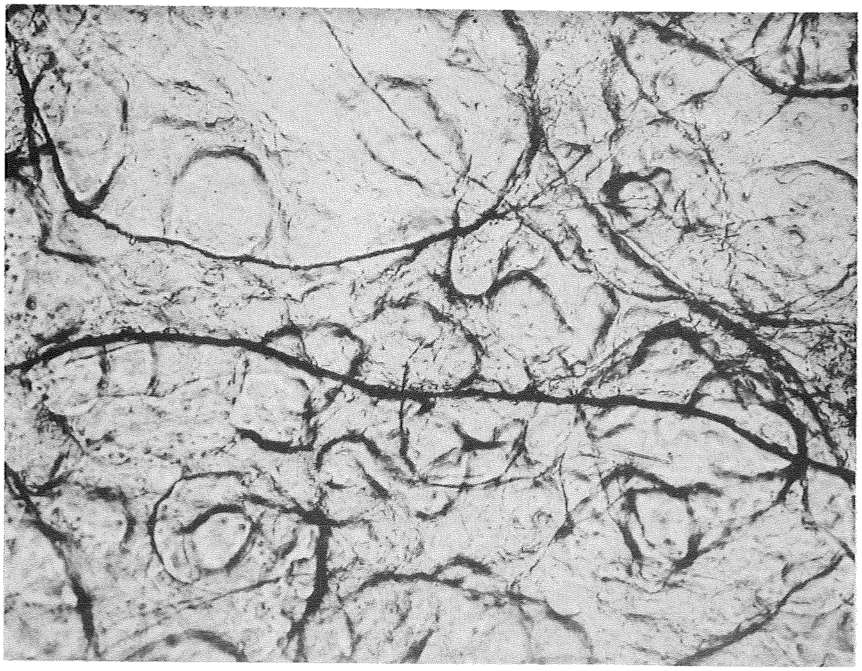

Figure 15: SILICON WAFER PRIOR TO DEPOSITION OF CONTACTS (200X)

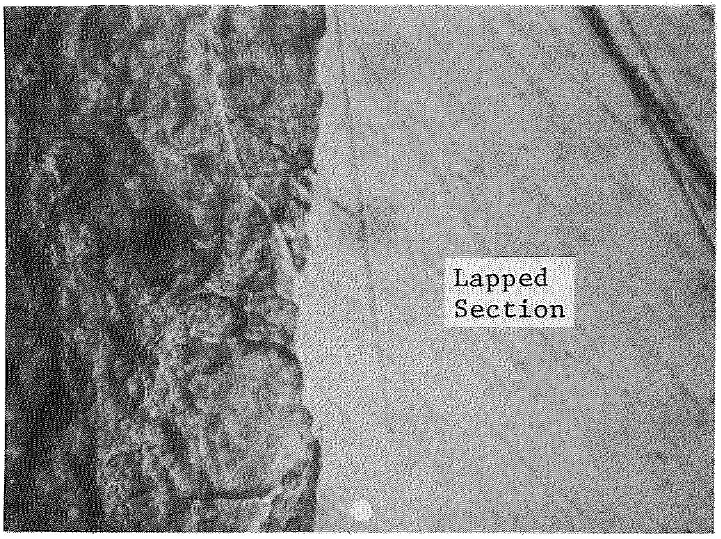

Figure 16: BEVELLED SILICON WAFER (143X)

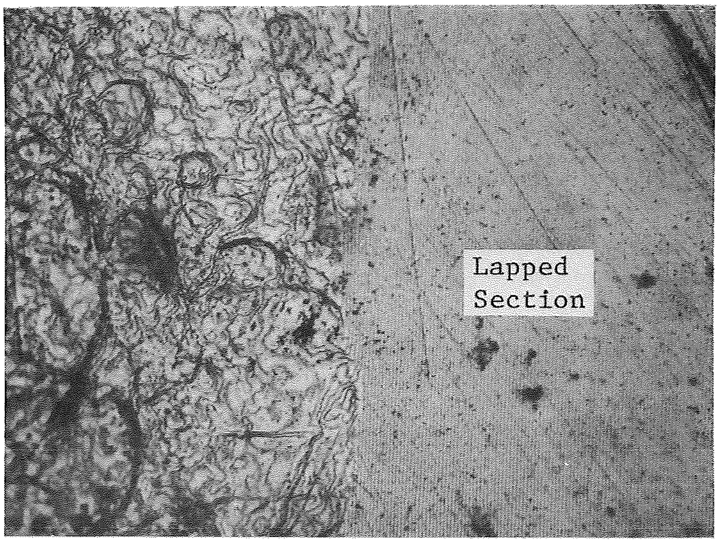

Figure 17: BEVELLED SILICON WAFER (143X)

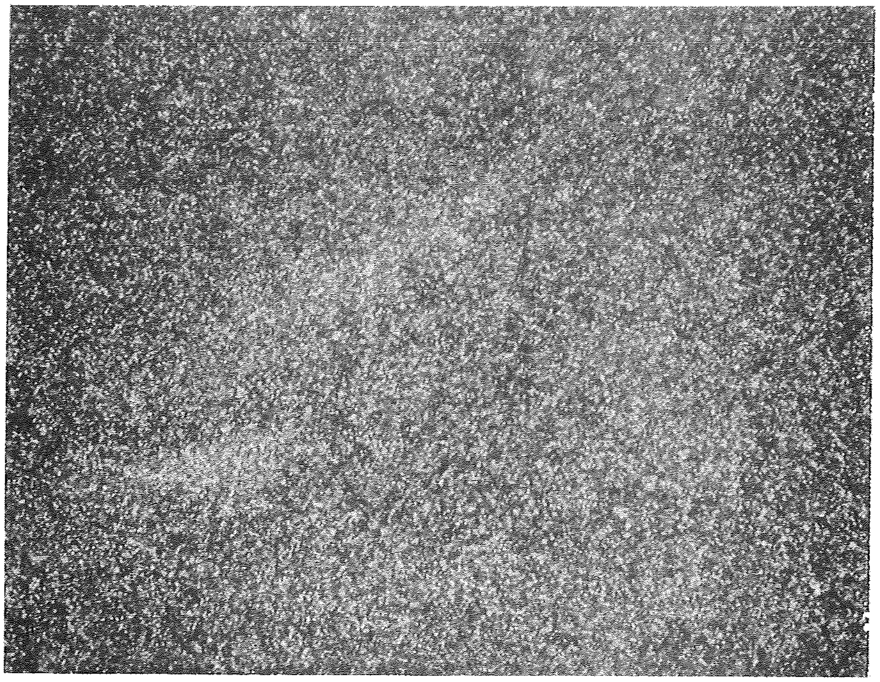

200X

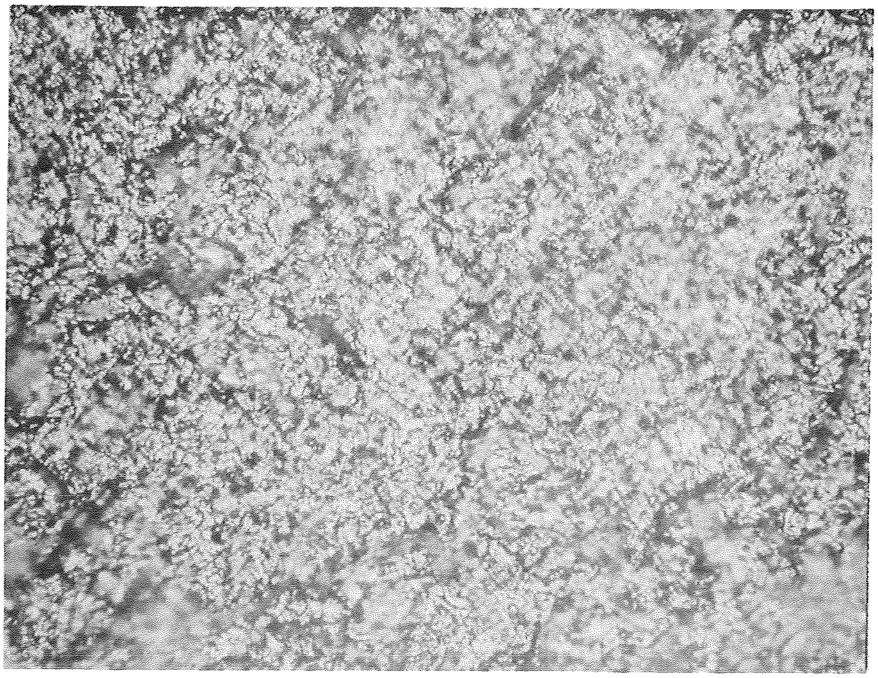

750X

Figure 18: CENTRALAB SILICON WAFER---BACK SIDE

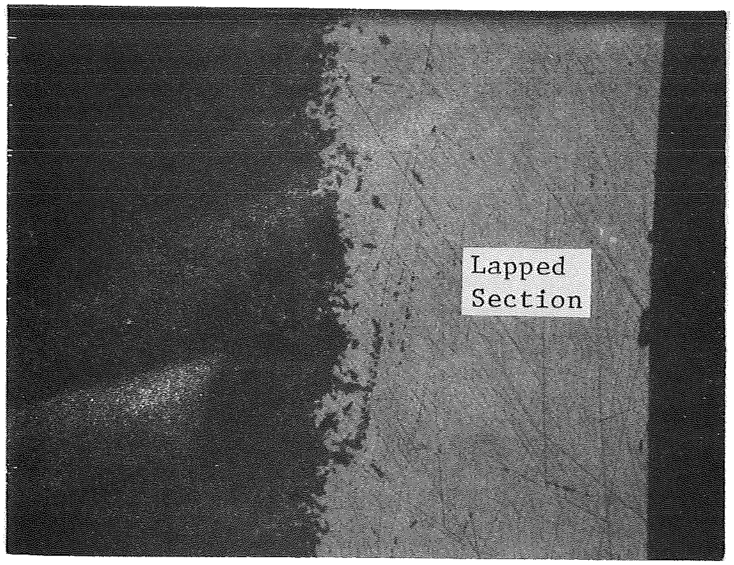

Figure 19: BEVELLED CENTRALAB SILICON WAFER (143X)

3.1.2 Mass Spectroscopy

Contaminants collected by a solar cell during manufacturing can affect the quality and degradation behavior of the finished cell. An excellent way to identify impurities in the solar cell is by mass spectroscopic analysis. For this work a spark-source mass spectrograph, CEC Model 21-110B, was used. Samples of complete solar cells and silicon wafers were analyzed. Tables 1 and 2 show the results of an analysis made on LASA and present day solar cells.

The results of the analysis show that even present day (1970) cells have many contaminants (Table 2). Most of the contaminants are readily explainable. Copper is an impurity in silver and also comes from evaporation of copper fixtures during contact deposition. Pb, Bi, W, and Zr are probably contaminants of the titanium and silver. Carbon may come from silicones used in masking or organic solvents used in cleaning. Some other species (CF_2, NH_3, CF) are due to recombination within the spectrograph.

Presence of fluoride and chloride ions is an important discovery. Halogens are noted for their ability to cause and/or enhance titanium corrosion (Ref. 12, 13). Thus their presence in solar cells may promote degradation. The fluoride ions come from the etching processes in which HF produces a surface with incomplete and porous oxide layers where fluoride and other ions can be trapped (Ref. 14). It is extremely difficult to obtain a "clean" surface after etching, even with careful washing. The chloride ion comes from subsequent handling of the product, or as impurities in titanium.

Non-uniformity exists from sample to sample and manufacturer to manufacturer, but care must be taken in interpreting these data in a quantitative manner. Differences in photographic processing and spark-produced crater shapes can introduce significant errors, but some general statements can be made. The Heliotek cell (Sample 1A and 2A are from the same cell) contains more titanium than the Centralab cell (Table 2). It is generally known that Centralab cells have more titanium, so this is surprising. The resistance method of monitoring titanium thickness used in manufacturing is not very accurate and may give rise to the observed differences.

The reason for the large variations in silicon content is due to variations in silver thickness or crater shape. Mass spectroscopic analysis is based on the collection of a specific number of ions (10^{-9} Coulombs for example). If the silver is thicker, then a larger fraction of the total charge is composed of silver at the expense of silicon which is the last layer to be analyzed. Crater shape variation can also alter the fraction of surface ions to bulk ions collected.

Silicon blanks which were ready for contact evaporation were obtained and analyzed (Table 3). Fluoride ion left from etching processes is evident even after elaborate cleaning processes.

Table 1: MASS SPECTROSCOPIC ANALYSIS (CONTACT OF LASA CELL)

Major 10,000 ppm	Minor 500-10,000 ppm	Lesser 10-500 ppm	Trace 1-10 ppm	Subtrace 1 ppm
Ag	Ti	F	B	S
Si	SiO	HO	P	NH_3
	SiO_2	H_2O	TiO	NH_4
		Cu	Cl	
		O	Pb	
		H	Bi	
		C	W	
			Zr	
			CF	
			CF_2	

Table 2: MASS SPECTROSCOPIC ANALYSIS (CONTACTS OF NEW CELLS)

	CENTRALAB		HELIOTEK	
	Sample 1A	Sample 2A	Sample 1A	Sample 2A
Silver	939,734 ppm	961,012 ppm	962,410 ppm	982,794 ppm
Copper	44	44	56	30
Titanium	1,138	1,310	9,460	5,300
Potassium	142	68	398	415
Chlorine	---	14	64	961
Oxygen	1,150	3,856	2,200	1,840
Aluminum	18	18	6	6
Silicon	47,500	21,886	25,350	10,400
Fluorine	9	7	15	17

Table 3: MASS SPECTROSCOPIC ANALYSIS (Silicon Wafers)

	HELIOTEK			CENTRALAB		
	Back		Front	Back	Front	
	Sample 1A	Sample 2A			Sample a	Sample b
Silicon	$\sim 10^6$ ppm	$\sim 10^6$ ppm	934,740 ppm	998,020 ppm	978,000 ppm	943,000 ppm
Oxygen	150	150	4,970	1,770	18,570	53,700
Potassium	15	300	190	160	639	750
Sodium	1-10	120	7	20	221	250
Phosphorus	4	1	3	--	247	35
Fluorine	20	500	0.1	1	26	20
Chlorine	1-10	260	--	--	177	7

Jacobson at 3M used Auger spectroscopy (Ref. 7) to study solar cell contaminants. His experiments, performed with Texas Instruments (TI) cells, did not show the presence of flouride ions. However, it was since learned that the Auger spectroscopic equipment was not capable of exploring the region where flouride ions are expected to appear (Ref. 15). Jacobson's results indicated the presence of some contaminants, namely boron or carbon and oxygen.

Becker, at the University of Pennsylvania, studied solar cell contaminants with an emission spectrograph (Ref. 16). He only looked for metals and reported trace amounts of Cu, P, Mn with the possibilities of Cd and Ca also being present. Neither Auger spectroscopy nor the emission spectrograph is as sensitive as mass spectroscopy, and contaminants in low concentrations could have been missed.

3.1.3 X-ray Diffraction

X-ray diffraction is an excellent way to determine the crystal structure of substances. We used X-ray diffraction in attempting to answer the following questions about solar cell contact degradation:

- Does the bond break at the silver-titanium or titanium-silicon interface?
- What is the form of the titanium on degraded solar cells?

Material scraped from the region of blisters on several degraded cells was analyzed with a Phillips Electronics 114.6 MM Debye X-ray diffraction powder camera. The results were inconclusive, indicating the presence of some compound(s) which resembles titanium but whose X-ray spectrum lacked certain characteristic lines for titanium or titanium oxide. The X-ray spectrum appeared to be caused by some amorphous substance with a tendency towards a cubic type structure. Titanium does not produce good X-ray diffraction patterns, having a tendency to appear amorphous. It is also possible that the grain size was so small that it caused the substance to appear amorphous.

3M had similar problems with X-ray diffraction studies. They likewise could see no evidence of titanium or titanium compounds in crystalline form when using either the forward/backward scattering technique or the powder camera method. They concluded that titanium was not necessarily absent, only that it did not exist in a well-defined state (Ref. 7).

We were able to locate the place where the contact separated with an electron microprobe. We peeled off the silver layer of a badly degraded solar cell and bombarded its back side with 30 KV electrons from an Applied Research Laboratory microprobe. The stripped solar cell itself was also analyzed. The characteristic X-ray from titanium was detected with a X-ray detector, the output of which was displayed on an oscilloscope. Photographs of the scanned samples are shown in Figures 20 and 21. White areas indicated the presence of titanium on the solar cell. The silver contact, on the other hand, had only a small patch of titanium present. Similar studies at 3M also indicated that peeled contacts contained only traces of titanium compared to the amount left on the cell. We thus conclude that the contact failure occurs at the silver-titanium interface.

It is appropriate to mention the electron diffraction work of Becker (Ref. 16), showing that undegraded cells contain varying amounts of Ti and TiH_2 whereas degraded cells had mainly TiO_2 in the anatase form. This oxide normally forms only under conditions where moisture is present. Under dry conditions TiO_2 will form in the rutile structure. This excellent evidence supports the degradation mechanism involving the reaction of titanium and water.

It is evident from our diffraction work that:

- The contact separates at the silver-titanium interface rather than at the titanium-silicon interface.
- X-ray diffraction methods are not sensitive enough to identify the nature of titanium films in solar cells.

3.1.4 Internal Reflection Spectroscopy

An important criterion for the proposed titanium corrosion mechanism is the ability of water to condense in the pores of the silver contact. Internal reflection spectroscopy offers a unique method of studying the porosity of silver to moisture.

Internal reflection spectroscopy involves the reflection of infrared radiation through single crystal silicon (Ref. 17). If the entering angle of incidence is greater than the critical angle, the radiation is internally reflected at the surface of the crystal (Figure 22). Material on the silicon surface will

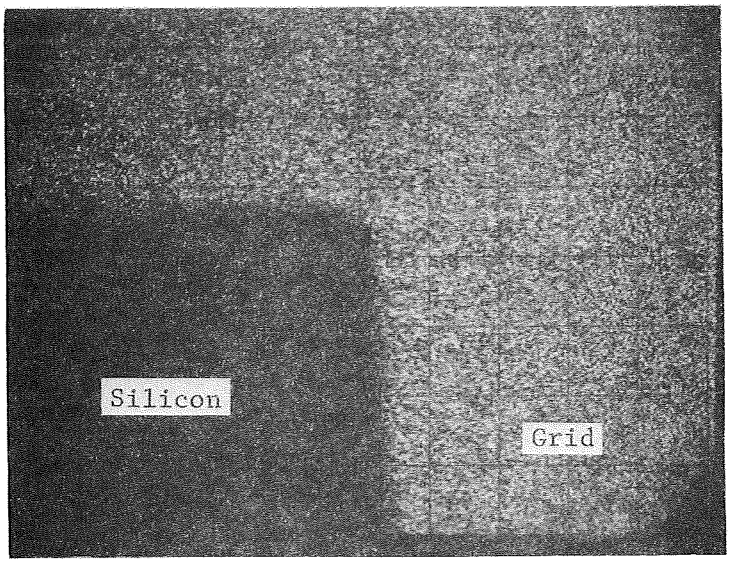

Figure 20: MICROPROBE PHOTOGRAPH OF CELL SURFACE WITHOUT SILVER CONTACT (200X)

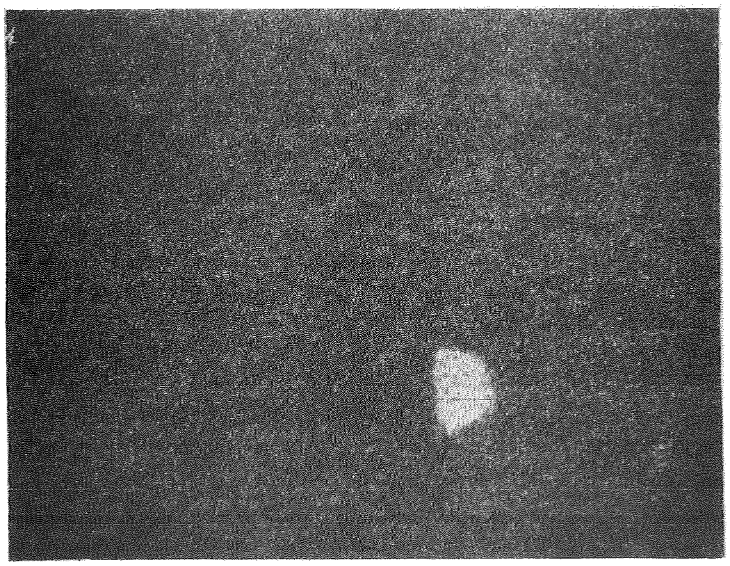

Figure 21: MICROPROBE PHOTOGRAPH OF PEELED SILVER CONTACT-BACKSIDE (200X)

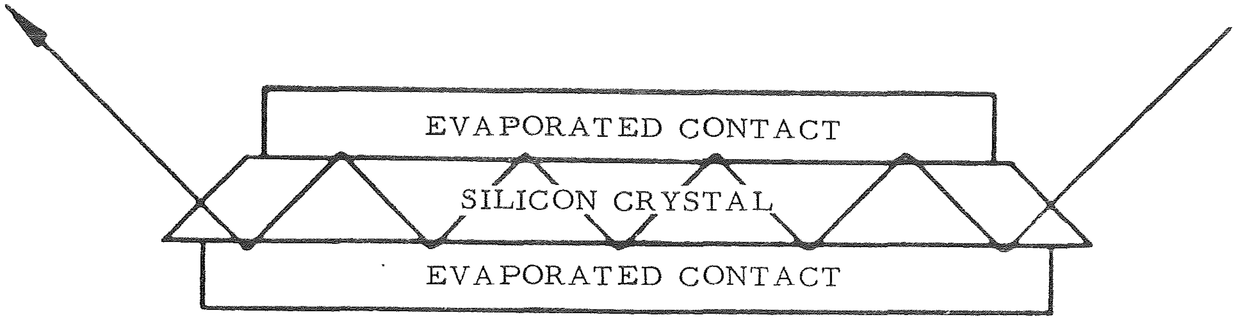

Figure 22: MULTIPLE INTERNAL REFLECTION EFFECT

selectively absorb radiation. Spectral transmission measurements will then give valuable information about chemical or physical changes occurring at the interface between silicon and a coating. The presence of water at the interface of the silicon and an evaporated sample will be indicated by a decrease in transmission (or increase in absorbance) in the region of 3400 cm^{-1}, the stretching frequency of the O-H bond in water (Figure 23).

Samples having three microns of silver evaporated on silicon wedges were prepared by the Boeing Microelectronics laboratory, Centralab, and Heliotek. Centralab and Heliotek prepared samples using the same methods employed in fabricating solar cells. Relative humidities (RH) of 32%, 52%, 75%, and 96% were initially chosen to test the hypothesis that there exists a critical humidity at which condensation occurs. Humid atmospheres were generated in a closed container using saturated salt solutions at room temperature as shown in Figure 24 (Ref. 18). Infrared transmission or absorption spectra were measured periodically.

The initial tests were made with the Boeing-prepared wedge. A spectrum taken after 48 hours in a 96% RH showed the presence of water (Figure 23), proving that the silver layer is porous to water. Others (Ref. 9, 11) had assumed that the silver layer on solar cells was porous but this is the first actual measurement of the porosity.

A silicon blank without contacts was placed in 96% RH for 144 hours to determine if adsorbed water on the silicon surface will absorb infrared radiation. Results (Figure 25) indicated no water adsorption, hence any water absorption which appears in the IR spectrum must be due to condensed water at the silicon-silver interface.

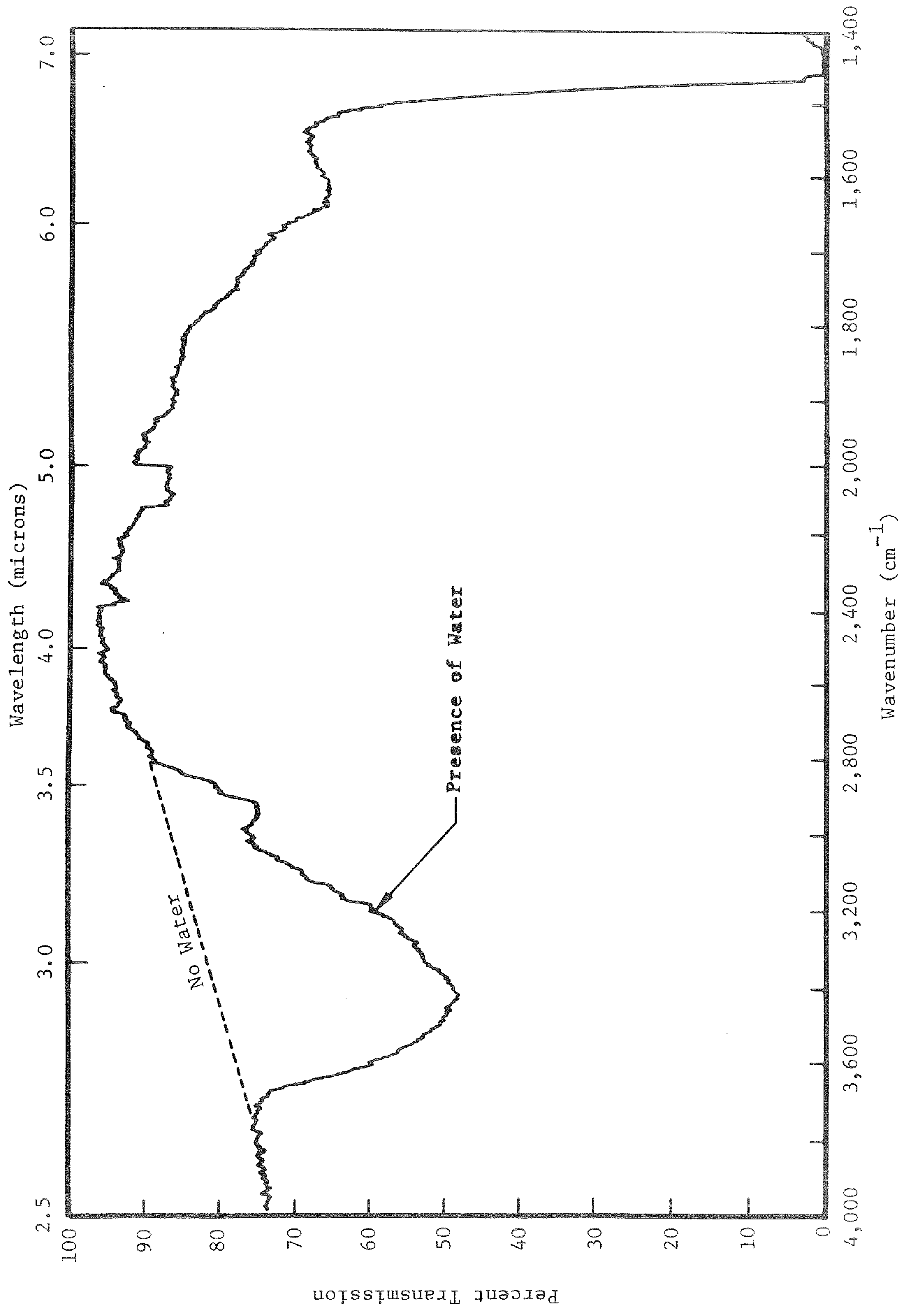

Figure 23: IR TRANSMISSION SPECTRUM

Figure 24: SPECIMEN IN HUMIDITY CHAMBER

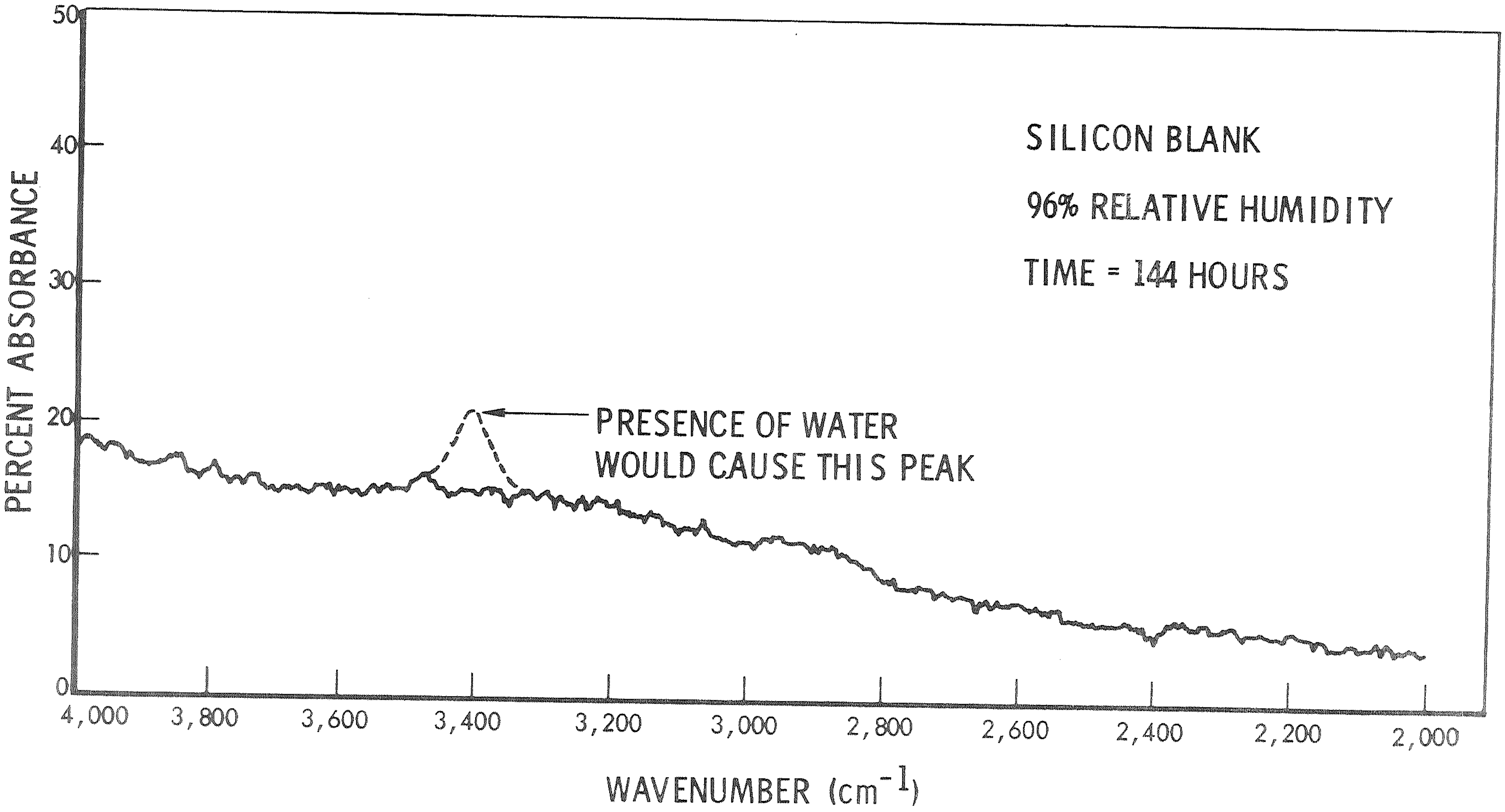

Figure 25: IR ABSORPTION SPECTRUM OF SILICON BLANK

The silicon wedge with Heliotek-made contacts was placed in 32% RH atmosphere for 168 hours, 52% RH for 168 hours, and 75% RH for 192 hours. No water absorption appeared in the IR spectrum. This sample was then placed in a 96% RH atmosphere, and water absorption appeared within 24 hours. The amount of water at the interface can be estimated quantitatively by subtracting the peak absorbance at 3400 cm^{-1} from an assumed linear background. Errors associated with absorbance readings are in the order of ± 0.005 units. The water content within the sample was seen to increase very slowly with time (Figure 26), indicating that the presence of water does not rapidly catalyze further condensation.

To study the condensation process further the sample was dried out in a vacuum desiccator. It was not possible to get it completely dry, an absorbance reading of 0.01 being the best we could achieve. We then placed the sample in an 81% RH atmosphere. Twenty-four hours later, the water content had increased. Transfer of the sample to higher humidities brought further increases in the water content (Table 4).

Table 4: INTERFACE WATER IN HELIOTEK SILVER-ON-SILICON SAMPLE

RELATIVE HUMIDITY	TOTAL TIME (hours)	WATER CONTENT (absorbance units)
32%	168	—
52%	168	—
75%	192	—
96%	24	0.03
	144	0.04
	168	0.05
DRIED	SAMPLE	(0.01)
81%	24	0.02
	148	0.025
85%	96	0.03
	288	0.03
91%	144	0.09
	216	0.11

The size of the capillaries needed to condense water at various humidities can be calculated using the Kelvin equation (Ref. 19):

$$RT \ln \frac{P}{P_o} = \frac{2\alpha V}{r}$$

where
R = gas constant = 8.314 x 10^7 ergs/deg mole
T = absolute temperature, °K (298°K for room temperature)
P = vapor pressure of water in pore, mm Hg
P_o = vapor pressure of water on flat surface, mm Hg
(P/P_o = relative humidity at which condensation will occur in a pore of radius r)
α = surface tension of liquid, dyne/cm (72 for water)
r = pore radius, cm
V = molar volume, cm^3/mole (18 for water)

The capillary sizes needed to condense water at various relative humidities are shown in Figure 28. Condensation occurring at 81% RH implies a minimum pore size of about 50 Å for the Heliotek sample. As the humidity is increased the water content at the interface increases more rapidly than an increase expected from a time factor (Figure 27) and implies a pore size distribution, the upper limit of which cannot be predicted by this method. Because the silver is typically 30,000 Å thick it is very unlikely that the porosity in silver is caused by individual capillaries which extend all the way through the sample. A more reasonable model is a "sponge" type structure which presents an average pore radius of 50 Å to the humid air.

Internal reflection spectroscopy with a Centralab-made sample brought quite different results. Initial infrared spectra before exposure to humid air indicated the presence of water, suggesting condensation at laboratory humidity (about 50% RH). The corresponding pore radius would be <15Å for such samples. The sample was dried in a vacuum desiccator reducing the water content to 0.02 absorbance. Introduction of the sample into 36% RH resulted in an increase in the water content to 0.045 after 144 hours. Increases in humidity brought increases in water content (Table 5).

A second silicon wedge with a contact made at Centralab and shipped with a desiccant to keep it dry behaved very differently from the first Centralab sample, as shown in Table 6. Water began to appear at the interface at 85% RH, and increased as the humidity was raised.

A silicon wedge with both 1000Å of titanium and three microns of silver was tested to see if titanium is also porous to moisture. Unfortunately the sample was not transparent to the infrared and no output signal was obtained. The wedge was stored in humid air to see if a change in chemical composition would alter the light absorbing characteristics of the sample. No change was observed in progressing from 32% RH to 96% RH and the test was terminated.

Four different samples were found to be porous to moisture. The porosity seems to vary from sample to sample. These results would explain the apparent dependence of cell degradation on humidity as reported by Springgate (Ref. 20). The fact that samples from the same source behaved quite differently suggests that there may be a day-to-day variation in silver porosity explaining the batch-to-batch variations in humidity degradation previously observed (Ref. 3, 4).

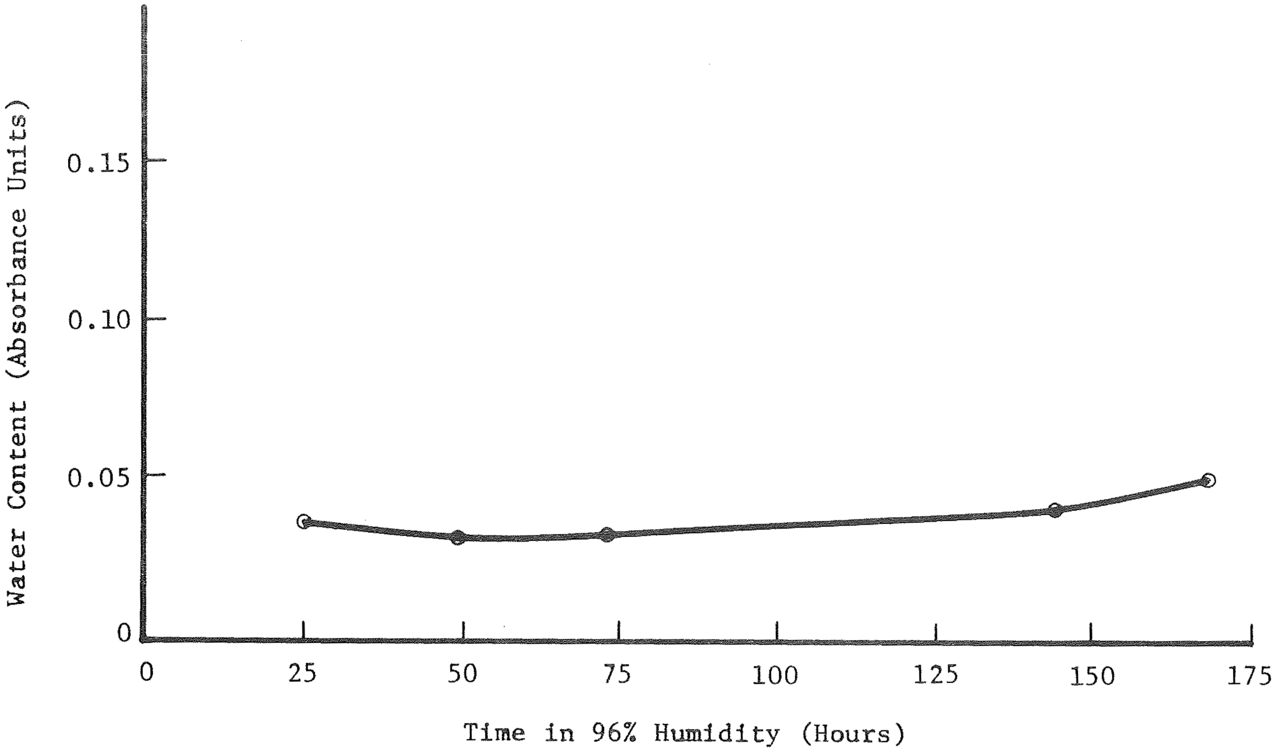

Figure 26: WATER BUILD-UP VERSUS TIME AT CONSTANT HUMIDITY

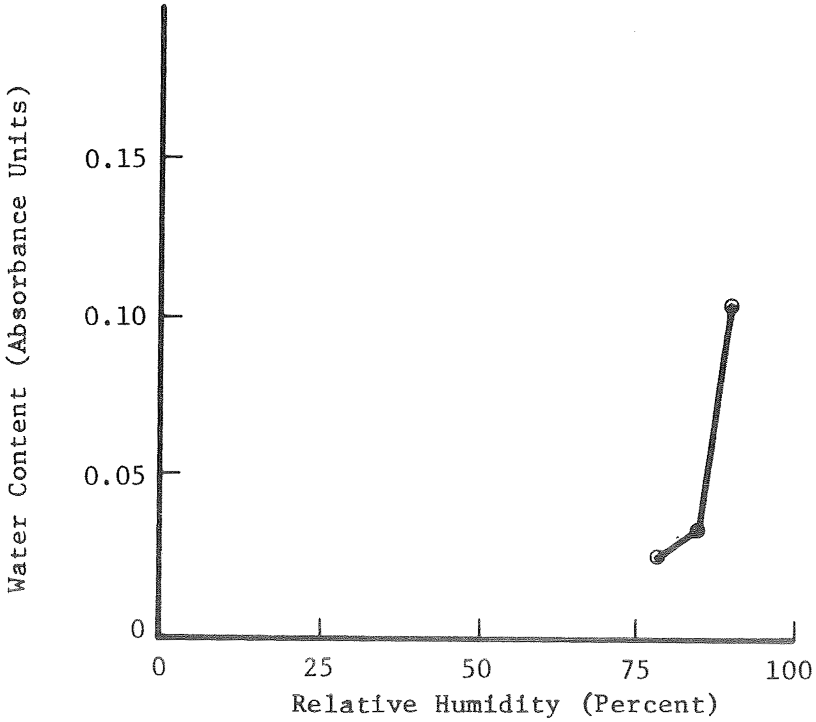

Figure 27: WATER BUILD-UP VERSUS HUMIDITY

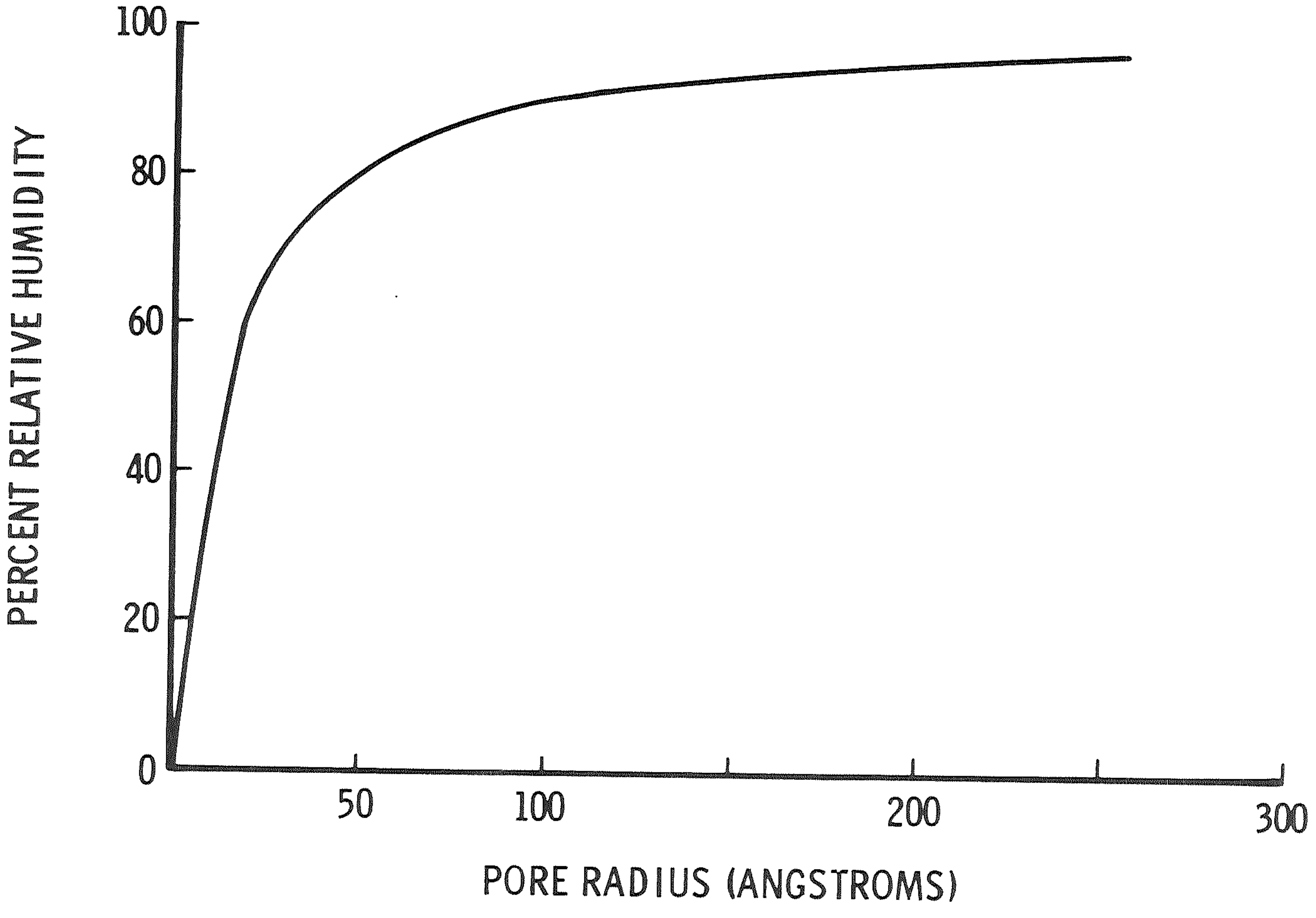

Figure 28: PORE SIZE REQUIRED FOR CAPILLARY CONDENSATION

Table 5: INTERFACE WATER IN CENTRALAB SILVER-ON-SILICON SAMPLE #1

RELATIVE HUMIDITY	TOTAL TIME (hours)	WATER CONTENT (absorbance unit)
DRIED	SAMPLE	(0.02)
32%	144	0.045
43%	72	0.05
52%	168	0.05
96%	168	0.11

Table 6: INTERFACE WATER IN CENTRALAB SILVER-ON-SILICON SAMPLE # 2

Relative Humidity	Total Time (Hours)	Water Content (Absorbance Units)
32%	96	---
43	96	---
52	72	---
66	96	---
75	72	---
81	96	---
85	504	0.06
91	192	0.11
96	144	0.18

Protection of the chemically reactive titanium with a non-porous layer would be one solution to the contact degradation problem. The use of gold instead of silver is a good prospect. A one-micron layer of gold was vacuum evaporated onto a silicon wedge used for internal reflection spectroscopy and placed in a 96% RH atmosphere at room temperature. After 1340 hours no evidence of water was seen (Figure 29) indicating that even one micron of gold is not porous to water.

Some other interesting results were obtained from the internal reflection spectroscopy work. Boeing, Heliotek, and Centralab-prepared silver-on-silicon samples developed blisters after exposure to >90% RH environments. These blisters were circular in shape (Figures 30 and 31) and characteristic of gas formation. The probable reaction involves the corrosion of silicon by the equation:

$$Si + 2H_2O \rightarrow SiO_2 + 4H^+ + 4e^-$$

and $$4H^+ + 4e^- \rightarrow 2H_2 \uparrow$$

Silicon is known to form imperfect oxide coatings. In fact, semiconductor manufacturers must take special care to grow oxide coatings which are passivating and not subject to corrosion (Ref. 21). This work suggests that solar cells could corrode where titanium does not cover the silicon. Fischer et al performed a test where titanium and silver were plated onto glass (Ref. 11). When placed in ∿ 100% RH, blisters developed which resembled those on solar cells. They then concluded that silicon did not take part in the corrosion mechanism. Our data indicate that their extrapolation of tests on glass to conditions on silicon is not necessarily valid. If the titanium forms an incomplete or porous layer, it is quite conceivable that silicon can also promote corrosion via the mechanism presented above.

To further test this hypothesis silicon wafers from both manufacturers were coated with three microns of silver in the Boeing Microelectronics laboratory and placed at 90°C above water in a closed container to generate ∿ 100% RH. The sun-facing side of the Heliotek sample developed blisters in 24 hours (Figure 32). The Centralab sample showed evidence of silver separation in the sample interior but no discrete blisters. Neither sample showed any evidence of blistering on the back side. From this we again concluded that silicon corrosion may contribute to the degradation mechanism. However the titanium layer would have to be porous or incomplete for this to occur. Also it should be noted that the back sides of solar cells appear sufficiently passivated to preclude silicon corrosion.

Internal reflection spectroscopy, the most significant of our physical tests, produced these conclusions:

- Condensation of water in the silver layer occurs rapidly above a critical humidity.
- The silver layer is porous with pores on the order of 10-65Å in radius.
- The small diameter of the pores compared to the thickness of the silver films (30,000Å) suggests an interconnected or "spongelike" structure.
- The pore size distribution in the silver varies from manufacturer to manufacturer and from batch to batch for a given manufacturer.

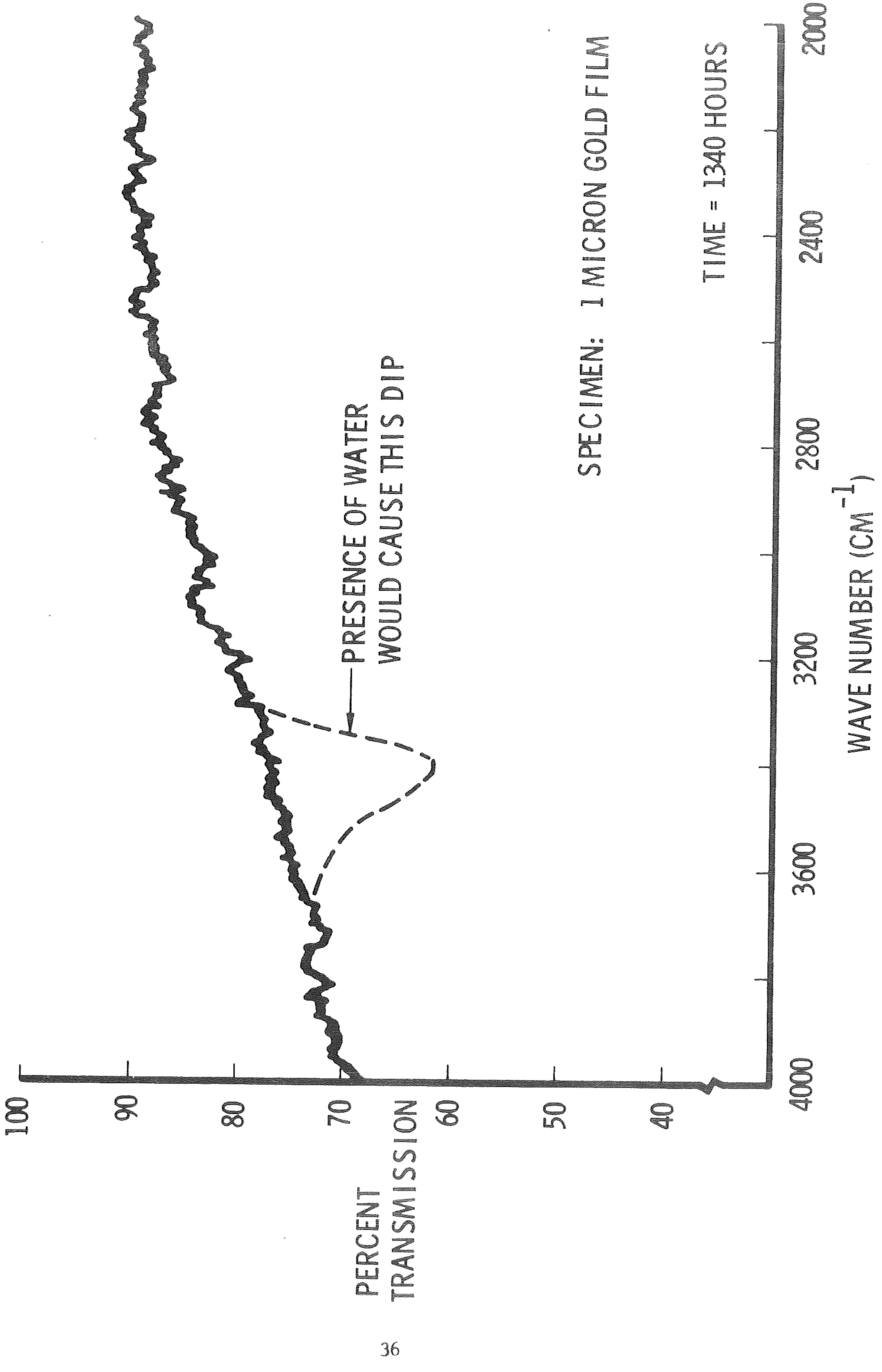

Figure 29: IR ABSORPTION SPECTRUM--GOLD COATED SAMPLE

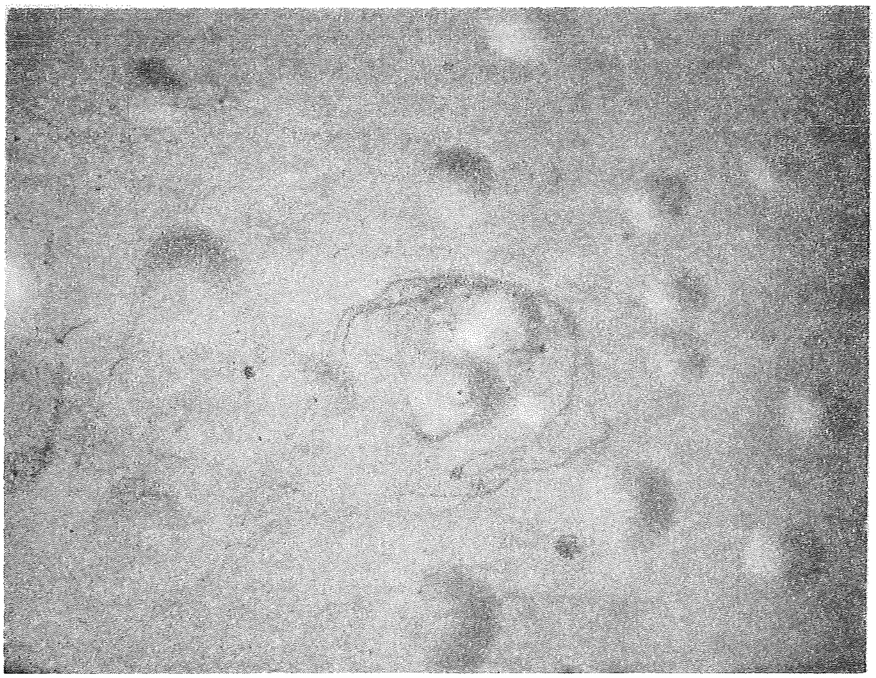

Figure 30 : BLISTERS ON HELIOTEK
SILVER-ON-SILICON SAMPLE (40X)

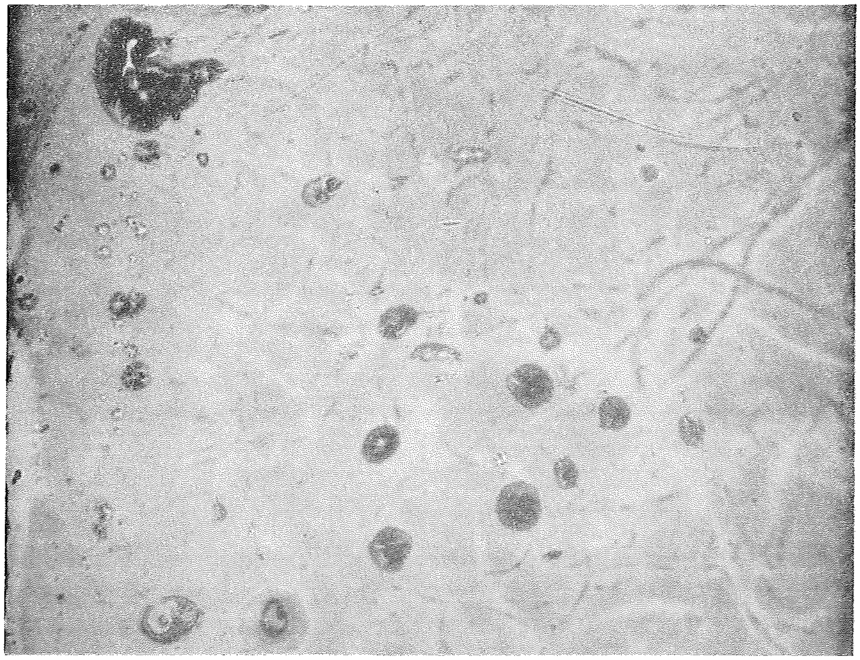

Figure 31 : BLISTERS ON CENTRALAB
SILVER-ON-SILICON SAMPLE (25X)

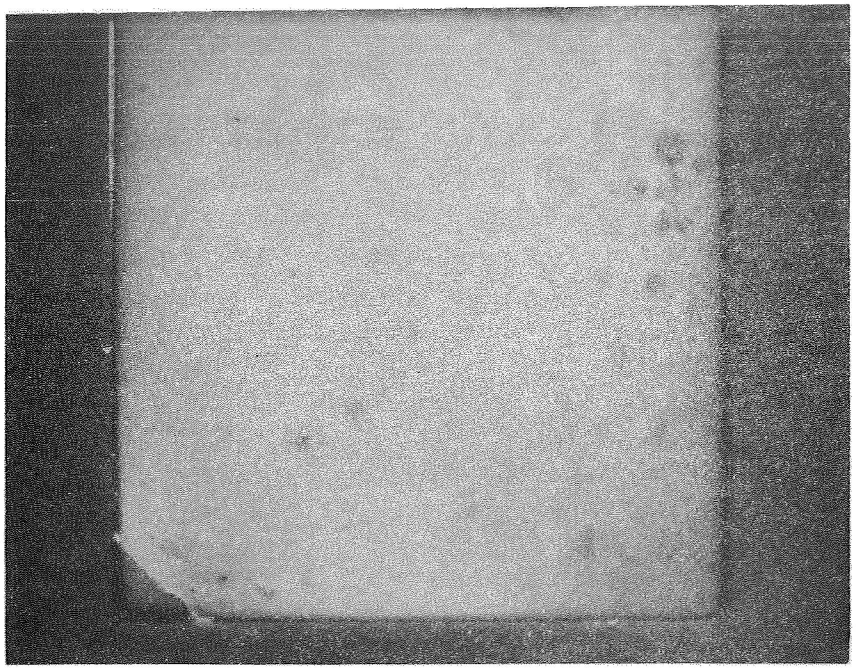

(4X)

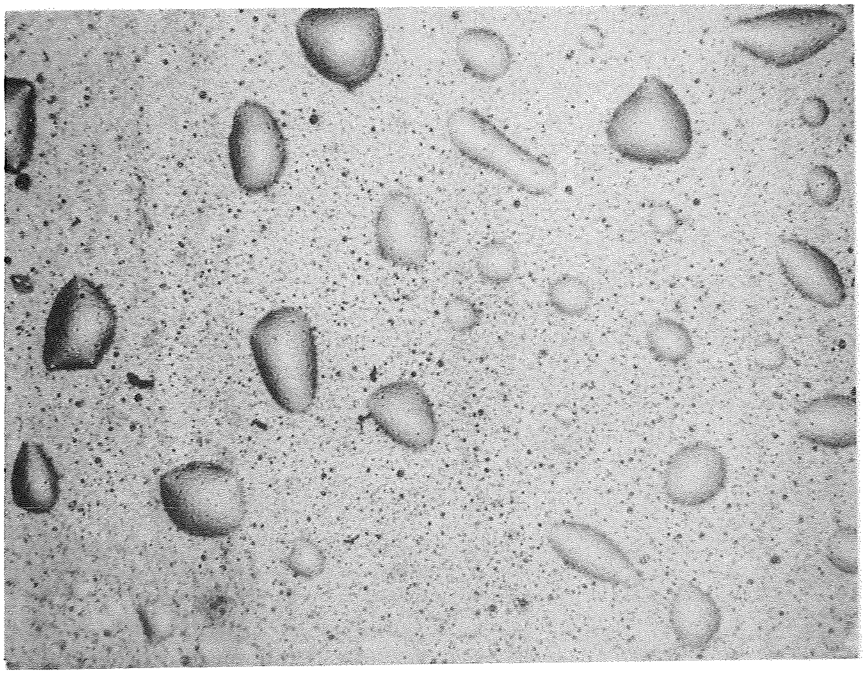

(7X)

Figure 32: SILVER/SILICON SAMPLE

- A one-micron gold film is non-porous and may be a substitute for the porous silver layer.
- Silicon can contribute to the contact degradation under certain conditions through the probable reaction: $Si + 2H_2O \rightarrow 2H_2 + SiO_2$.

3.2 Electrochemical Measurements

The electrochemical work done with solar cells contacts had two purposes: (1) to determine whether degradation can be accelerated under controlled laboratory conditions, and (2) to establish the effects of various chemical environments on solar cell degradation.

3.2.1 Polarization Tests

By imposing a potential on a solar cell in a chemical environment we hoped to control and accelerate degradation under controlled conditions and learn more about the degradation mechanism. Various chemical species are thermodynamically stable depending on the pH and the applied potential of the system. The potential-pH diagrams, developed by Pourbaix, for titanium-water (Ref. 22) and silver-water systems (Ref. 23) are shown in Figures 33 and 34. Regions where various species are stable are indicated on the diagrams. Lines a and b refer to the limits of stability of water. Above a, the reaction $2H^+ + 2e^- \rightarrow H_2$ is thermodynamically impossible for reactants and products at unit activities. Above b, the reaction $4H^+ + O_2 + 4e^- \rightarrow 2\ H_2O$ is impossible for the same conditions.

By imposing a potential of 0.0 volts with respect to the saturated calomel electrode (SCE) on a solar cell in a solution at pH = 0 the Pourbaix diagrams predict that Ag and TiO^{++} are the stable species. Silver would not react at this condition, whereas titanium would. This condition would therefore provide a test of which component results in cell failure. In the presence of chloride there is another equilibrium which must be considered in the Pourbaix diagram:

$$Ag + Cl^- \rightarrow AgCl + e^- \qquad E=0.22v$$

Above this potential AgCl is the stable species, while below Ag is stable.

Solutions of HCl NH_4F and NaOH were chosen to provide electrolytes with a wide range of pH values. The pH of the solutions as measured with a Beckman pH meter (Model G) are:

Solution	pH
1N HCl	0.0
1N NH_4F	7.1
0.01N NaOH	12.0

The solar cell, acting as the control electrode, was placed in a teflon cell filled with the appropriate solution (Figure 35). A platinum wire served as the counter electrode and a SCE was used as reference. A Magna Potentiostat (Model 4700M) was used to measure the current as a function of applied voltage. The resulting polarization curves did not show any unexpected results. Figure 36 shows the polarization curve for 1N HCl. The area labeled "A" corresponds

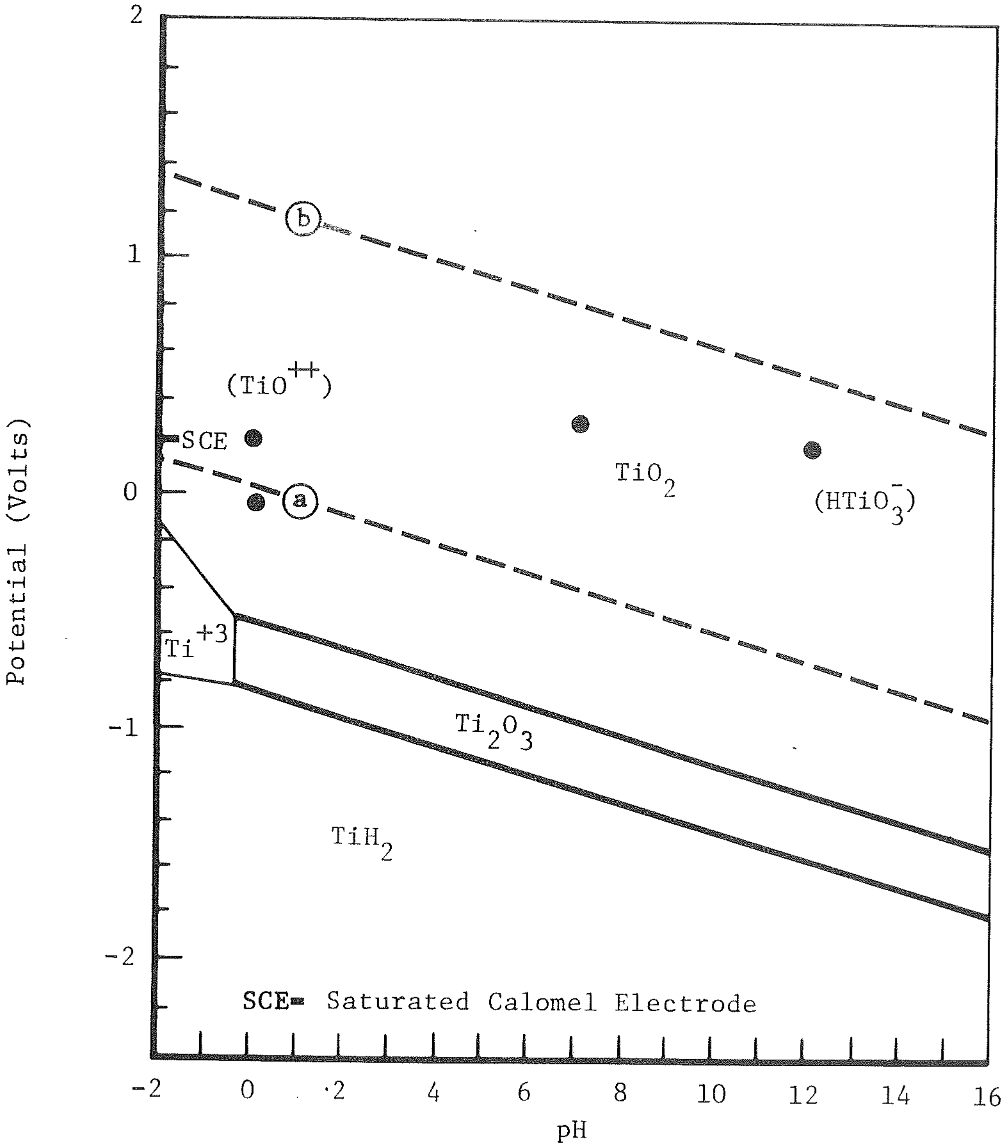

Figure 33: POTENTIAL-pH EQUILIBRIUM DIAGRAM FOR THE TITANIUM-WATER SYSTEM AT 25°C

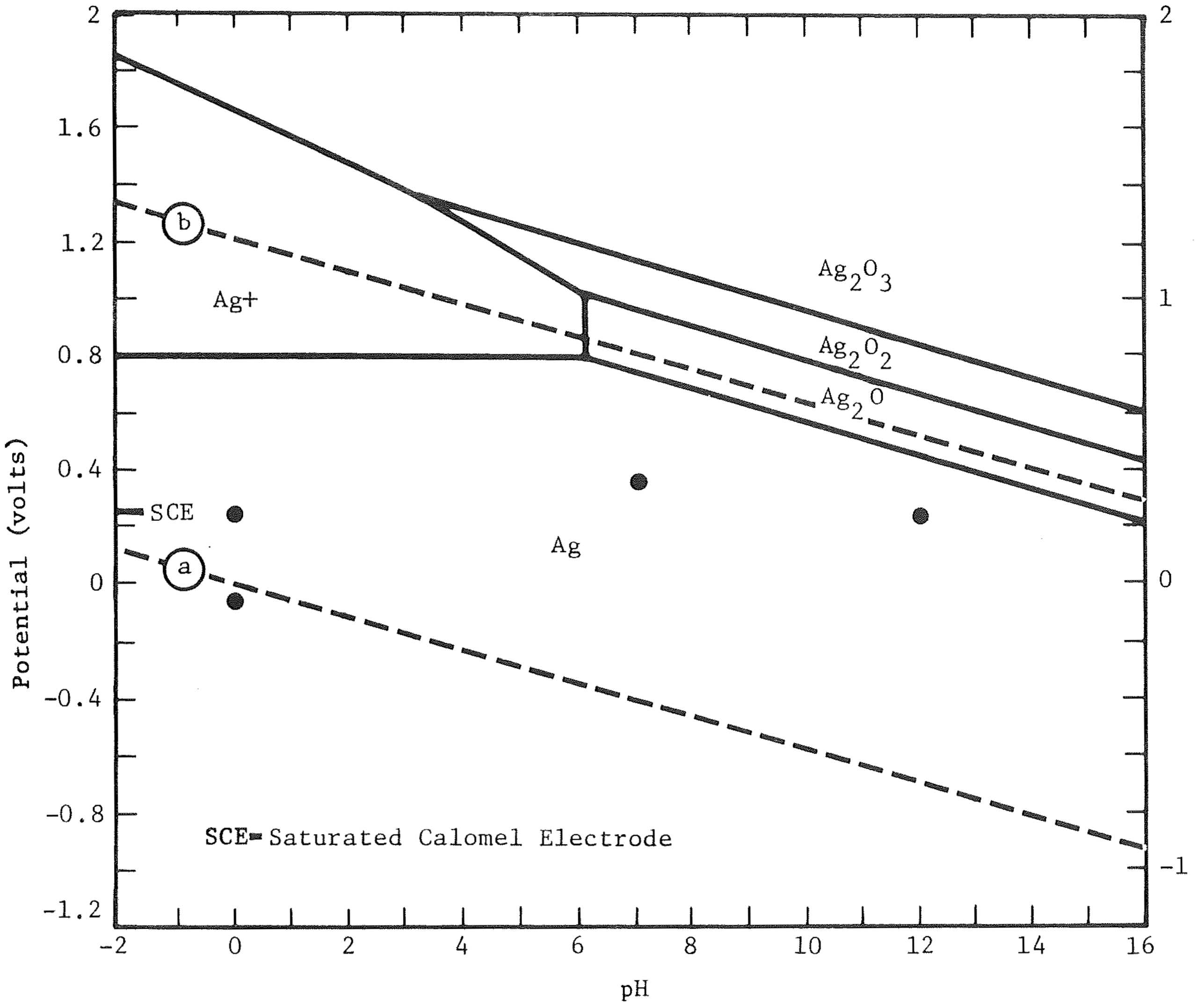

Figure 34: POTENTIAL-pH EQUILIBRIUM DIAGRAM FOR THE SILVER-WATER SYSTEM AT 25°C

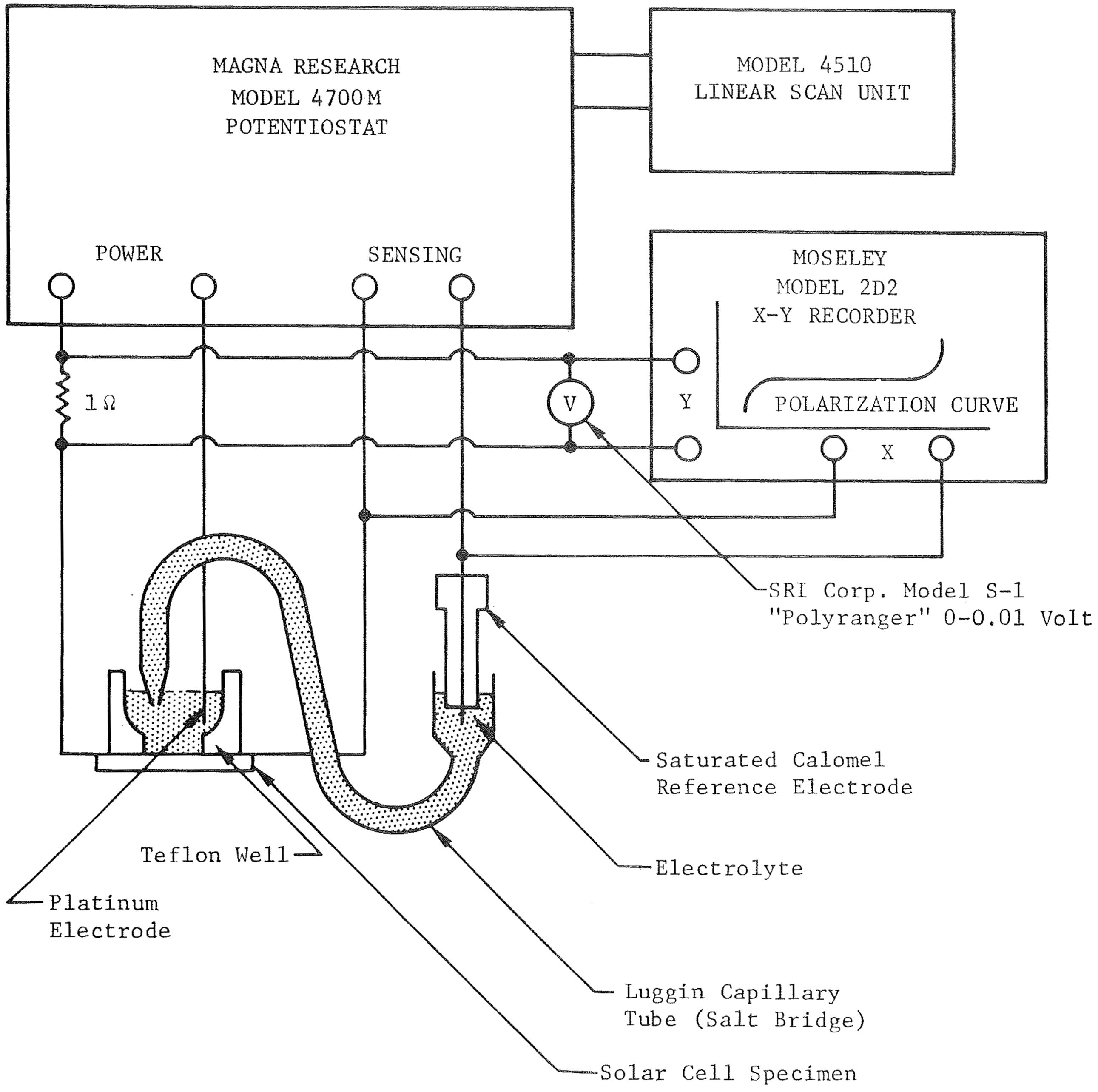

Figure 35: POLARIZATION APPARATUS

Specimen:	Cell No. 115
Solution:	**1 Normal HCl**

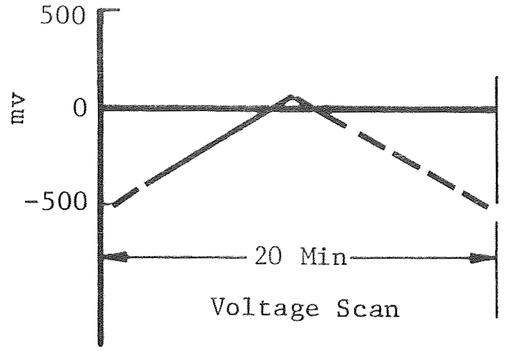

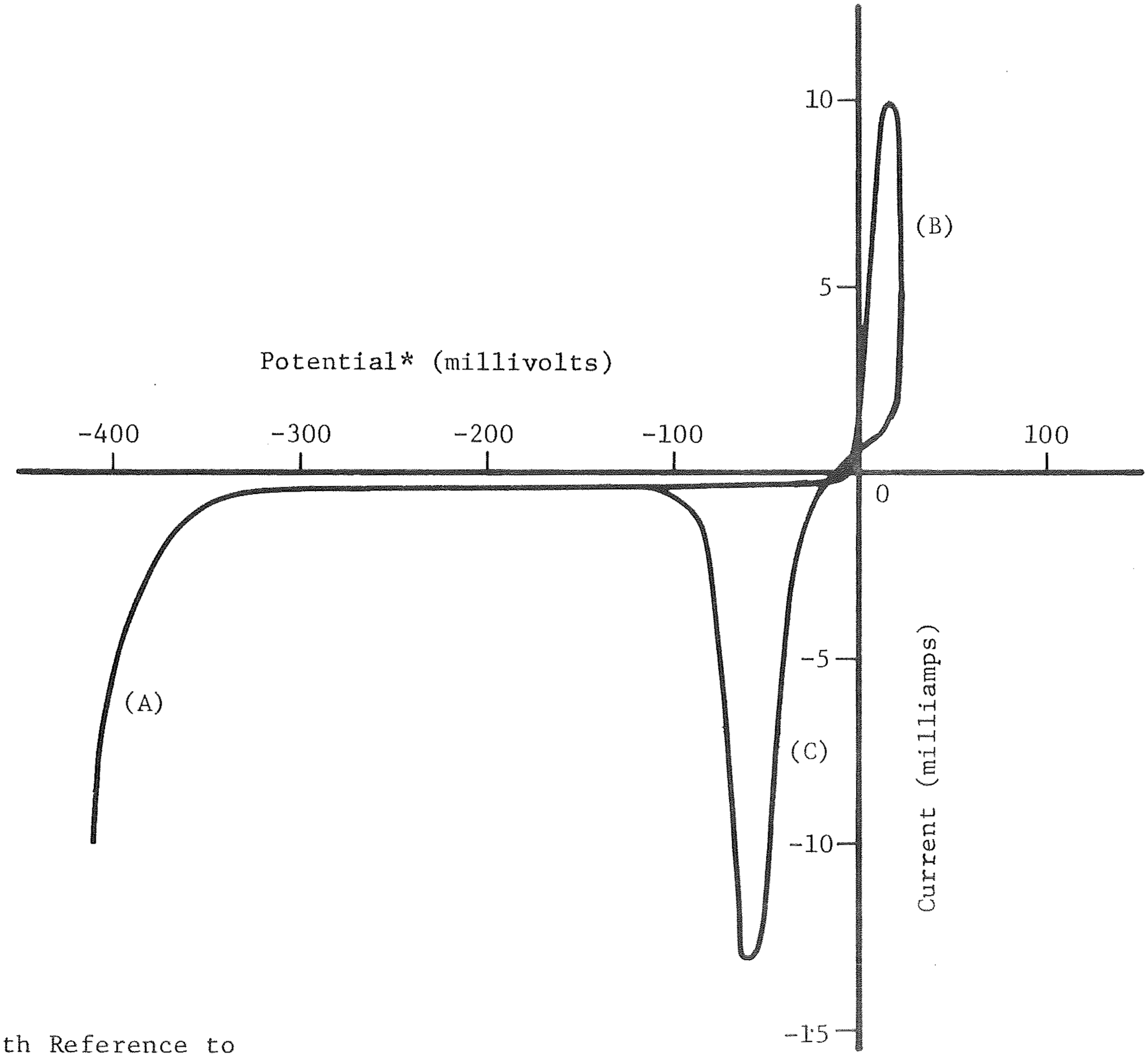

*With Reference to
Saturated Calomel Electrode

Figure 36 : POLARIZATION CURVE OF CELL IN HCl

to cathodic behavior of the cell where the reaction is $2H^+ + 2e^- \rightarrow H_2$. In area "B" the cell becomes anodic and silver oxidizes to give silver chloride by the reaction $Ag + Cl^- \rightarrow AgCl + e^-$. Region "C" corresponds to the reduction of the species oxidized in region "B" ($AgCl + e^- \rightarrow Ag + Cl^-$). The shapes of regions "B" and "C" are expected to vary as functions of the past history of the cell. The polarization curves indicate the irreversibility of the electrode process. Similar curves for NH_4F and NaOH are shown in Figures 37 and 38. The peak at positive potentials are due to the oxidation of silver to silver oxide (Ag_2O).

A reference current-voltage (I-V) curve was recorded for each solar cell before any electrochemical tests were performed with the cell. The potentiostatic tests were initiated and I-V curves were periodically obtained until degradation occurred. Solar cells in 1N HCl solutions at potentials of 0.0V (TiO^{++} and AgCl are stable) and -0.3V (TiO^{++} and Ag are stable) with respect to a SCE reference electrode degraded in 51 hours and 84 hours respectively, indicating that the environment accelerated the degradation. It is significant that applying a potential between the electrolyte and the silver-titanium contact of the solar cell produces rapid degradation at room temperature. Tests in solutions of 1 normal NH_4F (pH = 7.1) and 0.01 normal NaOH (pH = 12) showed no I-V degradation after 109 hours in the NH_4F solution maintained at 0.1 volt versus the SCE and 144 hours in NaOH at 0.0 volts.

The experimental conditions are plotted as points on the Pourbaix diagrams (Figures 33 and 34). In HCl the conditions are in the region where soluble titanium ions are the thermodynamically stable species, permitting degradation to occur. The increased degradation rate at 0.0 volts occurs because of the higher applied anodic potential which results in a higher overvoltage to drive the reaction. At a pH of 7 and at the potential applied the stable species is titanium oxide which would be expected to form a protective layer and hinder corrosion. The behavior at pH of 12 is harder to predict because of possible formation of soluble $HTiO_3^-$ species. Experimental results suggested that degradation had not occurred in either case. Subsequent rest potential tests (Section 3.2.3) showed, however, that solar cells in NH_4F and NaOH degrade with loss of silver on time scales similar to those used in the polarization tests. Upon examination of the cells we found that the silver layer would separate with gentle probing for both the NH_4F and NaOH samples. We then concluded that I-V electrical measurements alone might not be a good indication of contact degradation.

Summarizing, the polarization measurements have shown that solar cell degradation could be controlled and accelerated under controlled laboratory conditions. The measurements also indicated that the silver contact on solar cells is porous and that titanium is interacting with the chemical solution.

3.2.2 Rest Potential Tests

Rest potential is the open circuit equilibrium potential of an electrode in contact with an electrolyte. Samples of solar cells, silver, and silicon were placed in various chemical solutions and their rest potentials were measured as a function of time. Measurements were made with a high impedance voltmeter (Keithley, Model 200B) against a SCE reference electrode (Figure 39). Results for solar cells are shown in Figure 40. An interesting observation is that the

Electrolyte: 1 Normal NH_4F

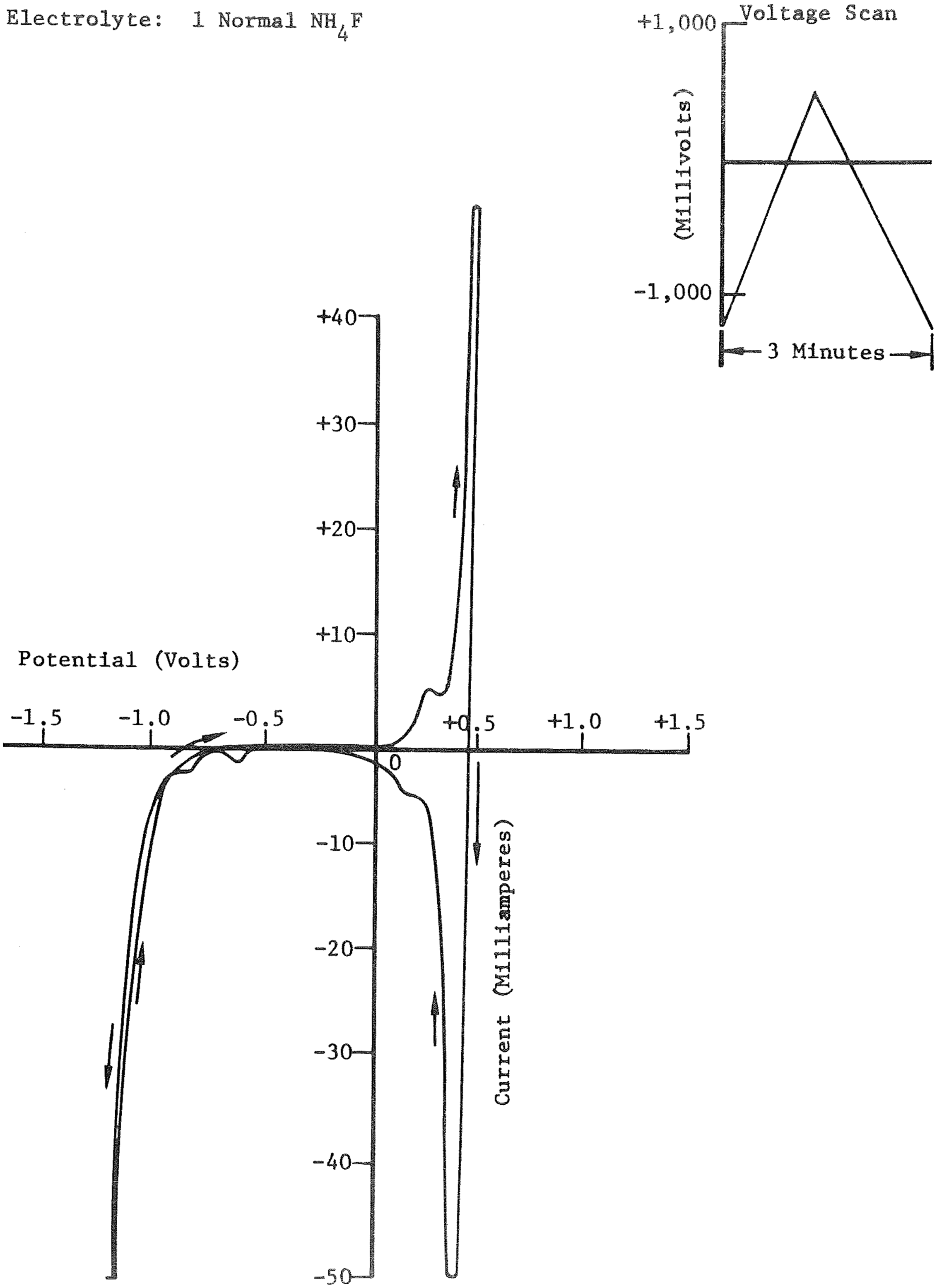

Figure 37: POLARIZATION CURVE OF CELL IN NH_4F

Electrolyte: 1 Normal NaOH

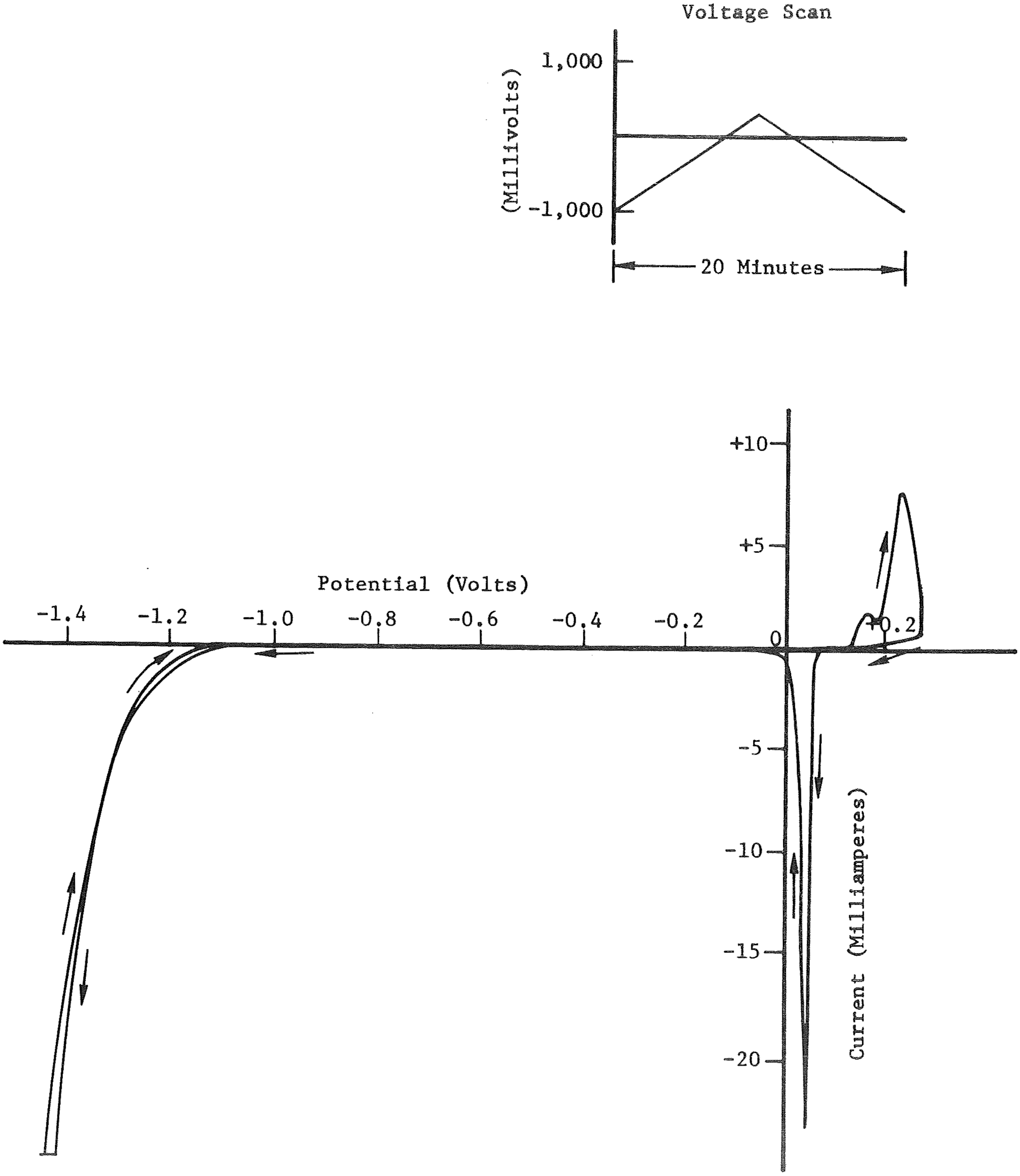

Figure 38: POLARIZATION CURVE IN NaOH

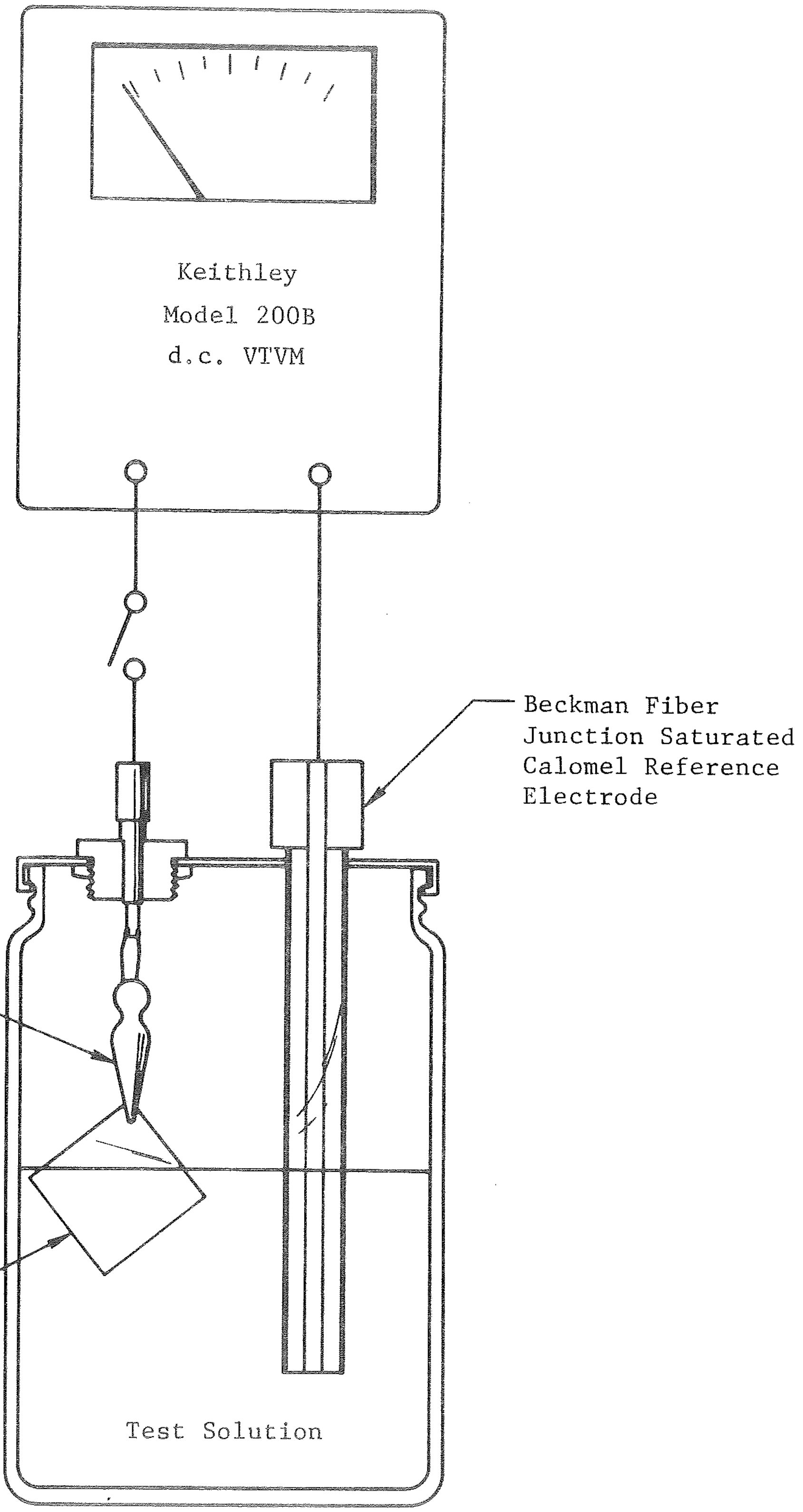

Figure 39: REST POTENTIAL TEST SETUP

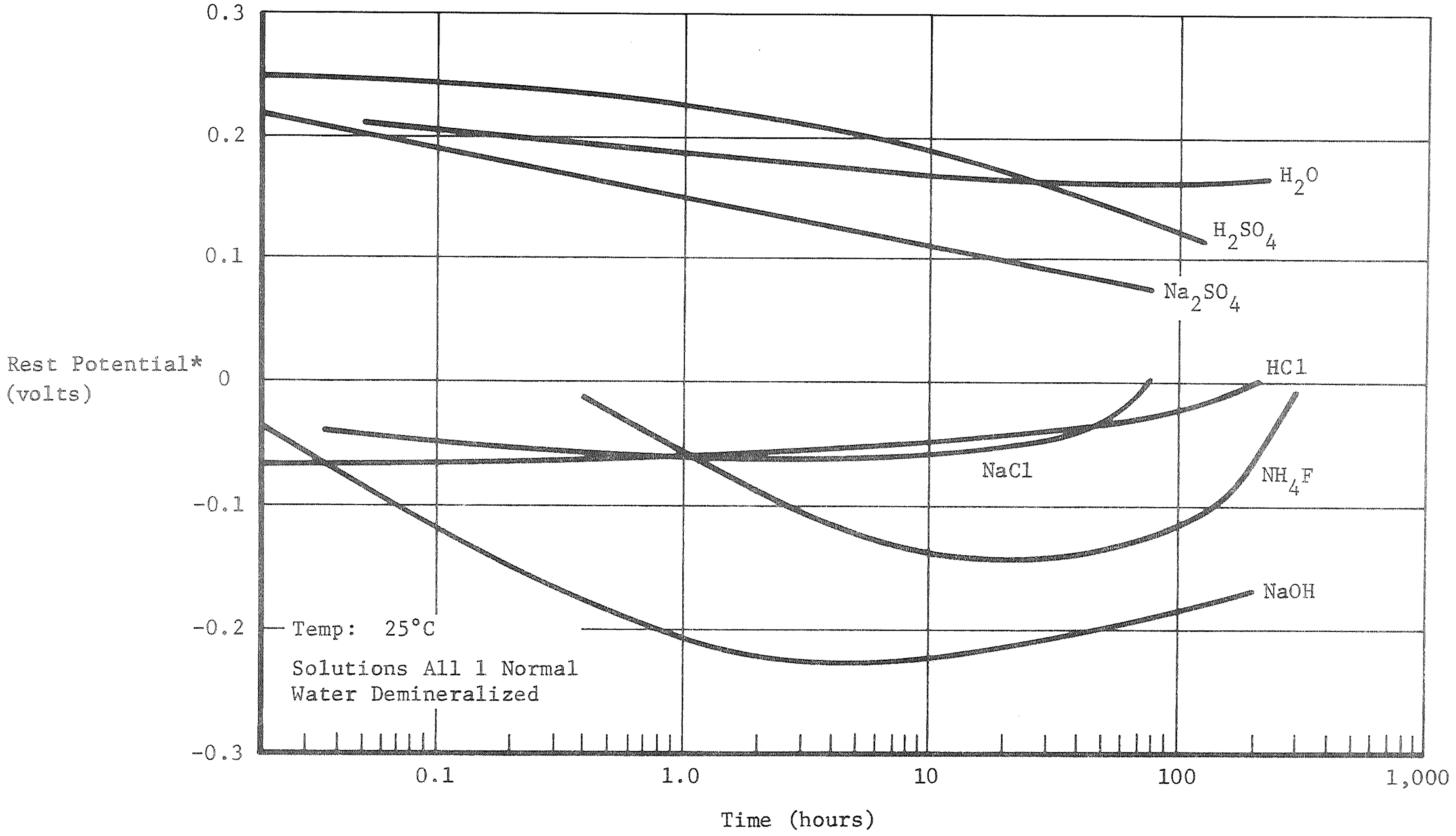

*With Reference to Saturated Calomel Electrode

Figure 40: REST POTENTIAL* VERSUS TIME

data fall into two distinct groupings. The possibility of predicting degradation behavior based on rest potential measurements was suggested (Ref. 5). It will be shown later that NaOH, HCl, NaCl and NH_4F promote rapid degradation in solar cells. However, so does H_2SO_4 which appears in the upper group. It is unlikely that rest potentials will prove to be a useful test for predicting solar cell degradation behavior.

The rest potentials of solar cells alone do not yield much information about the degradation process. There are three substances in the solar cell which can interact individually or when coupled with the solution. These are silver, silicon, and titanium. When two dissimilar substances are coupled in a conductive solution the potential exhibited by the system is called a mixed potential. The mixed potential depends on many factors and its actual value is impossible to predict. We can only state that the mixed potential will lie between the two individual rest potentials (Figure 41). Rest potentials of silver, silicon and silver-silicon couples were measured in the same solutions as the solar cells. It is interesting to compare solar cell rest potentials to silicon and silver rest potentials in the same solution. Table 7 shows such potentials measured 10 hours after immersion in various solutions. The ten-hour delay was to allow the system to equilibrate.

Table 7: REST POTENTIALS

SOLUTION	$^{\bullet}E_{SILVER}$	$^{\bullet}E_{SILICON}$	$^{\bullet}E_{SILVER-SILICON}$	$^{\bullet}E_{SOLAR\ CELL}$
1N HCl	-0.024	-0.045	-0.024	-0.046
1N H_2SO_4	+0.21	+0.11	+0.20	+0.16
1N NH_4F	+0.11	-0.37	-0.10	-0.13
1N NaOH	-0.14	-0.32	-0.16	-0.22

•VERSUS SATURATED CALOMEL ELECTRODE

For the silver-silicon system the data (Table 7) show that the mixed potential lies closer to that of silver. This implies that the exchange current for the silver reaction is greater than for the silicon reaction. Potentials of the solar cells are more negative than the silver-silicon couple in the solutions. This implies that an interaction is occurring, with a substance having a more negative rest potential than silver or silicon. Such a substance is titanium.

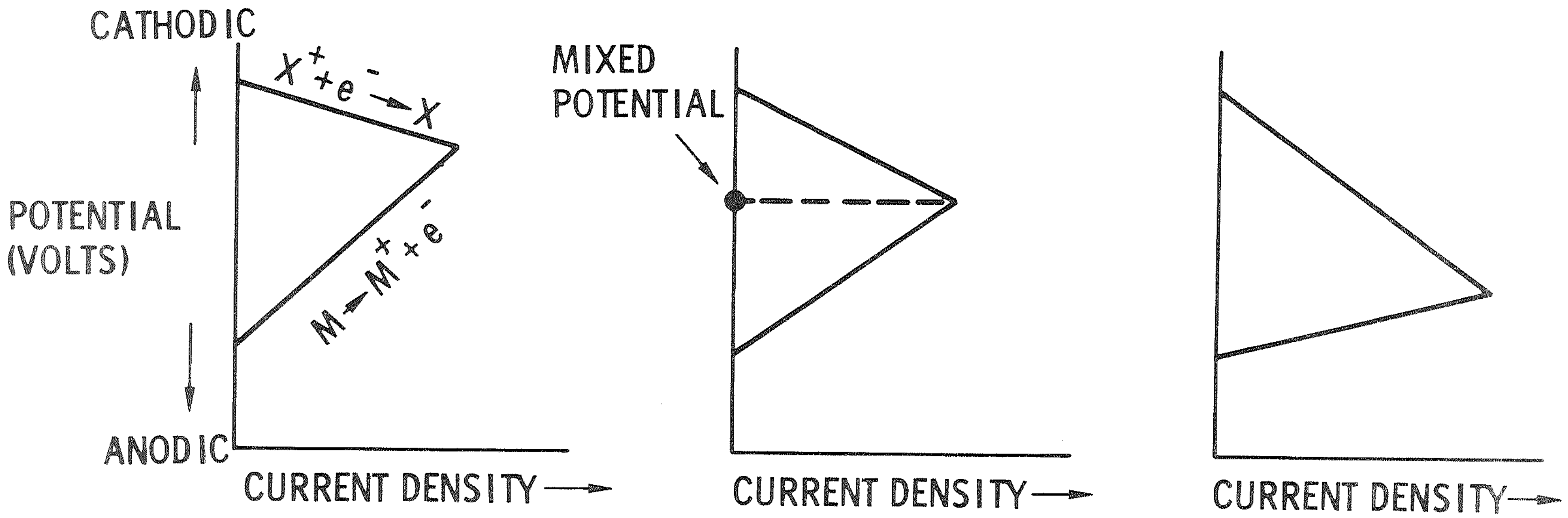

(a) ANODIC

(b) MIXED

(c) CATHODIC

Figure 41 : ELECTROCHEMICAL CONTROL

It is thus suggested that the silver contact is porous and interaction of the solution with titanium gives rise to the observed potential.

3.2.3 Effects of Chemical Environments

The cells from the rest potential tests were also used in studying the effects of various chemical species on degradation and degradation rates. If titanium is interacting with the environment it is expected that solar cells placed in acidic and basic solutions would degrade with the formation of Ti^{+3} and $HTiO_3^-$ type species respectively (Figure 33). The behavior of cells in more neutral solutions is expected to be more passive with the formation of the protective oxide layer (Figure 33).

The data from rest potential tests along with comments concerning degradation appear in Table 8. Blisters were determined by inspection under a 50X microscope. Probing with a dental tool established the adherence of the silver contact layer. Electrical degradation was determined from I-V curves.

Table 8 : EFFECTS OF ENVIRONMENT ON SOLAR CELLS

Solution	pH	Hours in Solution	Blisters	Silver Separation	Electrical Degradation
1N HCl	0	192	Yes	Yes	Yes
1N H_2SO_4	0.2	240	Yes	Yes	Yes
1N Na_2SO_4	6.7	168 960	No No	No No	No No
H_2O	7.0	213 621	Yes Yes	No Yes	No Yes
1N NH_4F	7.1	170	Yes	Yes	Yes
1N NaCl	7.2	73 253	Yes Yes	No Yes	Slight Yes
1N NaOH	14.0	94	Yes	Yes	Yes

The predicted acidic and basic solution behavior is confirmed in the results. Complete delamination of the silver layer occurred under both conditions. In Table 8 the time of exposure to solutions indicates when the observations were made, but the degradation probably began much earlier. Therefore, one should not conclude for example that NaOH is more corrosive than HCl or H_2SO_4. 3M also reported blisters on silver-titanium samples immersed in solutions of

NaOH, KOH and humid air above HF, HCl but not H_2SO_4(Ref. 8,9). The NaOH, KOH, HF, and HCl results are predicted and agree with our observations. The absence of degradation in the H_2SO_4 could be explained by the very low vapor pressures of H_2SO_4 (<1mm) when compared to HCl(40 atm.) and HF(1 atm.).

The more neutral solutions of Na_2SO_4, H_2O, NH_4F, and NaCl exhibit interesting and surprising behavior. All cells except those in Na_2SO_4 eventually degraded. The only explanation we can offer for the behavior in Na_2SO_4 is that the precipitation of Ag_2SO_4, as evidenced by a visible yellowish coating on the silver contact, seals off moisture from the silver and thus acts as a barrier to prevent degradation. 3M also reported blistering when silver-titanium samples were placed in NaCl, but none in water (Ref. 8). However the test lasted only 10 days (240 hours), and our degradation in water wasn't readily apparent at 213 hours.

Both H_2O and NaCl initially produced blisters but no silver separation or significant I-V degradation. Pourbaix diagrams predict that in this pH range, titanium should form a protective oxide coating typically 50Å thick, inhibiting further corrosion.

3.2.3.1 Blister Generation

Several questions can be asked about these blisters:

(1) Would a 50Å oxidation of titanium produce enough hydrogen to cause the blisters seen?

(2) Would the pressure generated under the silver be sufficient to raise a blister?

Using the following assumptions we can calculate the amount of hydrogen generated by the titanium being oxidized:

Diameter of typical blister = 0.005 inches (1.27×10^{-2}cm)
$Ti + 2H_2O \rightarrow TiO_2 + 2H_2$ to a depth of 50Å

The area of the blister would be:

$$\text{Area} = \pi r^2 = 1.27 \times 10^{-4}\,\text{cm}^2$$

The amount of titanium corroded would be:

$$50\text{Å}(1\text{cm}/10^8\text{Å})(4.5\text{ gm Ti/cm}^3) = 2.25 \times 10^{-6}\text{ gm Ti/cm}^2$$

Each mole of Ti would generate two moles of hydrogen. Therefore the amount of hydrogen generated would be:

$$x = \frac{(2.25 \times 10^{-6}\text{gm Ti/cm}^2)(1.27 \times 10^{-4}\text{cm}^2)(2\text{ moles H}_2\text{/mole Ti})(22{,}400\text{ cm}^3\text{ H}_2\text{/mole})}{48\text{gm Ti/mole}}$$

$$x = 2.66 \times 10^{-7}\text{ cm}^3 \text{ or } 1.10 \times 10^{-11}\text{ moles hydrogen}$$

The volume of a blister can be estimated as shown in the sketch below. The slope of a blister was measured with an optical comparator and found to be typically less than 20°.

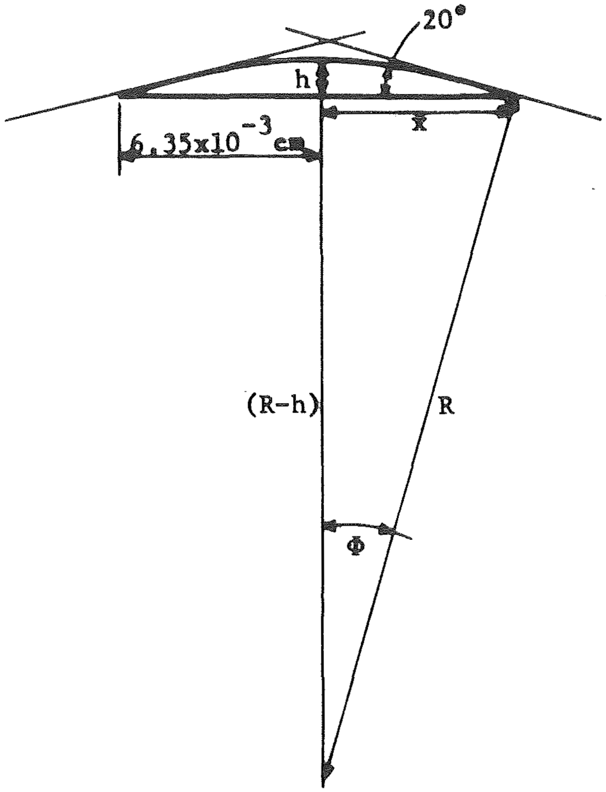

By geometrical arguments it can be shown that $\Phi = 20°$. R, the radius of the assumed spherical blister, can be calculated from:

$$\sin \Phi = \frac{x}{R}$$

$$R = 1.86 \times 10^{-2} \text{cm}$$

The height of the blister can now be obtained from:

$$R^2 = x^2 + (R-h)^2 \text{ or}$$

$$h^2 - 2Rh + x^2 = 0 \text{ which is a quadratic equation.}$$

$$h = 1.1 \times 10^{-3} \text{ cm or } 3.6 \times 10^{-3} \text{ cm}$$

Since h must be less than Tan $(20°)(6.35 \times 10^{-3}) = 2.3 \times 10^{-3}$cm, the correct value is 1.1×10^{-3}cm.

The volume of this blister, a spherical segment, can now be calculated:

$$(\text{Volume})_{\text{blister}} = 1/3\pi h^2(3R - h)$$

$$(\text{Volume})_{\text{blister}} = 6.95 \times 10^{-8}\text{cm}^3$$

This volume of the blister is less than the amount of hydrogen generated ($2.7 \times 10^{-7}\text{cm}^3$) and therefore it can be concluded that surface oxidation of titanium can provide enough hydrogen to fill the blister.

The second question involves the pressure required to raise the silver layer. The pressure needed to raise three microns of silver, a typical contact thickness can be estimated as follows:

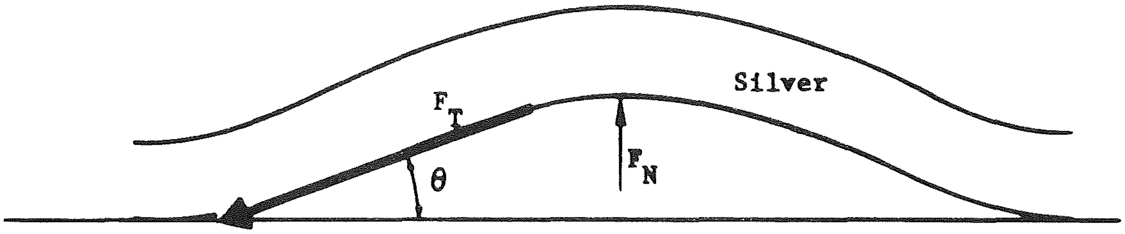

The force acting upward is: $F_N = P(\pi r^2)$

where P = pressure needed to raise the blister
πr^2 = area of the blister

The resisting force is: $F_T = \sigma_y t(2\pi r)$

where σ_y = yield stress of silver (estimated at 10^6 gm/cm^2)
t = thickness of the silver (3×10^{-4}cm)
$(2\pi r)$ = circumference of the blister
r = radius of blister (6.4×10^{-3}cm typical)

From geometrical arguments:

$$\frac{F_N}{F_T} = \sin\theta$$

Substituting we obtain:

$$P(\pi r^2) = \sigma_y t(2\pi r)\sin\theta$$

$$P = \frac{2\sigma_y t \sin\theta}{r}$$

As θ approaches zero the pressure(P) needed to raise the silver approaches zero. For $\theta = 20°$, $P = 31$ atmospheres.

The pressure needed to raise the blister would vary from 0 to something in the order of 31 atmospheres as the blister becomes larger. This calculation must be considered only approximate because it does not take into effect the possibility of an increase in r as the blister grows. Also if the silver is porous then σ_y would be less than for solid metal. The angle θ continually changes as the blister grows, and the yield stress was estimated.

The pressure produced within a blister by the corrosion of titanium can be calculated from:

$$PV = nRT$$

where
V = Volume of blister ($6.95 \times 10^{-8} \text{cm}^3$)
n = Number of moles of H_2 (1.19×10^{-11} moles H_2)
R = 0.082 l.atm/deg. mole
T = 298°K

$$P = \frac{(1.19 \times 10^{-11} \text{ moles } H_2)(0.082 \text{ l.atm/deg.mole})(298°\text{K})}{6.95 \times 10^{-11} \text{ liters}}$$

$$P = 4.2 \text{ atmospheres}$$

Again this pressure must be considered approximate as it does not allow for escaped gas, and blister volume was approximated. We can conclude, however, that the numbers are not unreasonable and that the pressure generated (4 atmospheres) is sufficient to raise a blister. Oxidation of titanium beyond 50Å or hydrogen migration from regions adjacent to a blister can increase the pressure.

Another question which arises concerning blisters is: If water can get in the silver, why can't the hydrogen generated get out? The pressure required to blow out the water in a pore can be estimated from:

$$r = \frac{2\sigma}{\Delta P}$$

Where
r = pore radius (assume 30 Å here)
σ = surface tension of water (72 dynes/cm)
ΔP = pressure

$$\Delta P = \frac{(2)(72 \text{ dynes/cm})}{30 \times 10^{-8} \text{cm}}$$

$$\Delta P = 480 \text{ Atmospheres}$$

It is unlikely that pressures of this magnitude can be generated and thus the hydrogen could not escape. This does not mean, however, that the hydrogen cannot diffuse away from the area where it is generated and find other avenues of escape. Estimates of hydrogen diffusion rate away from the corrosion site can be made:

$$j = -D \frac{dC}{dx} \sim -D \frac{\Delta C}{\Delta X}$$

where j = diffusion rate

D = diffusion coefficient (approximately $10^{-5} cm^2/sec$)

$\frac{dC}{dx}$ = differential concentration gradient

$$\Delta C \sim C_{\text{Saturation of hydrogen in water}} \sim \frac{1.5\times10^{-6} gm\ H_2}{cm^3} \sim \frac{7.5\times10^{-7} mole\ H_2}{cm^3}$$

$$\Delta X = 3 \times 10^{-4}\ cm\ Ag$$

$$j \sim 10^{-5} cm^2/sec\ \frac{(7.5 \times 10^{-7}\ moles\ H_2/cm^3)}{(3 \times 10^{-4}\ cm\ Ag)}$$

$$j \sim 2.5 \times 10^{-8}\ moles\ H_2/cm^2 Ag.sec$$

Assume the fraction of voids in silver (porosity) is 0.1%.

$$J_{eff} \sim (0.001)\ (2.5 \times 10^{-8}) = 2.5 \times 10^{-11}\ moles\ H_2/cm^2 Ag.sec$$

$$\text{Volume of gas diffusing} \sim (2.5 \times 10^{-11}\ moles\ H_2/cm^2 Ag.sec)(22{,}400\ cm^3/mole\ H_2)$$

$$\text{volume of gas diffusing} \sim 5.6 \times 10^{-7} cm^3 H_2/cm^2 Ag.sec$$

The amount of hydrogen generated(x) is $2.66 \times 10^{-7} cm^3$ in an area (A) of $1.27 \times 10^{-4} cm^2 Ag$.

$$\frac{x}{A} = \frac{2.66 \times 10^{-7}}{1.27 \times 10^{-4}} = 2.09 \times 10^{-3} cm^3 H_2/cm^2 Ag$$

The time available to form a blister before the hydrogen can diffuse away is

$$T = \frac{x/A}{\text{volume}} = \frac{2.09 \times 10^{-3} cm^3 H_2/cm^2 Ag}{5.6 \times 10^{-7}\ cm^3 H_2/cm^2 Ag.sec} = 3730 \text{ seconds}$$

The corrosion current needed to produce hydrogen on this time scale is:

$$i = \frac{(2.09 \times 10^{-3} cm^3 H_2/cm^2 Ag)(1.93 \times 10^5\ \text{Coulombs/mole}\ H_2)}{(3.73 \times 10^3 sec)(2.24 \times 10^4 cm^3 H_2/mole\ H_2)}$$

$$i = 4.8\ \mu A/cm^2$$

This is the order of magnitude of corrosion currents for titanium corrosion (Ref. 24). We therefore conclude that hydrogen is generated fast enough to form blisters before it can diffuse away from the blister site.

Thus surface oxidation of titanium can explain initial blistering of solar cells. The next question that comes to mind is: what happens on further degradation? Several mechanisms can operate: (1) The area under a blister can continue to oxidize enlarging the blister, (2) areas adjacent to the blister can oxidize with hydrogen migrating into the blister, (3) new blisters can form in new areas, or (4) no new blisters form because hydrogen escapes.

This question was answered by performing the following test. We identified an area on the back contact of a solar cell with a scribe and placed the cell in a 90°C oven above a tray of water to generate ∿ 100% RH. We periodically removed the cell from the environment and photographed it with a Zeiss Ultraphot II. These photographs (Figures 42 and 43) showed that:

(1) New blisters appeared with the passage of time (labelled N).
(2) Old blisters grew to random sizes (labelled G) and then stopped growing (labelled S). There seemed to be no relation to final blister size or to time.
(3) Silver peeled away in areas where no blisters appeared.

It thus seems probable that all four proposed mechanisms above are in operation.

Becker's work tends to support these mechanisms (Ref. 16). He showed the presence of relatively thick layers of oxide on degraded cells, and in some cases the presence of TiH_2, indicating to him that not all of the surface was oxidized. It should be noted that Becker's method of detection (electron diffraction) involved the use of replicas to remove the desired layers from solar cells. It is not known if the replication process removes all of the layers from the solar cell surface. The fact that thick layers (500 to 1000Å) of oxide were removed implies that degradation involves more than surface oxidation. This raises the question of why surface oxidation does not protect the titanium from further oxidation. The presence of halides, as explained later, can break the passivity of the oxide to allow further reaction. It is also possible that titanium oxide in the anatase form does not protect as well as does rutile, thus allowing further degradation to occur.

The area of the electron beam used in Becker's work was $\sim 1.77 \times 10^{-2} cm^2$ which is $\sim 10^2$ times larger than a typical blister. Oxidation of titanium must occur in areas adjacent to blister sites since in many instances he reported only oxides on degraded cells. If oxidation only occurred in the region of a blister his results would have shown the presence of titanium or titanium hydride in all cases.

3.2.3.2 Fluoride and Chloride Ions

The data in Table 8 suggests that both NaCl and NH_4F accelerate and enhance degradation of solar cells. This observation prompted another test where cells were placed in 1N NaCl (pH = 6.65), 1N NH_4F (pH = 6.5), and H_2O (pH = 6.7), and kept in a 90°C oven for 18.5 hours. The high temperature was used to accelerate the corrosion rate. The cells exposed to fluoride and especially chloride ions developed severe degradation with blisters and contact peeling (Figure 44). The cells from the water had no blisters and no silver separation.

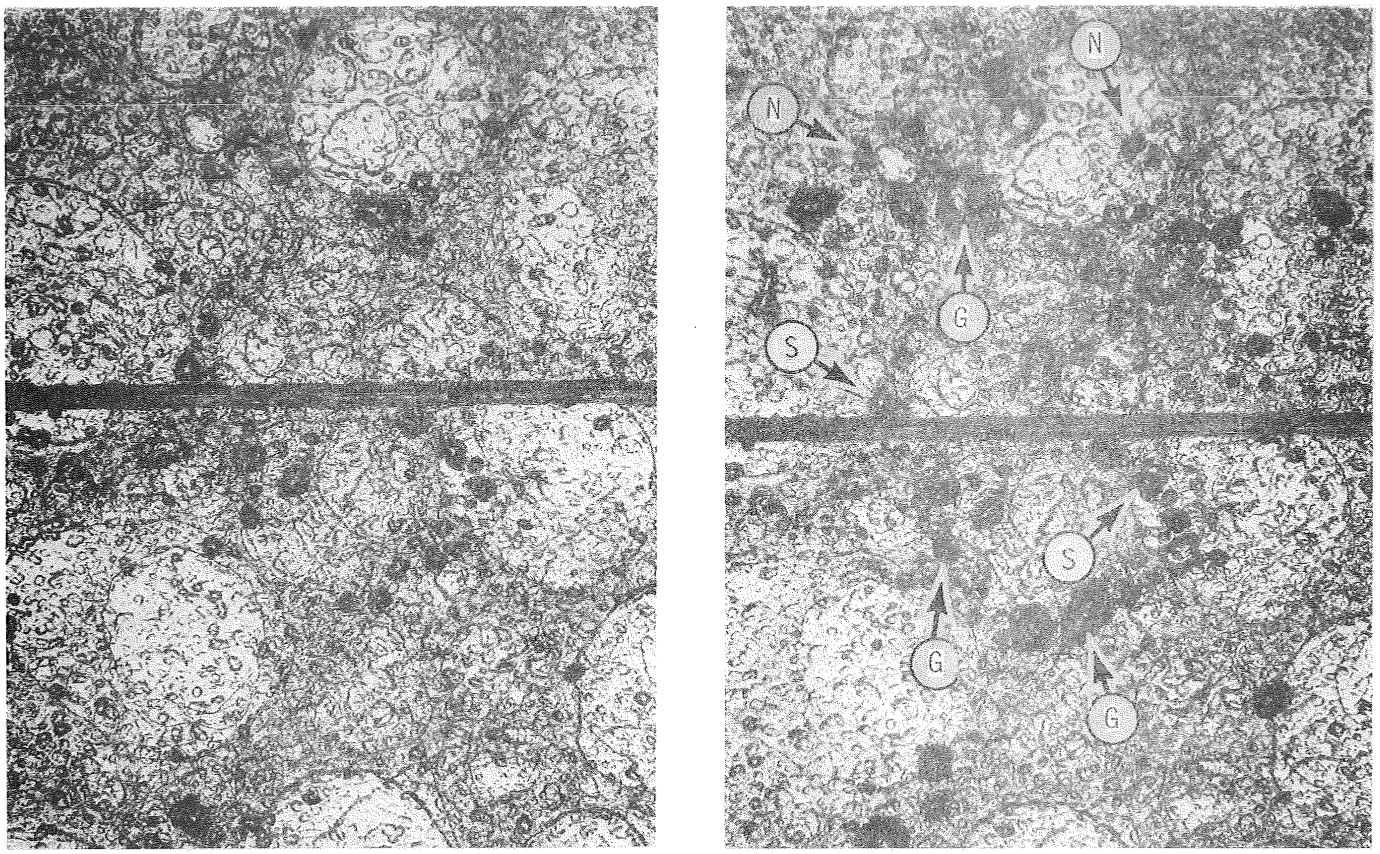

16.5 Hours

35 Hours

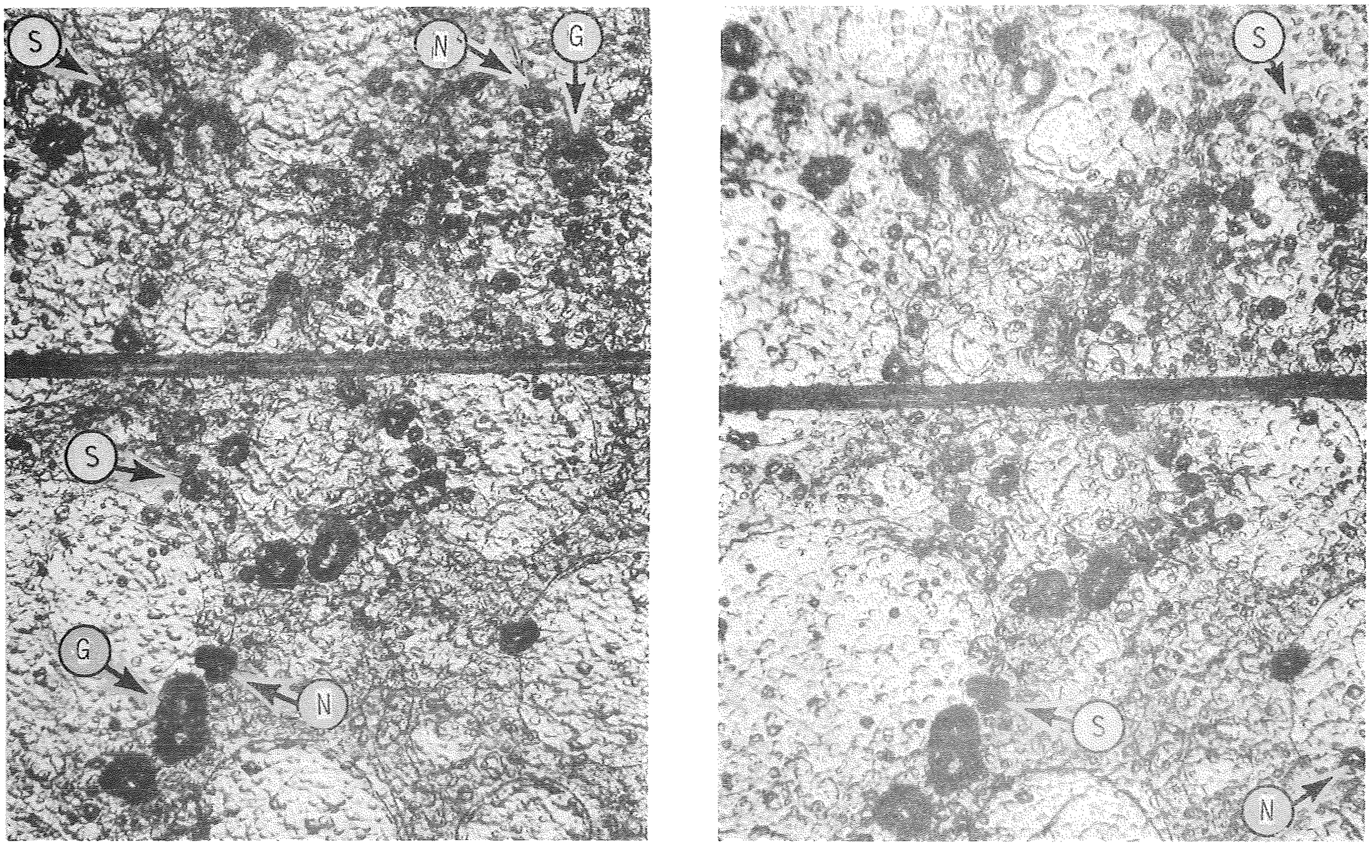

52 Hours

69 Hours

Figure 42: BLISTER GROWTH (45X)

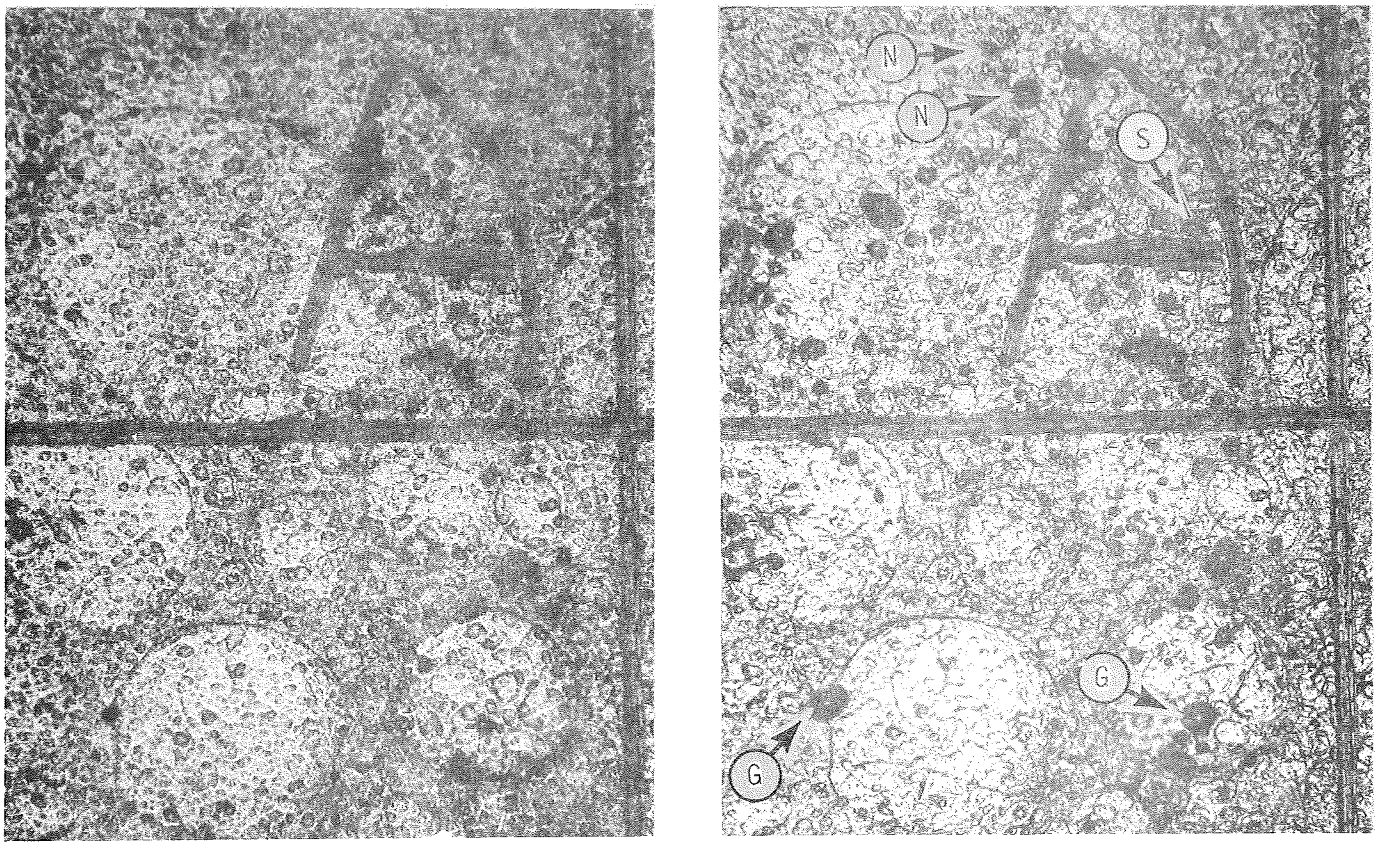

16.5 Hours

35 Hours

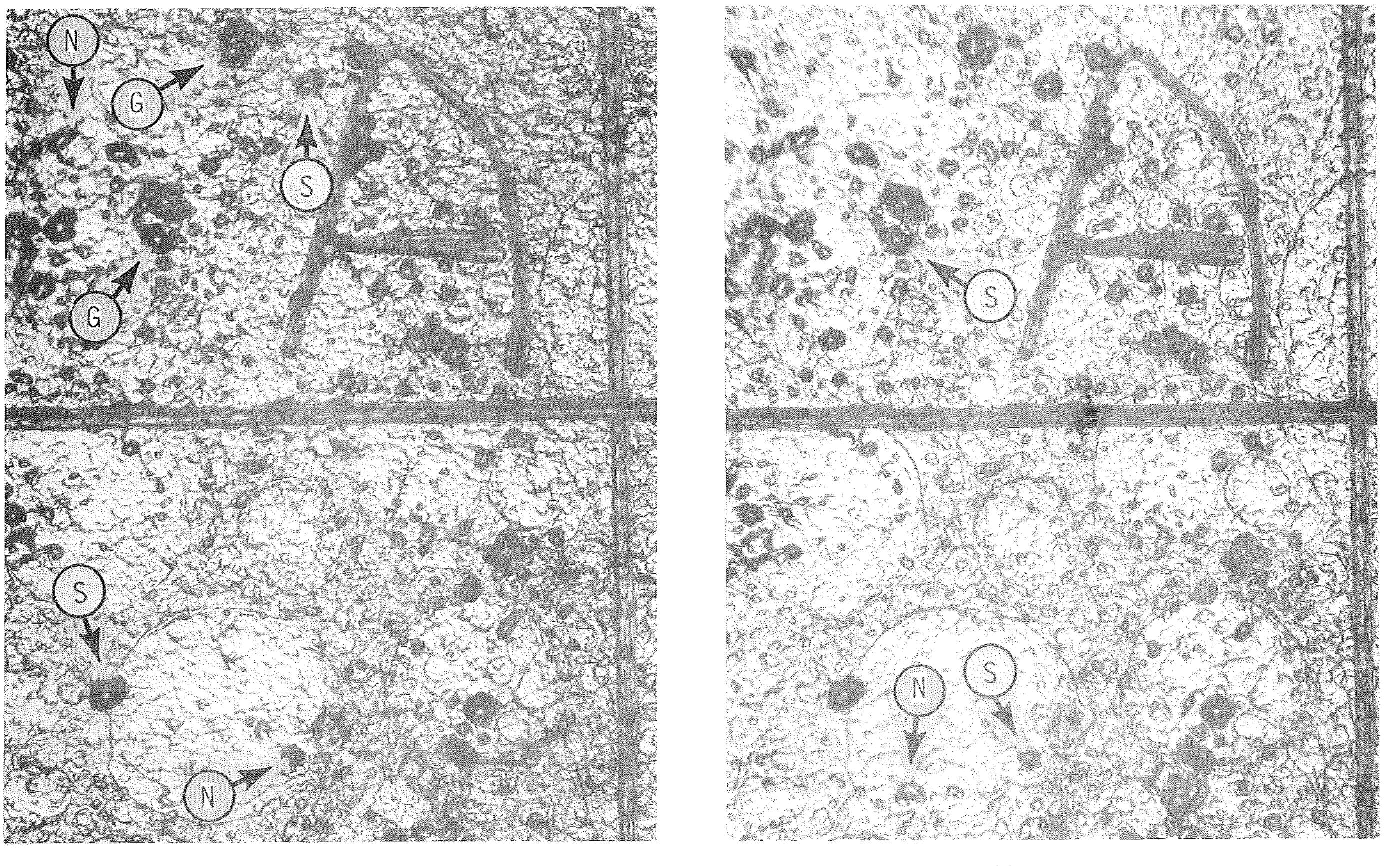

52 Hours

69 Hours

Figure 43: BLISTER GROWTH (45X)

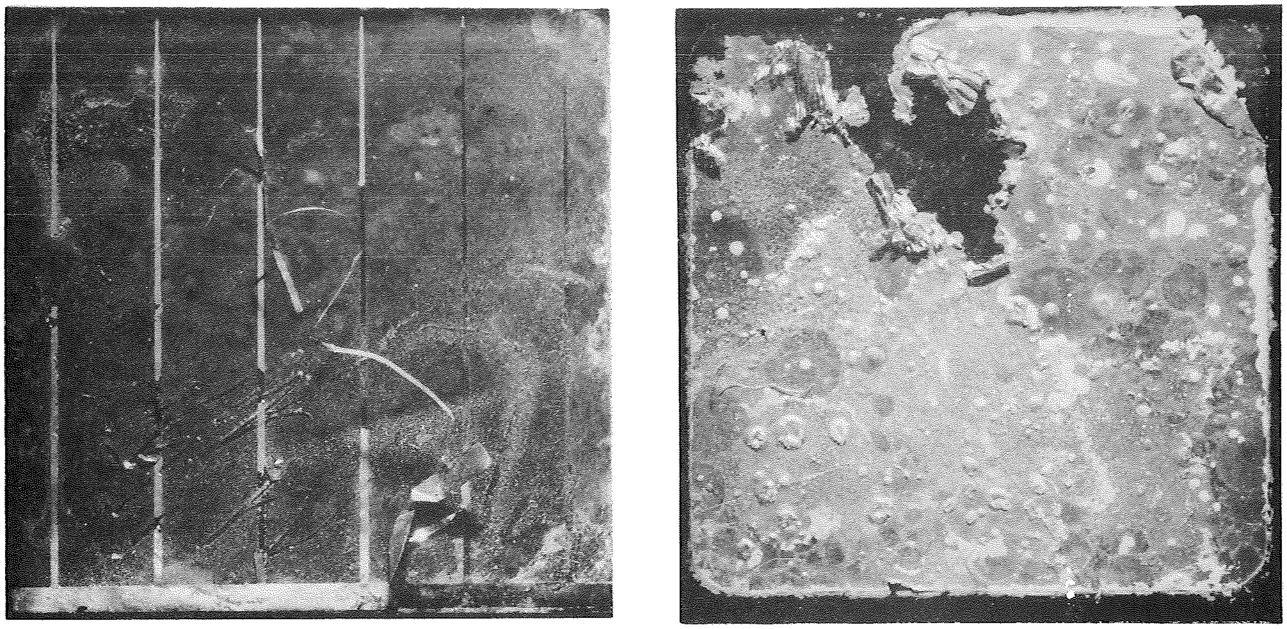

1N NH_4F, 90°C

1N NaCl, 90°C

Figure 44: DEGRADATION WITH HALIDES PRESENT

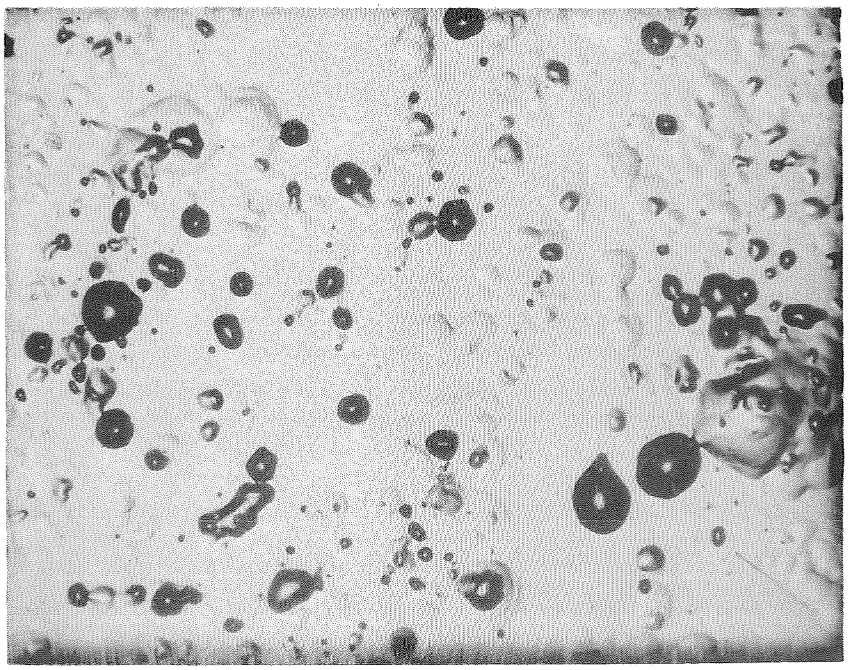

Figure 45: Si/Ti/Ag IRS SAMPLE (25X)

To see what role ion concentration played, the test was repeated using 0.02N fluoride and chloride solutions. After 16.5 hours at 90°C both samples showed blistering with the chloride sample having more and larger blisters. The control cell in water had no degradation. We concluded that the presence of chloride and fluoride ions accelerates degradation of solar cell contacts. More quantitative work is discussed in the next section.

A question which might be raised now is whether the presence of fluoride or chloride is necessary to obtain the fast degradation seen. Solar cells contain fluoride and chloride contaminants, as shown by mass spectroscopy data (section 3.1.2). Several items of evidence indicate the halogens are not necessary but that their presence enhances the degradation. For example, the silver-titanium sample made by Heliotek for the internal reflection spectroscopy studies had not been subjected to etching or cleaning processes which might have left appreciable quantities of halogens. Yet when placed in 96% RH the sample developed many blisters on its surface (Figure 45). The light colored spots are blisters just beginning to form. Also Fischer et al (Ref. 11) evaporated titanium and silver onto a glass slide which was presumably kept clean and not subjected to etching and other contaminating processes. Blisters formed on this sample when exposed to high humidity.

In a final confirming test we evaporated 1000Å of titanium and three microns of silver onto a glass slide in the Boeing Microelectronics laboratory where we could use special precautions to maintain cleanliness. After 48 hours in humid air (∿ 100% RH) at 90°C silver separation occurred along edges but no blisters were seen. After 120 hours blisters could be seen on the surface mainly along the edges (Figure 46). A second sample made at a different time showed blisters after 17 hours under the same conditions (Figure 47). Thus solar cell degradation can occur even in the absence of halogen contaminants. It is not known whether oxidation of the entire titanium layer takes place, as it is probable that even surface oxidation could result in loss of silver adhesion.

3.2.3.3 Experimental Observations

During these tests and observations we noted that blisters were not necessarily accompanied by electrical degradation as observed on an I-V curve. If the cells were degraded so badly that the silver could be easily separated with gentle probing, the I-V characteristics would show drastic degradation (Figure 48). In this illustration the curve of the blistered cell (curve 1) was the same as the original I-V curve taken before the test began. These results further support the observation that the use of I-V curves alone may not be sufficient to establish degradation in a solar cell.

Blisters tend to form along the edges of the contact first. Even the silver-titanium-glass samples initially formed blisters along the edges. Further degradation is accompanied by blister formation in the cell interior. The cell contact layers have no overlap at edges, thus exposing titanium to the atmosphere and providing a surface where corrosion can start. Blisters are less likely to form on the sun-facing contact. This may be due to the narrow width of the grid fingers, allowing the gas to escape before a blister can be formed. As a result grids very often separate without the appearance of blisters.

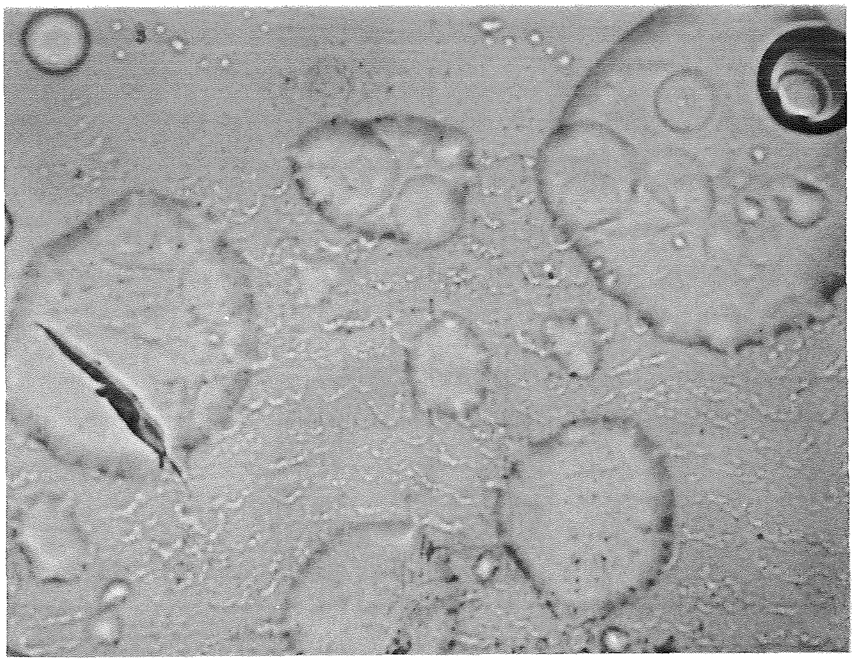

Figure 46: SILVER-TITANIUM-GLASS SAMPLE #1 (25X)

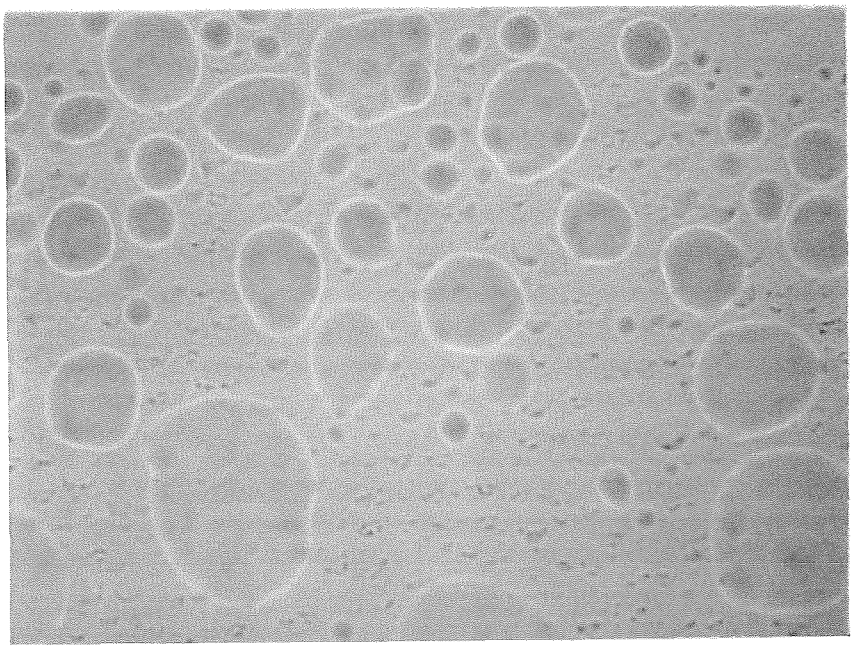

Figure 47: SILVER-TITANIUM-GLASS SAMPLE #2 (25X)

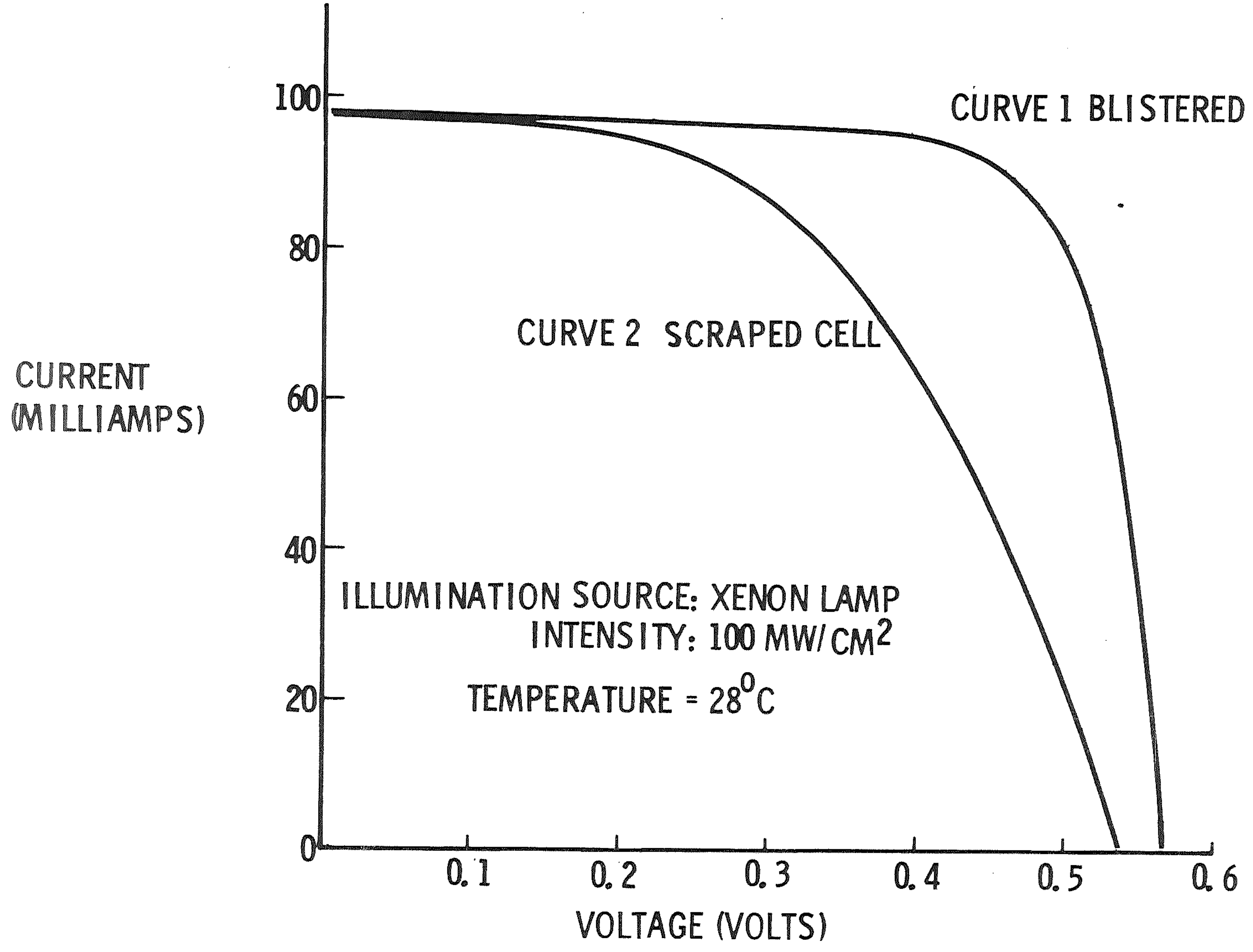

Figure 48: I-V CHARACTERISTICS OF SOLAR CELL

Silver separation does not necessarily occur on both sides of the cell at the same time. Data imply that the grids tend to separate faster than the back contact. This may be linked to the larger titanium surface area which is exposed to the atmosphere because of edge effects.

Summarizing:

- Exposure of solar cells to aqueous solutions caused contact degradation.
- Calculations indicated that surface oxidation (50 Å) of titanium can generate enough hydrogen and sufficient pressure to form blisters. The generation of hydrogen is fast enough to preclude diffusion away from the corrosion site before blister formation.
- New blisters formed and old blisters grew to random sizes as contact degradation progressed.
- The presence of fluoride and chloride ions, even in small quantities, accelerated solar-cell contact degradation, especially at elevated temperatures.
- Contacts free from halogen contamination degraded in humid atmospheres.
- I-V curves by themselves are not good indicators of contact degradation.

3.2.4 Titanium Corrosion

Titanium corrosion in acidic solutions in the presence of various ions has been studied by several investigators (Ref. 12, 13, 25). However, no experimental data were found for corrosion behavior in slightly acidic (pH 5 to 7) solutions. This acidity range is attainable in water exposed to the atmosphere. Fluoride ions were shown to be present in solar cells (Section 3.1.2), and other experiments indicated that the presence of fluoride and chloride ions enhanced corrosion (Section 3.2.3.2).

3.2.4.1 Fluoride Ion

Pieces of 1-mil-thick titanium were abraded with emery cloth, cleaned with alcohol, and placed in solutions of water, 1 normal NH_4F, and 1 normal NH_4F adjusted to a pH=5. The resulting rest potentials are plotted as a function of time in Figure 49. Points 1 and 2 on the water curve represent the addition of approximately 10^{-3} moles of fluoride ions to the solution, and the adjustment of the solution pH to 5, respectively. The changes seen in the rest potentials reflect these perturbations.

The titanium in the 1 normal NH_4F (pH = 5) solution immediately began turning black with the evolution of a gas, presumably hydrogen. After 17.5 hours, the solution contained a solid residue and exhibited a pale violet color, characteristic of Ti^{+3}. At the air-titanium-solution interface, the titanium was corroded almost all the way through. In a subsequent test where the titanium was not abraded it behaved similarly. Within a few minutes, gas was evolved and the rest potential measured -1.2 volts against a saturated calomel electrode, indicating that the protective oxide of the titanium had been attacked and the titanium was corroding.

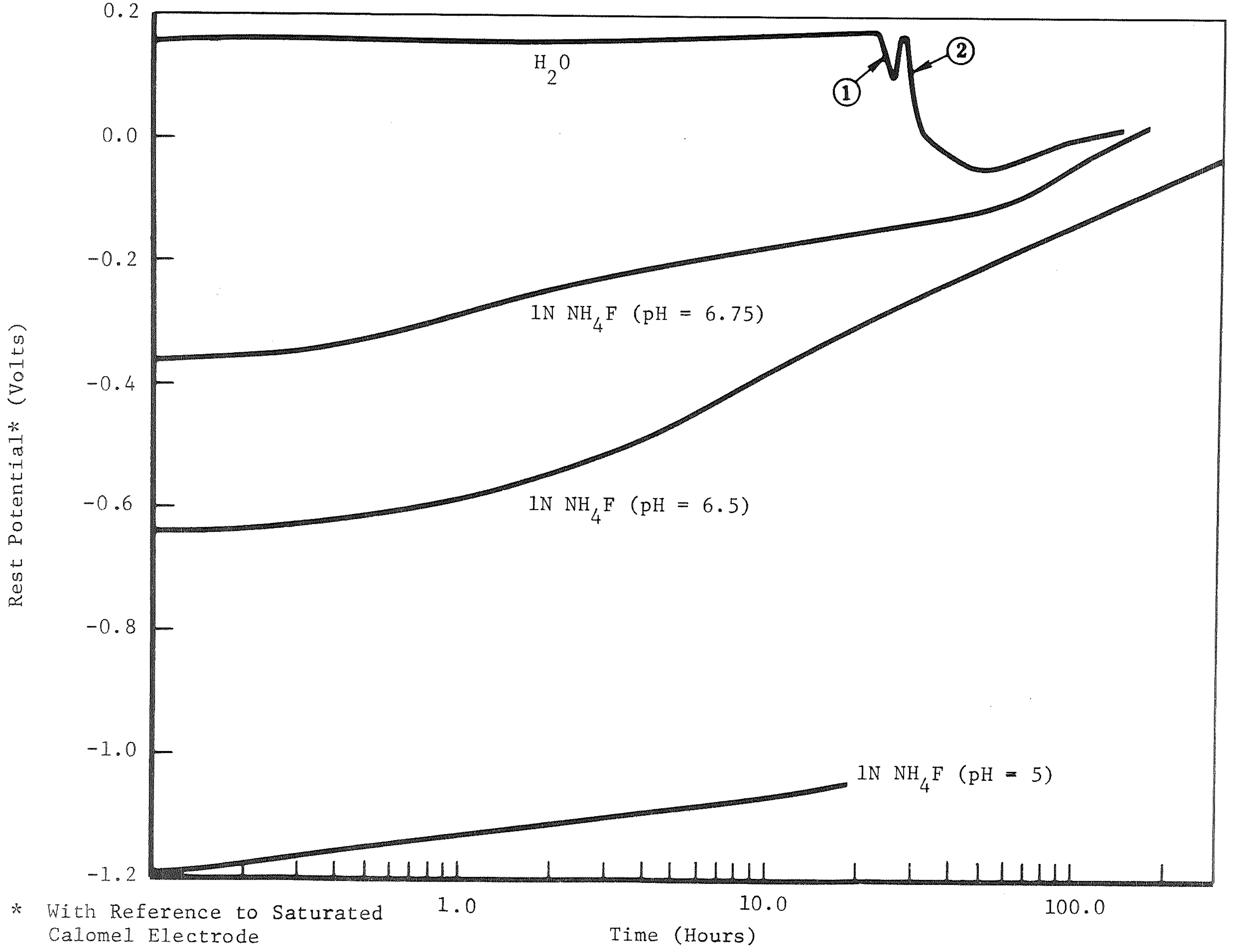

* With Reference to Saturated Calomel Electrode

Figure 49 : **REST POTENTIAL OF TITANIUM**

The titanium placed in the other solutions, however, showed no visible evidence of corroding. This result is in apparent disagreement with the results previously discussed (Section 3.2.3.2) where a pH of 6.5 in 1N NH_4F and 1N NaCl solutions accelerated degradation of solar cells. However, part of the previous tests were at 90°C. Since reaction rates depend quite strongly on temperature, another test was performed where one-mil titanium foil was inserted into a 1N NH_4F (pH = 6.5) solution which had been heated to 90°C. Bubbles appeared and a potential of -1.18V was recorded. Obviously the room temperature corrosion rate was too small to be observed. This is a good example of the effect of temperature on corrosion rates.

It is significant that titanium will corrode in the presence of fluoride at moderate pH. The absorption of CO_2 in water at standard temperature and pressure results in a 0.038M solution. The pH of such a solution can be as low as 3.7 (Ref. 26). Water condensation in pores in the silver layer of the solar cell contacts can thus provide a conductive, acidic solution where titanium would corrode in the presence of fluoride ions.

To obtain more quantitative data on the corrosion of titanium at moderate pH, polarization curves were taken in solutions of fluoride ion at various pH values and concentrations. Existing experimental apparatus was used (Figure 35). A teflon cell was built to expose 0.75 cm^2 of titanium metal to the solution. To minimize concentration effects, approximately 50 ml of solution was used in each test. The pH of the fluoride solutions was adjusted with H_2SO_4 and/or KOH. The titanium was abraded with emery cloth, cleaned with alcohol, and "conditioned" at a current of -10 or -20 mA/cm^2 for several minutes before the polarization curve was taken. Sweep speeds of 100 to 300 mv/min were used in the studies.

A typical polarization curve (Figure 50) for 1 normal NH_4F(pH=5) shows the presence of a positive current in the region of -800 mv, indicating corrosion. Assuming that the unstirred solution is diffusion-limited by fluoride ions, the limiting corrosion current can be defined (Ref. 27) as:

$$i_j = \frac{D_j \, z \, F \, a_j}{\delta}$$

where:

D_j = diffusion coefficient for ion j (approximately 7.5×10^{-6} cm^2/sec);
a_j = bulk activity of j (10^{-3} moles/ml for a 1 normal solution);
F = Faraday constant (96,500 Coulombs/mole);
z = number of electrons transferred (four);
δ = diffusion layer thickness (approximately 5×10^{-2} cm).

Using these values, the limiting current i_1 can be estimated to be approximately 58 mA/cm^2, which agrees well with the experimentally observed value of 53.5 mA/cm^2 for the 1 normal NH_4F(pH=5) solution.

Corrosion was found to occur for only some combinations of halide ion concentrations and pH. For example, titanium in 1 normal NH_4F(pH=6.65) exhibits no visible corrosion current (Figure 51).

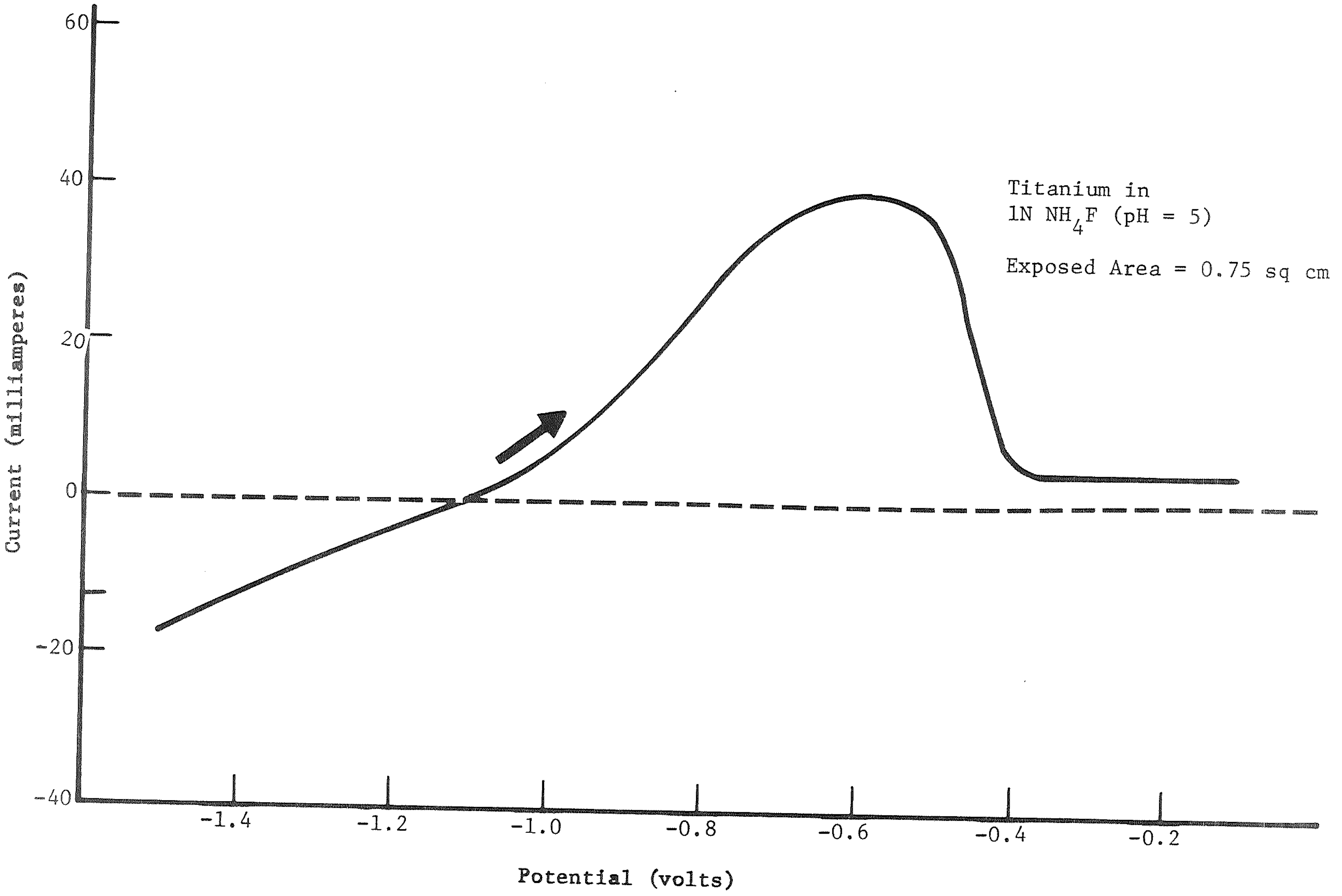

Figure 50: POLARIZATION CURVE (1 Normal NH_4F, pH = 5)

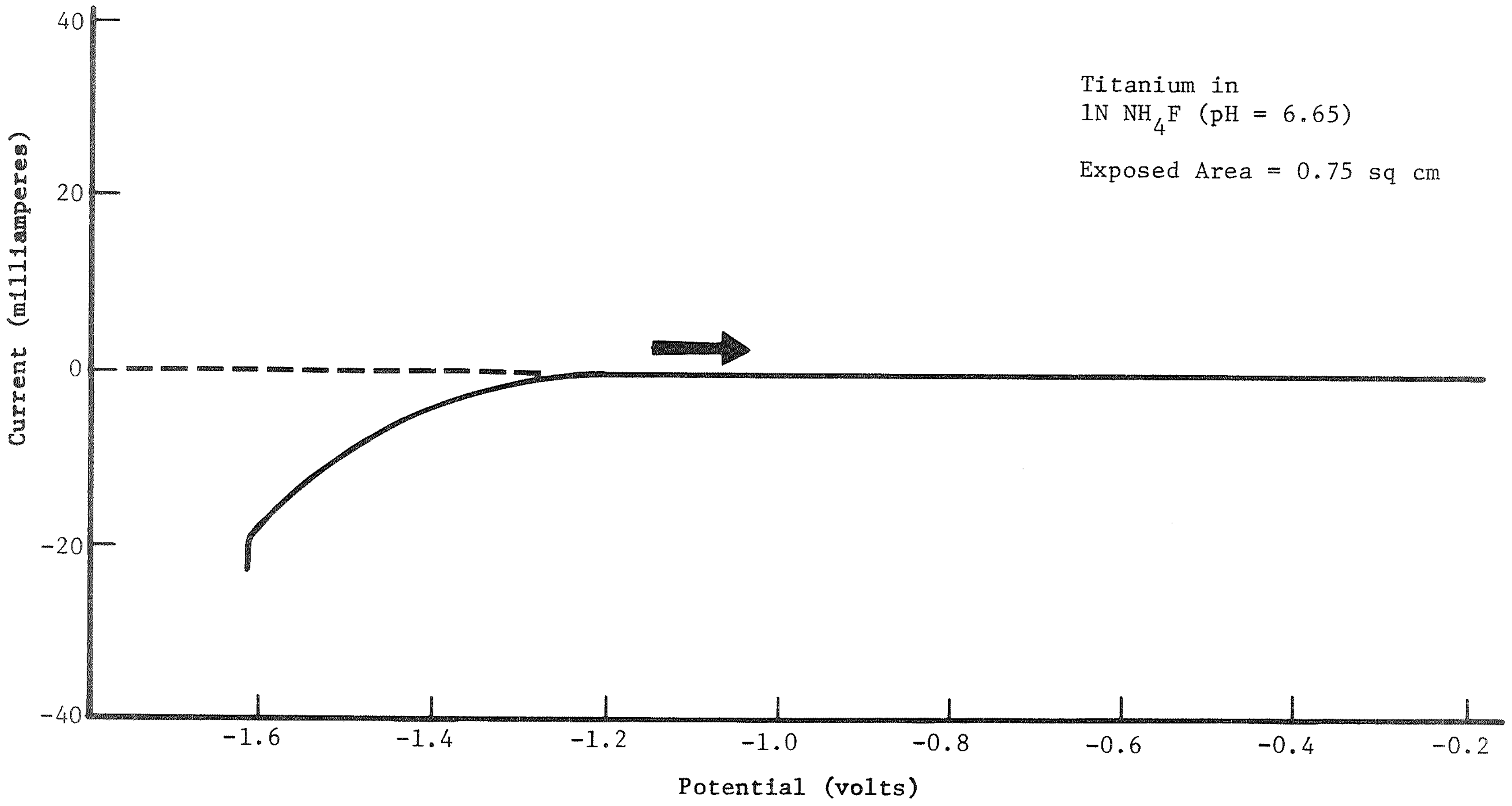

Figure 51: POLARIZATION CURVE (1 Normal NH_4F, pH = 6.65)

The results from the polarization tests are summarized below. YES implies that a positive corrosion current was observed; NO indicates that corrosion did not occur under those conditions. Blank spaces represent conditions that were not tested.

Fluoride Solutions	Concentration			
pH	0.01N	0.1N	1N	5N
4	NO	YES	YES	
5		NO	YES	YES
6			NO	YES
6.65			NO	
7				NO

These data are in seemingly partial disagreement with the previous section where data indicated that fluoride solutions at a pH > 6 also enhanced degradation of solar cells. The time for the fluoride degradation is less than 260 hours at room temperature (Table 8). The corrosion current (I) needed to give corrosion of titanium in this time can be estimated using Faraday's Laws (Ref. 27).

$$W = \frac{I\ t\ A}{z\ F}$$

where W = weight of titanium reacted
t = time (seconds);
A = molecular weight (47 gm/mole);
z = number of electrons transferred
F = Faraday constant (96,500 Coulombs/mole).

Assuming that 50 Å of titanium corrodes via the reaction $Ti + 6F^- \rightarrow TiF_6^{=} + 4e^-$, the corrosion current required would be:

$$I = \frac{50\ \text{Å Ti}\ (4.5\ \text{gm Ti/cm}^3)\ (10^{-8}\text{cm/Å})\ (4)\ (96.5 \times 10^3\ \text{Coulombs/mole})}{(47\ \text{gm/mole})\ (260\ \text{hours})\ (3600\ \text{sec/hour})}$$

$$I = 1.97 \times 10^{-8}\ \text{Amps/cm}^2$$

$$I = 0.0197\ \mu\text{A/cm}^2$$

The times used for this calculation must be considered as approximate because the definition of degradation is subjective and the quantitative amount of degradation in a solar cell is difficult to determine.

The equipment used in polarization measurements is not sensitive enough to measure the 0.0197 μA corrosion currents calculated above so it is probable that corrosion was indeed occurring during these measurements, but it proceeded undetected. The fact that large corrosion currents were seen in some solutions at pH < 5 would imply that corrosion also occurs at pH > 5 but at reduced rates.

There is also the possibility that film thickness can affect corrosion rate. The titanium film in solar cells is very thin (10^3 Å) whereas polarization was measured with thick films (1 mil). Data by Beck (Ref. 23) on reactivity of titanium indicated that small grain titanium reacted much more vigorously than thick films. This phenomenon occurs with other substances, such as platinum black.

We do not yet know by what reaction mechanism the titanium corrodes in fluoride solution. The initial attack on the titanium foil can be explained by a reaction:

$$4H^{+} + 6F^{-} + TiO_2 \rightarrow TiF_6^{=} + 2H_2O \qquad \Delta F = 28 \text{ kcal/mole}$$

Since titanium dissolves the reaction that most likely occurs is:

$$Ti + 6F^{-} \rightarrow TiF_6^{=} + 4e^{-} \qquad \Delta F = -110 \text{ kcal/mole}$$

The potential for this reaction, -1.19v (Ref. 28), is very close to the measured value. The formation of some type of oxyfluoride complex is also possible. The presence of the violet color in the rest potential test indicates the presence of Ti^{+3} which would come from the reaction: $Ti \rightarrow Ti^{+3} + 3e^{-}$. Beck has also seen evidence for this reaction in high pH systems (Ref. 29). It is also possible that the fluoride acts in a catalyst role through a series of reactions where it is an intermediate, being regenerated as the corrosion proceeds.

The data show that the corrosion current depends on concentration and pH. We cannot estimate the actual fluoride concentration and pH within a solar cell contact but the overall fluoride concentration must be small (Section 3.1.2). Local concentrations, however, can be higher depending on the amount of water present. Some of the mass spectroscopy work showed equal amounts of fluoride and water (Table 1) indicating a saturated solution of fluoride in that particular case. The overall evidence suggests that even small amounts of fluoride ion will enhance the corrosion of titanium in solar cells over long periods of time, especially at elevated temperatures.

3.2.4.2 Chloride Ion

Chloride ions also break down the passivity of oxide coatings (Ref. 30). Because our previous work implied that the presence of chloride also enhances degradation, polarization studies were conducted using various pH chloride solutions. The results are shown below.

Chloride Solutions	Concentration			
pH	0.01N	0.1N	1N	5N
4		NO	NO	NO
4.5				NO
4.85			NO	
5.0			NO	

Again a disagreement exists. The time scales for the chloride degradation ($\leq$ 73 hours for blister formation) would require a corrosion current of $\sim$ 0.06 $\mu A/cm^2$ to corrode 50 Å of titanium. This current is below the sensitivity of our instrument.

Rest potentials of titanium in chloride solutions were not measured. However, to test the temperature effect, a solution of 1N NaCl was heated to 90°C, and the rest potential of titanium in the solution found to be -0.032V. There were no visible signs of corrosion activity.

3.2.4.3 Noble Metal Couples

It is known that titanium alloyed with a noble metal reduces the corrosion rate of the titanium (Ref. 31). It should be noted, however, that the corrosion is not completely halted. To explore the behavior of titanium-noble metal systems in the presence of fluoride ion we coupled titanium to platinum in a one-normal NH_4F(pH = 5) solution and recorded the rest potential as a function of time (Figure 52). When coupled to the platinum, fewer bubbles were emitted from the titanium surface, suggesting that the corrosion slowed, but did not stop. After one hour, the one-mil thick piece of titanium had almost corroded through (Figure 53). Buck et. al. (Ref. 13) also noted that the presence of fluoride increased the corrosion rate of titanium-platinum alloy appreciably.

Summarizing:

- We find that titanium corrodes in fluoride solutions more neutral than previously described in the literature.
- High temperature accelerates degradation of solar cells in fluoride solutions. The high-temperature degradation phenomena agree qualitatively with polarization data when temperature is taken into account.
- Room temperature solar cell degradation in fluoride solutions cannot be correlated directly with the polarization data which suggests that no corrosion is taking place. Either the corrosion currents are below the threshold of detection of the polarization apparatus, or the thin film of titanium in the solar cell does not behave in the same manner as does the titanium strips that we tested.
- Solar cell behavior in chloride solutions does not correlate with titanium behavior in chloride solutions. Again the corrosion currents may be too low to be measured with our equipment, or the thin film of titanium in solar cells determines its reactivity towards these solutions.
- Coupling of titanium with platinum reduces the corrosion rate of titanium in the presence of fluoride ion, but does not halt it.

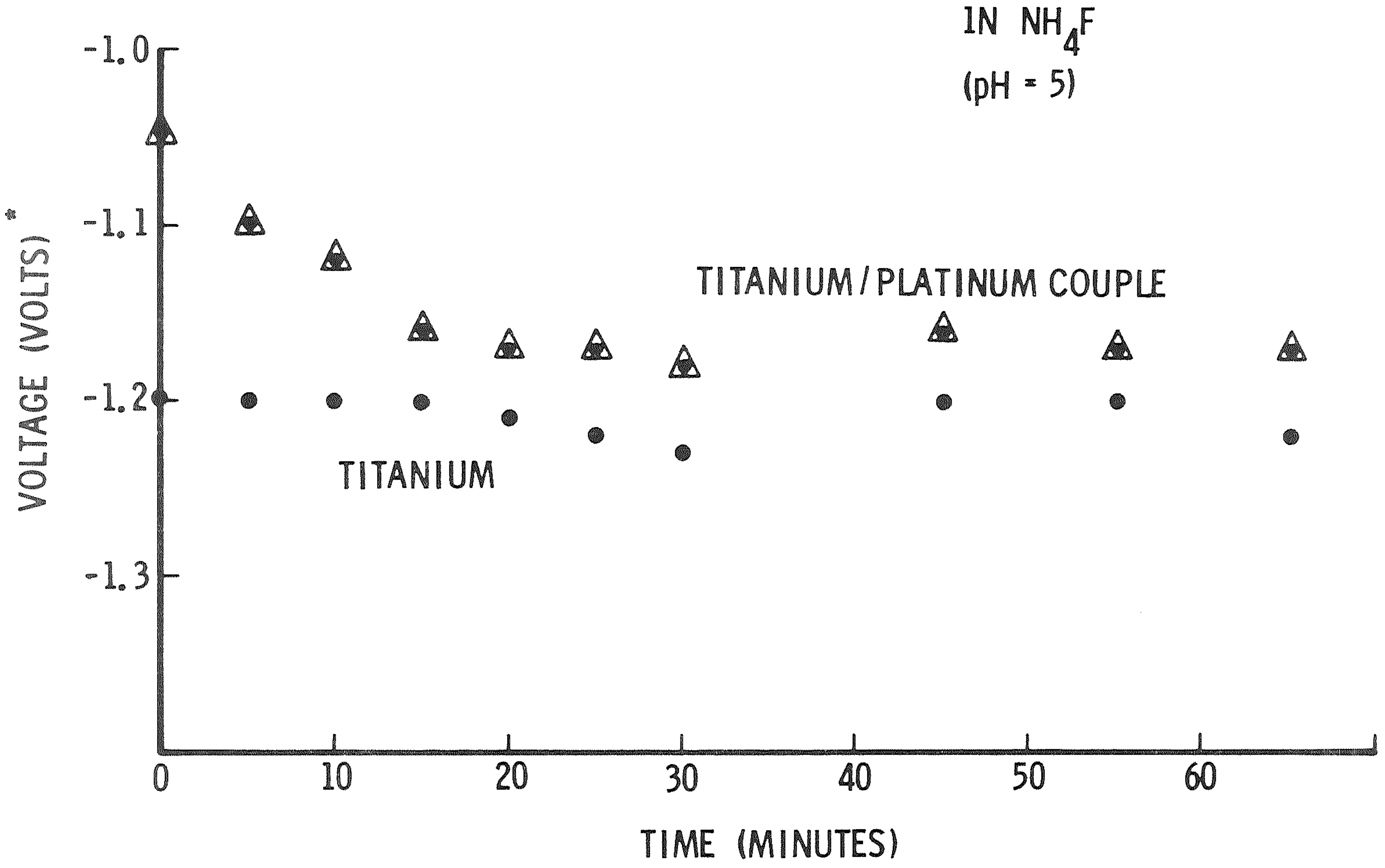

* VERSUS SATURATED CALOMEL ELECTRODE

Figure 52 : REST POTENTIAL OF TITANIUM---PLATINUM COUPLE

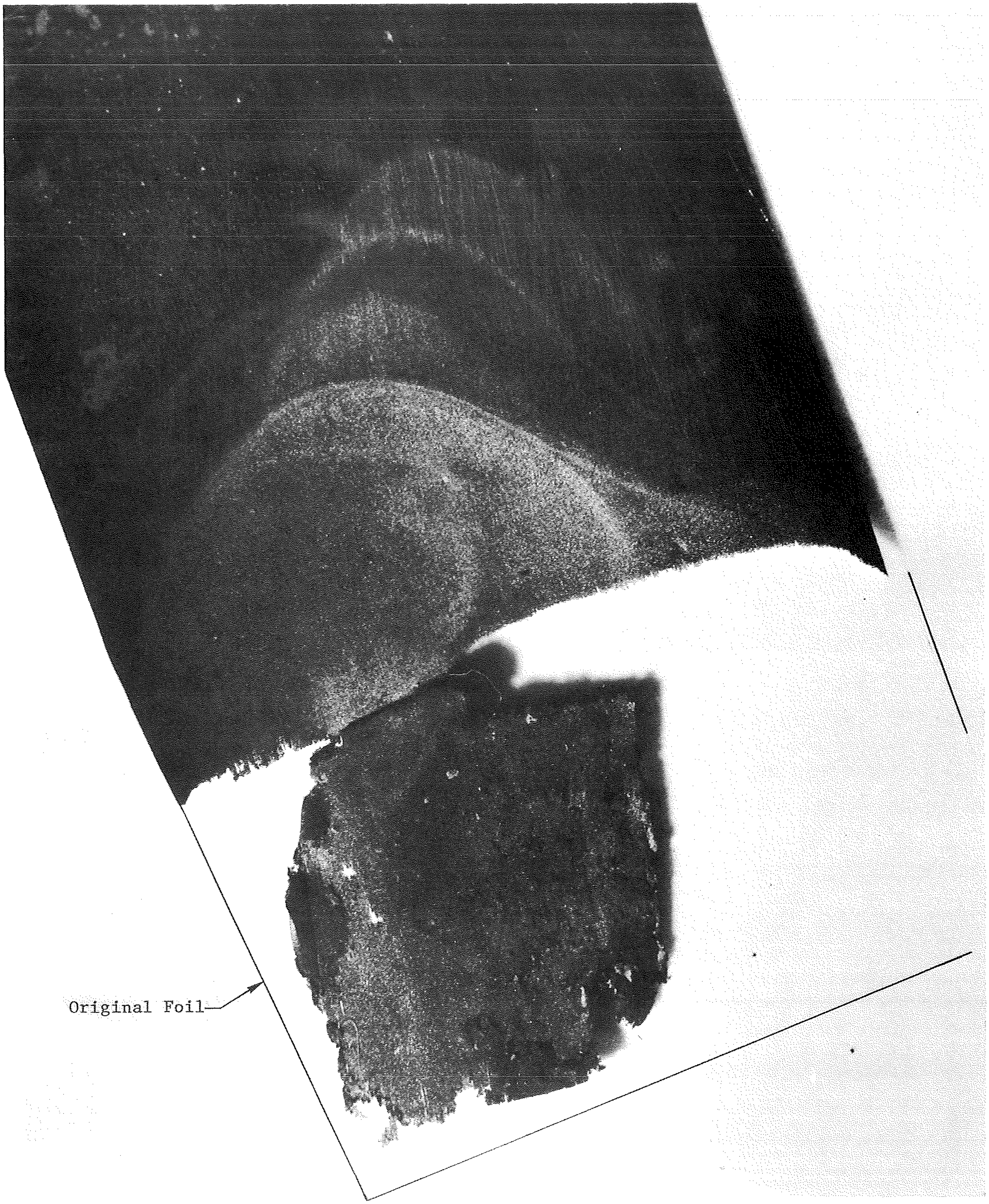

Figure 53: CORRODED TITANIUM FOIL

4.0 PRESENT DAY SOLAR CELL BEHAVIOR

Based on the work done up to this point, the behavior pattern of present day solar cells in a humid atmosphere can be predicted:

- When subjected to ∿ 100% RH the solar cell will degrade because water will condense in the pores of the silver layer and react with the titanium.

To test this hypothesis, nine cells (4 Heliotek, 5 Centralab) were obtained from production lines and exposed to a 90°C, ∿ 100% RH environment. I-V curves were taken periodically. After 288 hours, two Heliotek cells and one Centralab cell showed increased series resistance and I-V degradation. After 936 hours, I-V curves were recorded for all nine cells. The I-V characteristics of some cells were satisfactory even after the 900 hours. The cells were then examined for evidence of contact degradation (Table 9). All cells lost contact adherence on the critical sun-facing side. Centralab cells lost adherence mainly in the bar contact; Heliotek showed more tendency to lose both the bar contact and the grids. This might be related to the SiO coating that is placed on finished cells.

Table 9: SOLAR CELL DEGRADATION BEHAVIOR (TEST NO. 1)

Cell	Contact	Blisters	Silver Separation	Manufacturer
1	Sun-Facing Back	Yes Yes	Extensive Yes	Heliotek
2		Yes Yes	Extensive Yes	
3		Yes Edges	Extensive Yes	
4		Yes Edges	Yes Yes	
5		? No	Yes No	Centralab
6		Yes Few	Yes No	
7		Yes No	Yes No	
8		Yes Few	Yes Edges	
9		No No	Yes No	

Test Conditions: 90°C, ~ 100% RH

Time: 936 Hours

The surprising result was the good contact adherence and lack of blisters on most of the Centralab back contacts. The reason for this is not known. Several possibilities exist. The sun-facing sides of Heliotek and Centralab cells are similar in surface characteristics, and both types show silver separation on this side. Differences in surface characteristics exist with the back contact (Section 3.1.1). Possibly adhesion characteristics are linked to the surface structure. A second possibility is that non-porous silver was deposited on these cells. This is unlikely since all of the internal reflection spectroscopy samples were porous to high humidity (Section 3.1.4). Mass spectroscopy did not indicate a drastic difference in contamination between manufacturers. We are hesitant to attribute the difference in behavior to cleanliness. Furthermore, our data indicate that even clean systems will degrade (Section 3.2.3).

We repeated the test using subsequently produced cells. Again the test conditions were 90°C and above ∿ 100% RH. After 24 hours all four Heliotek cells had extensive peeling of the silver grids (Table 10). One of the Centralab cells

Table 10: SOLAR CELL DEGRADATION BEHAVIOR (TEST NO. 2)

Cell	Contact	Blisters		Silver Separation		Manufacturer
		24 Hours	48 Hours	24 Hours	48 Hours	
300	Sun-Facing Back	No Few	No Yes	Extensive Edges	Extensive Yes	Heliotek
301	↓	No No	One One	Extensive Edges	Extensive Edges	
302	↓	No No	No Yes	Extensive Edges	Extensive Yes	
303	↓	No No	No Yes	Extensive Edges	Extensive Edges	
200	↓	Yes No	Yes No	No (?) No	Yes Yes	Centralab
201	↓	No No	Yes No	Yes (?) No	Yes Yes	
202	↓	Few Extensive	Yes Extensive	No Yes	Yes Yes	
203	↓	Few No	Yes No	No (?) No	Yes No	

Test Conditions: 90°C, ~100% RH

had blisters all over the back contact and two other Centralab cells had blisters on the sun-facing side. After 48 hours at these conditions all of the Centralab cells lost contact adhesion on the sun-facing side and three of the four back contacts had silver separation. The inconsistent behavior of solar cells shows up well in these tests; some cells with no blisters, yet silver separation; some contacts blistering, others not; silver separation only along edges, others all over.

As shown by the first test care must be taken not to rely only on I-V characteristics when determining the degradation behavior of the cells. Even though some cells show signs of resistance to electrical degradation the fact that silver separation occurs indicates that the useful life of the cell is reduced. Most degradation is seen to occur on the critical sun-facing side of of the cell.

These tests show that present day 1970 cells will degrade consistently in a high humidity atmosphere.

5.0 APPENDIX 1: STEPS IN MANUFACTURE OF SILICON SOLAR CELLS

One of the goals of this study was to identify steps in solar cell manufacturing where contamination might occur. Listed below is a composite of steps used by manufacturers to produce solar cells. This composite is based on data obtained from NASA Lewis Research Center, Heliotek and Centralab. Individual steps vary depending on the manufacturer. Proprietary cleaning steps used by the manufacturers are only generalized here.

1. Grow ingot.
2. Clean ingot.
3. Cut flat on ingot.
4. Mount ingot for sectioning.
5. Section into disks.
6. Demount sections.
7. Production inspect sections.
8. Lap sections.
9. Mount sections for slabbing (barring).
10. Cut slabs (bars).
11. Demount slabs.
12. Lap slabs.
13. Mount slabs for slicing (wafering).
14. Mount billet in diamond-saw wafering machine.
15. Slice slab.
16. Demount slices.
17. Mount slices for polishing (alternate-etch slices).
18. Polish slices with 20 micron alumina powder.
19. Polish slices with 5 micron powder.
20. Polish slices with 1 micron powder.
21. Demount slices.
22. Production inspect slices.
23. Clean slices in trichloroethylene (alternates-acetone, isopropyl alcohol, sulfuric acid).
24. Etch slices in acid solution (acetic, nitric, hydrofluoric):
    a. Mix acetic and hydrofluoric acid and pour over slices.
    b. Add nitric acid to start etch.
    c. Etch required time, e.g., 4 minutes.
    d. Quench etch with deionized water.
25. Clean slices in deionized water.
26. Dry slices in alcohol.
27. Dry slices in stream of nitrogen gas.
28. Store in plastic containers.
29. Diffuse in quartz tube or boat with $POCl_3$ carried with O_2.
30. Anneal slices.
31. Store in covered Pyrex container.
32. Mask N layer with tape (alternate-cover with wax).
33. Sandblast cells to expose p layer (alternate-chemically etch).
34. Remove mask or wax.
35. Clean cells in trichloroethylene.
36. Clean in nitric-hydrofluoric-acetic acid solution.
37. Clean in deionized water.
38. Dry with methyl or isopropyl alcohol.
39. Dry slices in stream of nitrogen gas.

40. Store slices in Pyrex container with desiccant, e.g., $CaSO_4$.
41. Load fixtures for evaporation of contacts.
42. Clean titanium filament with SiC paper.
43. Clean silver filament.
44. Measure vacuum, must be less than 5×10^{-5} Torr.
45. Evaporate titanium.
46. Evaporate titanium and silver.
47. Evaporate silver.
48. Break vacuum with dry nitrogen.
49. Place cells in sintering oven.
50. Admit hydrogen gas to oven.
51. Sinter cells at 605°C in gas.
52. Clamp cells between rubber wafers (alternate-mask cell faces with wax).
53. Remove N layer from cell edges with HF acid.
54. Clean cells in deionized water.
55. Evaporate silicon monoxide on cell.
56. Fire silicon monoxide coating.
57. Perform tape test on silver coating.
58. Clean cell after tape test.
59. Production test cells mechanically.
60. Production test cells electrically.
61. Store cells in polystyrene slotted boxes.
62. Package for shipment.

Contamination from fluorides comes from the HF etching processes which are used several times during the manufacturing process. Handling of cells at various times even with cotton gloves can introduce or spread contamination, especially chloride-containing compounds. Cleaning processes offer opportunities to introduce contaminants from impure wash solutions. Tape tests leave traces of residue on solar cell surfaces observable in X-ray diffraction studies.

REFERENCES

1. Morrison, G., "Solar Cell Contact Deposition Parameter Study," Contract NAS5-11612, NASA Goddard (November 1968).

2. Lepselter, M.P., U.S. Patent 3, 106, 489, Bell Telephone Laboratories, October 8, 1963.

3. Luft, W., McCraven, C.C., and Aroian, L.A., "Temperature and Humidity Effects on Silicon Solar Cells," 7th Photovoltaic Specialists Conference, Pasadena, California, 1968.

4. Ralph, E.L., "Solar Cell Development Survey," Intersociety Energy Conversion Engineering Conference, Boulder, Colorado, 1968.

5. Springgate, W.F., "Investigation Into the Mechanism of Degradation of Solar Cells with Silver-Titanium Contacts," 1st Quarterly Report, Contract NASW-1859, NASA Headquarters (June 1969).

6. Bishop, C.J. "Investigation Into the Mechanism of Degradation of Solar Cells With Silver-Titanium Contacts," 2nd Periodic Progress Report, Contract NASW-1859, NASA Headquarters (December 1969).

7. Jacobson, R.J., "Solar Cell Contact Development," 1st Quarterly Report, Contract NAS5-11595, NASA Godddard (September 1968).

8. Jacobson, R.J., "Solar Cell Contact Development," 2nd Quarterly Report, Contract NAS5-11595, NASA Goddard (December 1968).

9. Jacobson, R.J., "Solar Cell Contact Development," 3rd Quarterly Report, Contract NAS5-11595, NASA Goddard (March 1969).

10. Morrison, G., "Solar Cell Contact Deposition Parameter Study," Contract NAS5-11612, NASA Goddard (February 1969).

11. Fischer, H., Gehrke, J., Gereth, R., and Pschunder, W., "A Study on the Development of Improved Interconnection Techniques for Silicon Solar Cell Arrays," Contract 459/67AA, European Space Research Organization (January 1969).

12. Straumanis, M.E. and Gill, C.B., "The Rate of Dissolution and the Passivation of Titanium in Acids With Ammonium Fluoride Added," J. Electrochemical Society 101, 10 (1954).

13. Buck III, R., Sloope, B.W., and Leidheiser Jr., H., "Corrosion of Titanium in Boiling 2M Hydrochloric Acid," Corrosion 15, 566t (1959).

14. Larrabee, G.B., Heinen, K.G., and Harrell, S.A., "Measurement of the Retention of Fluoride by Silicon and Silicon Dioxide Surfaces," J. Electrochemical Society 114, 867 (1967).

15. Jacobson, R.J., private communication.

16. Becker, W.H., "The Formation and Degradation of Titanium-Silver Solar Cell Contacts," Ph.D. Thesis, University of Pennsylvania (1970).

17. Rawlins, T.G.R., "ATR Spectroscopy," Canadian Spectroscopy 9, 12 (1963).

18. Anon., "Recommended Practice for Maintaining Constant Relative Humidity by Means of Aqueous Solutions," 1969 Book of ASTM Standards, Part 30, American Society for Testing and Materials, Philadelphia, Pa., p. 211 (1969).

19. Adamson, A.W., Physical Chemistry of Surfaces, 2nd ed., Interscience, New York, p. 58 (1967).

20. Springgate, W.F., "Investigation Into the Mechanism of Degradation of Solar Cells with Silver-Titanium Contacts," in Ohmic Contacts to Semiconductors edited by B. Schwartz, The Electrochemical Society, New York, p. 263 (1969).

21. Atalla, M.M., Tannenbaum, E., and Scheibner, E.J., "Stabilization of Silicon Surfaces by Thermally Grown Oxides," Bell System Technical Journal 38, 749 (May 1959).

22. Pourbaix, M., Atlas of Electrochemical Equilibria in Aqueous Solutions, Pergamon Press, New York (1966).

23. Beck, T.R., "Stress Corrosion Cracking of Titanium Alloys: Electrochemistry of Freshly Generated Titanium Surfaces," Quarterly Report No. 9, Contract NAS7-489 (September 1968).

24. Stern, M., and Wissenberg, H., "The Electrochemical Behavior and Passivity of Titanium," J. Electrochemical Society 106, 755 (1959).

25. Shibamori, S., Yoshizawa, S., and Hine, F., "Electrochemical Behavior of Titanium in HCl Solutions Containing Ferrous and Ferric Ions," J. Electrochemical Society, Japan 35, 10 (1954).

26. Heslop, R.B., Robinson, P.L., Inorganic Chemistry, Elsevier, New York (1960).

27. Potter, E.C., Electrochemistry: Principles and Applications, Cleaver-Hume Press, Ltd., London (1954).

28. Latimer, W.M., Oxidation Potentials, 2nd Ed., Prentice Hall, New Jersey (1952).

29. Beck, T.R., Blackburn, M.J., Smyrl, W.H., and Speidel, M.O., "Stress Corrosion Cracking of Titanium Alloys: Electrochemical Kinetics, SCC Studies with Ti:8-1-1, SCC and Polarization Curves in Molten Salts, Liquid Metal Embrittlement, and SCC Studies with other Titanium Alloys," Quarterly Progress Report No. 14, Contract NAS 7-489 (December 1969).

30. Uhlig, F.H., Corrosion and Corrosion Control, John Wiley, New York (1963).

31. Stern, M. and Wissenberg, H., "The Influence of Noble Metal Alloy Additions on the Electrochemical and Corrosion Behavior of Titanium," J. Electrochemical Society 106, 759 (1959).

32. Lepselter, M.P. and Andrews, J.M., "Ohmic Contacts to Silicon," in Ohmic Contacts to Semiconductors edited by B. Schwartz, The Electrochemical Society, New York, p. 159 (1969).

33. Shinoda, D., "Ohmic Contacts to Silicon Using Evaporated Metal Silicides," in Ohmic Contacts to Semiconductors edited by B. Schwartz, The Electrochemical Society, New York, p. 200 (1969).